DYE ENCAPSULATION AND EXCHANGE

IN BLOCK COPOLYMER MICELLES

by

Emma De Baets

A thesis submitted to the Faculty of the University of Delaware in partial fulfillment of the requirements for the degree of Master of Chemical Engineering

Spring 2017

DYE ENCAPSULATION AND EXCHANGE

IN BLOCK COPOLYMER MICELLES

by

Emma De Baets

Approved: _____
Thomas H. Epps, III, Ph.D.
Professor in charge of thesis on behalf of the Advisory Committee

Approved: _____
Millicent O. Sullivan, Ph.D.
Professor in charge of thesis on behalf of the Advisory Committee

Approved: _____
Abraham M. Lenhoff, Ph.D.
Chair of the Department of Chemical & Biomolecular Engineering

Approved: _____
Babatunde A. Ogunnaike, Ph.D.
Dean of the College of Engineering

Approved: _____

Ann L. Ardis, Ph.D.
Senior Vice Provost for Graduate and Professional Education

ACKNOWLEDGMENTS

iv

TABLE OF CONTENTS

LIST OF TABLES

LIST OF FIGURES

ABSTRACT

Amphiphilic block copolymers, consisting of covalently attached hydrophobic and hydrophilic polymer blocks, can self-assemble into spherical micelles in aqueous solution. Block copolymer micelles can solubilize molecules for use as nanocarriers in applications of drug delivery, catalysis, and self-healing materials. Guest exchange dynamics are known to affect the stability, performance and lifetime of the nanocarriers, so thorough understanding of this process is critical. This work first explores the encapsulation of cyanine3 (Cy3) alkyne and BHQ-2 amidite dyes by poly(1,4-butadiene-*b*-ethylene oxide) (PB-PEO) micelles in aqueous solution using dynamic light scattering, UV-Vis spectroscopy, and fluorescence spectroscopy. The highly hydrophobic BHQ-2 amidite molecules were stably encapsulated within the micelles. Cyanine3 alkyne molecules were found to be less hydrophobic and could migrate out of the PB-PEO micelles into the aqueous solution. Additionally, this work investigates the guest exchange mechanism with fluorescence resonance energy transfer. Apparent guest exchange occurred within one minute under quiescent and magnetically stirred conditions. Multiple hypotheses were examined but no conclusive theory could be presented as to why this effect occurred. Vortex mixing induced significant guest exchange compared to quiescent and magnetically stirred conditions. Within 2 to 5 min, complete guest exchange had occurred. This time frame was found to be in concurrence with theoretical estimates of a guest exchange process mediated through the air-water interface.

Chapter 1

INTRODUCTION

Amphiphilic block copolymers are made up of hydrophobic and hydrophilic polymer blocks, which are covalently attached.[1,2] In aqueous solution, block copolymers can self-assemble into various nanostructures, such as spherical micelles, cylindrical micelles or vesicles.[2,3] These micelles are very similar to their low molecular weight surfactant micelle counterparts but have several advantages including a lower critical micelle concentration (CMC), the possibility to modify the size or chemical nature, a higher stability, etc.[1,2,4]

Like surfactant micelles, amphiphilic block copolymer micelles can solubilize hydrophobic molecules and increase their solubility in aqueous solution significantly.[5-8] This property is very useful for applications in the field of drug delivery, where micelles can be used as vehicles of hydrophobic drugs. Currently, many molecules developed for pharmaceutical use are poorly soluble in water: this is true of approximately 40% of market-approved drugs and almost 90% of all drugs in development.[9] In this regard, new techniques, such as polymeric nanocarriers, are developed to provide a solution to this solubility problem. Therefore, it is of crucial importance that the properties and behavior of amphiphilic block copolymers in solution are well understood.

Many applications of polymer nanocarriers require the encapsulation of cargoes, including drug delivery, catalysis, and self-healing materials.[10] The stability, performance and lifetime of the nanocarriers are dependent upon the guest exchange

dynamics, and in a broader sense, upon the molecular chain exchange dynamics.[10,11] It is therefore important to understand these dynamic processes thoroughly.

The first part of this chapter (1.1) includes an introduction into block copolymers, their self-assembly into micelles in solution, and techniques or theories that are used to characterize or predict these micelle characteristics. Finally, some applications of block copolymers and their micelles are discussed. In part two of the introductory chapter (1.2), the solubilization of (hydrophobic) molecules and the advantages of block copolymers for drug delivery are covered. The release of molecules from the polymer nanocarriers, i.e. "drug release" is covered in the third part of the first chapter (1.3). Finally, the fourth part (1.4) introduces the different mechanisms of cargo exchange between polymer micelles.

1.1 Block copolymer micelles

1.1.1 Block copolymers

In general, a block copolymer consists of multiple, covalently bonded, polymer chains of different chemistries.[1,2] The most common is a linear diblock copolymer, which consists of two covalently bonded polymers of different composition. It is often represented as an AB diblock copolymer, with A and B representing the two chemically distinct blocks.[2]

Controlled polymerization techniques like anionic and living radical polymerization are most commonly used to synthesize block copolymers because they provide a lot of control over the composition, molecular weight and architecture of the block copolymer.[2,3] The two segments of a block copolymer are usually immiscible, which can result in microphase separation in bulk or in solution.[2-4] Complete phase

separation is not possible because the blocks are covalently bonded, resulting in the formation of self-assembled nanostructures with sizes that range from 10 to 100 nm.[4]

Block copolymers can be classified into different categories depending on their solubility in water: amphiphilic, double hydrophobic or double hydrophilic.[2] Amphiphilic diblock copolymers consist of a hydrophobic block and a hydrophilic block. Three types of these amphiphilic block copolymers exist: non-ionic, anionic and cationic block copolymers.[1] Here, the focus will be on non-ionic amphiphilic block copolymers.

1.1.2 Micellization

Block copolymers can form nanostructures by self-assembly in a selective solvent, as they also can in bulk.[2] This self-assembly in solution occurs when the solution is a thermodynamically good solvent for one block and a precipitant (poor solvent) for the other block.[3] Nanostructures formed by self-assembled block copolymers in solution can organize into many different morphologies; for example: spherical micelles, cylindrical micelles, vesicles, etc. [2,3]

When, at a fixed temperature, block copolymers are dissolved in a selective solvent, micelles form when the concentration is higher than the CMC.[1,3] Once the CMC is reached, the additional block copolymer unimers undergo a closed association process or "self-assembly" to form micelles.[1] A dynamic equilibrium exists between the micelles and unimers in solution, which means chains are constantly exchanged between the micelle and the bulk solution.[7] The concentration of unimers in solution remains the same (i.e. equal to the CMC) when the concentration of block copolymer is increased above the CMC, while the number of micelles increases with concentration.[4,7]

A micelle consists of a core and an outer shell or corona. The insoluble blocks will aggregate into a more or less swollen core.[3,4] Around this core, the corona will be formed by the chains that are soluble in the selective solvent. [3,4] Two structural types of micelles exist: "star-like" and "crew-cut" micelles (Figure 1.1). Star-like micelles have a smaller core and larger corona than crew-cut micelles, due to the hydrophillic chains of the block copolymer being much longer than the hydrophobic chains. [Mai, p. 5972], [Gohy, p. 75]

(a) (b)
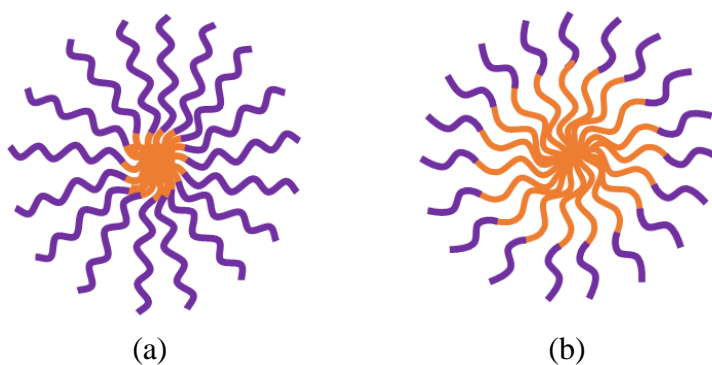
Figure 1.1: Depending on the relative chain lengths of the blocks in a block copolymer micelle, star-like (a) or crew-cut (b) micelles are obtained. This figure was used with permission from Laurens Heusele.

For amphiphilic block copolymers, the selective solvent is usually water. The hydrophobic blocks will form the core and the hydrophilic blocks will form the corona. Due to these coronal hydrophilic chains, the micelles are soluble in water. The hydrophobic core can encapsulate hydrophobic molecules and hence solubilize these molecules which are otherwise often insoluble.[1,2]

The driving force for self-assembly is the minimization of the Gibbs free energy.[7] In this specific case of block copolymer micelles in aqueous solution, the dominant driving force it is the hydrophobic effect, an entropic effect.[1,7] In this effect, the enthalpy is decreased when the hydrophobic blocks are arranged in the micelle core due to the removal of unfavorable interactions between hydrophobic chains and water molecules.[2] The configurational entropy of the block copolymer chains has a contrary effect, as it is less favorable for chains to be arranged in the micelle versus being unrestricted in solution.[2] However, the main contribution to the Gibbs free energy is the increase in entropy of the solution due to the hydrophobic effect. Because water molecules arrange in "cage-like" structures around the hydrophobic blocks, there is a large increase in entropy of these molecules once the hydrophobic blocks are shielded by the hydrophilic blocks when arranged in micelles.[2,7]

In short, attractive forces between the hydrophobic chains lead to the aggregation of these chains.[3] The repulsive forces between the hydrophilic chains in a micelle result in a certain equilibrium size for the micelle and their interactions with the solvent are responsible for the stabilization of the micelle.[1,3,12]

It is worth noting that this situation of block copolymer micellization in aqueous medium is quite different from the micellization of block copolymers in organic medium, which is a process dominated by the enthalpic contribution to the Gibbs free energy.[1]

1.1.3   Micelle characteristics and characterization

1.1.3.1   Critical Micelle Concentration (CMC)

Micellization is characterized by the CMC, at which point micelles are formed in a solution of surfactants.[1,3] The CMC of block copolymers is much lower than for conventional low molecular weight surfactants.[1,4] The low CMC, on top of the fact that block copolymer micelles take a long time to equilibrate due to lower diffusion coefficients, makes the determination of the CMC more complicated than for low MW surfactants.[1] Surface tension measurements are most often used to determine the CMC of low MW surfactants and block copolymers.[4,7] However, scattering techniques, fluorescent techniques or other methods monitoring certain physical properties of the solution like the osmotic pressure can also be utilized.[4,7] The value of the CMC can be dependent upon which technique is used to obtain it.[4] CMC measurements might also be complicated by "kinetically frozen" micelles.[1] These "frozen micelles" are a result of block copolymers consisting of a core-forming (insoluble) block with a high glass transition temperature (T_g) or a large insoluble block. Due to their glassy core, these micelles do not exhibit unimer-micelle exchange in solution and do not reach unimer-micelle equilibrium.[1,3,4] A common example of a block copolymer that forms frozen micelles is PS-PEO due to the high glass transition temperature of the PS polymer block.[4]

1.1.3.2   Morphology

The morphology which self-assembled block copolymers adopt in solution depends primarily on the inherent molecular curvature of the block copolymer chains stemming from the relative sizes of the soluble and insoluble blocks.[3] The relative sizes of the soluble and insoluble blocks can be described by the critical packing

parameter, or simply called the packing factor.[3] This packing factor indicates the most likely morphology of self-assembled block copolymer nanostructures in solution.[2,3,7] The packing parameter was initially introduced for surfactants, but it can also be used in the case of amphiphilic block copolymers as they are so similar.[2,3] This packing factor (p) is determined by the following equation:[2,3,7,12]

$$p = \frac{v}{a_0 \, l_c} \tag{1.1}$$

The volume and the maximum possible length of the insoluble (hydrophobic) segment/chain are denoted by v and l_c, respectively. The optimal surface area of the insoluble (hydrophobic) block at the interface of both blocks is denoted by a_0.

The value of the packing factor determines which block copolymer nanostructures are formed, in bulk as well as in solution (Figure 1.2).[2] When the packing factor is smaller than 1/3, spheres or spherical micelles are formed. If it is between 1/3 and 1/2, cylinders or cylindrical micelles are formed, while between 1/2 and 1, the morphology consists of flexible lamellae or bilayers, or vesicles (polymersomes). In the case of planar lamellae or bilayers, the packing factor is equal to 1 and if it is larger, the structures are inverted.[2,3,7,12]
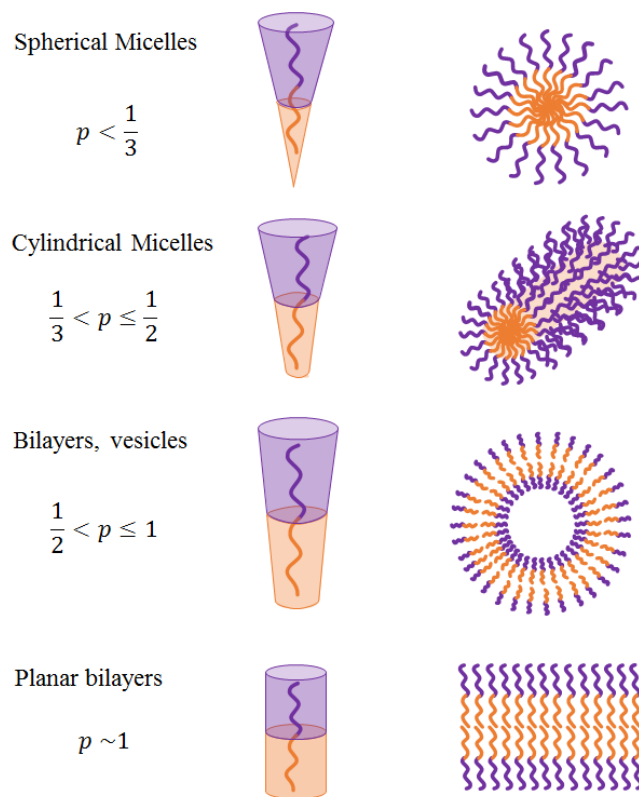
Figure 1.2:   The value of the packing factor determines which block copolymer nanostructures are formed in solution. Different packing factors lead to different morphologies, which include spherical micelles, cylindrical micelles, bilayers or vesicles, and planar bilayers. This figure was used with permission from Laurens Heusele.

To characterize the morphology of block copolymer micelles, many different methods and technologies exist, such as conventional transmission electron microscopy (TEM) or cryo-TEM, atomic force microscopy (AFM), small angle neutron and X-ray scattering (SANS and SAXS), etc.[1,4] A detailed look into all of the characterization methods for block copolymer micelles is beyond the scope of this thesis, but good summaries can be found elsewhere. Riess, for example, gives a

summary of these characterization methods and their applications.[1] Gohy explains the characterization methods in detail and enumerates their advantages and limitations.[4]

1.1.3.3   Size

The size of the (spherical) micelles is usually obtained with Dynamic Light Scattering (DLS).[1] DLS determines the hydrodynamic radius (R_h) of the micelles.[1,4] More detailed information on DLS can be found in chapter 2 (section 2.3.1). The sizes of micelles usually range from 10 nm to 100 nm.[1,4] Static Light Scattering (SLS) gives different information than DLS: instead of providing the hydrodynamic radius, it delivers the radius of gyration (R_g). The R_g/R_h ratio allows determination of the compactness and shapes of nanoparticles; a ratio of about 0.78 indicates spherical particles.[13]

1.1.4   Theories to predict micelle characteristics

Several theories exist to predict micelle characteristics like the (hydrodynamic) radius $R_{(h)}$, radius of the core R_c, thickness of the corona L, CMC, aggregation number Z, etc.[1,4] These micelle characteristics are then presented as a function of the characteristics of the block copolymer, like the composition (N_A and N_B for diblock copolymers) and molecular weight.[1,4] The two main theories used are based on scaling concepts and mean-field theories.[1,4]

Both theories use the concept of minimization of the free energy to obtain the micelle characteristics. The total free energy of the micelle system has contributions from the free energy of the micelle ($G_{micelle}$), the mixing of free block copolymers and solvent (G_{mix}), and a translational entropy term (TS_m).[14] A "pseudo-phase" approximation can be made when the interfacial energy is large, so that large micelles

9

(i.e. large aggregation number Z >> 1) and little free block copolymer chains are present (i.e. small CMC).[14] For dilute conditions (polymer volume fraction φ < 0.01), the total free energy is approximately equal to the free energy of the micelle.[14]

The basic concept of the scaling and mean-field theories is the minimization of this Gibbs free energy of the micelle. The free energy of the micelle can be subdivided into contributions from the core (G_{core}), the corona (G_{corona}), and the core/corona interface ($G_{interface}$):[1,14]

$$G_{micelle} = G_{core} + G_{corona} + G_{interface} \qquad (1.2)$$

The correlations between the characteristics of the block copolymer and the micelle are obtained by minimizing these contributions to the Gibbs free energy of the micelle with respect to the micelle parameters.[1,14]

For scaling theories usually AB diblock copolymers are considered with B being the hydrophobic block that forms the core of the micelle.[1] Different correlations are obtained for star-like (or hairy) micelles versus crew-cut micelles.[1,4] For star-like micelles (in good solvents), i.e. when $N_B < N_A$, the radius of the micelle R scales with $N_A^{3/5} Z^{1/5}$. The aggregation number Z scales with $N_B^{4/5}$, which means that in terms of the composition of the block copolymer, the radius of the micelles scales as $R \sim N_A^{3/5} N_B^{4/25}$. For crew-cut micelles ($N_A < N_B$) the core radius scales as $R_c \sim \gamma^{1/3} N_B^{2/3} a$ and the aggregation number Z scales with γN_A.[1] The interfacial tension between the A and B blocks is denoted by γ. In scaling theories, the segment length a is introduced to simplify the system ("coarse-grained" approach).[14]

There are some limitations with these simpler scaling theories: 1) they can only be used for long chains in good solvents and 2) nor finite chain effects, nor polymer-solvent interactions are considered.[1,4] Only correlations are obtained with scaling

theories, therefore only trends and no absolute values are predicted for the micelle characteristics.[1] Mean-field theories, however, can be used to calculate structural properties of micelles in solution.[14] When correlations based on mean-field theories are obtained, most are specifically for one type of block copolymer, like PS-PB or PPO-PEO.[15-18] Mean-field theories are only applicable for systems which are relatively homogeneous and have weak interactions.[14]

Apart from theoretical models, computer simulations are also generated to obtain a prediction of the micelle characteristics. To study self-assembly of block copolymers, Monte Carlo simulations have been used by several authors.[1] Scaling and mean-field theories have several advantages, for example the fast numerical results, but also include assumptions and approximations.[1] Computer simulations need a lot of computational power and time for longer polymers, but are able to obtain results without having to use as many assumptions or approximations.[1]

1.1.5   Applications of block copolymer micelles

Due to their similarity with low molecular weight surfactants, non-self-assembled (amphiphilic) block copolymers can be used for surface activity: as dispersants, emulsifiers, wetting agents, foam stabilizers, flocculants, demulsifiers, etc.[1] Block copolymer micelles are used in very diverse fields, like biomedicine, biomaterials, catalysis, micro-/photo-electronics, etc.[1-4]

In the biomedical field, block copolymers are used as biomaterials for applications such as implants and drug delivery systems (e.g. drug carriers for gene therapy).[1] Block copolymer micelles are used as nanoreactors, with one application being the preparation of colloidal metal particles.[1,4]

1.2   Loading of micelles with (hydrophobic) molecules

1.2.1   Block copolymer micelles for drug delivery

One of the most important applications of self-assembled block copolymers in a selective solvent is their use as vehicles for drug delivery because these soft systems are flexible, i.e. their properties can be tailored, and many block copolymers are also biocompatible.[7] The ultimate goal is to improve drug delivery by having improved drug targeting/delivery and reduced toxicity.[6,7] This goal can be achieved by encapsulation, as the drug itself can be more easily dissolved and either the drug is protected from a harmful external environment or tissues are protected against a harmful drug until it reaches its target destination.[7] At the same time, therapeutic activity, biocompatibility and safety have to be maintained.[7]

Amphiphilic micelles are able to solubilize hydrophobic substances in their (hydrophobic) core.[1,6,7] This physical entrapment has been shown to lead to a large increase in aqueous solubility of hydrophobic drugs, of up to 30,000-fold.[5-8] An estimated 40% of new small molecule drug candidates fail further development, mainly due to poor aqueous solubility.[6,19,20] Therefore, it is extremely important to find ways to increase the solubilization of drug compounds.

1.2.2   Solubilization

1.2.2.1   Introduction

As per definition, (micellar) solubilization is the incorporation of a component, the solute, into or onto micelles.[21] The block making up the core of the micelle is insoluble in the selective solvent and will provide a microenvironment for the solute.[17]

The goal is to enhance the solubility of the solute, which is usually a hydrophobic drug in the specific case of drug delivery.[1,22]

In general, there are two causes of insolubility of a molecule: limited ability to form hydrogen bonds or a high lattice energy. Hydrophobic molecules are limited in their ability to form hydrogen bonds and are thus not soluble in water.[19] When in the solid state, molecules with a high lattice energy do not break apart easily, causing the molecules to stay in an aggregated state instead of dissolving.[19] For molecules to be soluble in water, they must compete with clusters of water molecules that are tightly linked by hydrogen bonds.[19] Competition with this strong hydrogen bond network of water is possible in two ways: reduction of the lattice energy by modification of the solid phase (i.e. lower melting point) or disruption of hydrogen bonds by changing the drug delivery method.[19] Many drug molecules are hydrophobic, so the primary reason for insolubility is their limited ability to form hydrogen bonds. To overcome this insolubility, they can be incorporated into amphiphilic block copolymer micelles of which the hydrophilic corona chains are able to break up the hydrogen bond network of water.

The most common (thermodynamic) parameter describing solubilization is the micelle – water partition equilibrium coefficient.[1,22] The partition coefficient is defined as the ratio of the mole fractions of the solute in the micelle (X_m) and in the aqueous phase (X_w).[1,22] The mole fraction of the solute in the micelle (X_m) is related to another commonly used parameter, the molar solubilization ratio (MSR) through the equation:[22]

$$X_m = \frac{MSR}{1+MSR} \tag{1.3}$$

The MSR is the ratio of the number of solute molecules encapsulated by the micelle and the number of molecules that make up the micelle.[22] Closely related, and effectively expressing the same, is the solubilization capacity. The solubilization capacity is the volume fraction, mass fraction or number of moles of the solute in the core of the micelle per gram of hydrophobic block.[1]

1.2.2.2   Thermodynamics of solubilization

What follows is a short introduction to the theory of solubilization of low molecular weight compounds in spherical block copolymer micelles formed in a selective solvent. This theory is the work of Nagarajan and Ganesh (1989) and Nagarajan (1996).[17,22] The system is considered to be a multicomponent solution, consisting of solvent molecules, micelles encapsulating solute molecules, and free solute molecules. The micelles may be polydisperse in size and in amount of solute molecules it encapsulates. To obtain the distribution of the micelle size and composition at equilibrium, the free energy of solubilization is minimized.

Depending on which model is used for the system entropy, different expressions for micelle size and for the composition distribution equation are obtained. When the ideal solution model is used for the system entropy, the micelle size and composition distribution equation is:

$$X_{gj} = X_1{}^g\, X_{1J}{}^j\, \exp\left[-\frac{\mu^0{}_{gj} - g\mu^0{}_1 - j\mu^0{}_{1J}}{kT}\right] \qquad (1.4)$$

In this equation, X_{gj} denotes the mole fraction of a micelle with g block copolymer molecules and j solute molecules, X_1 denotes the mole fraction concentration of the singly dispersed block copolymer molecules, and X_{1J} is the mole fraction of the singly dispersed solute molecules. The standard chemical potentials of the singly dispersed

copolymer, the singly dispersed solute, the micelles, and the solvent are denoted as μ°_1, μ°_{1J}, μ°_{gj} and μ°_s. The Boltzmann constant is denoted as k and the temperature of the system as T. This equation is valid for dilute solutions, for which intermicellar interactions are not important.

When the system entropy is written in terms of the Flory-Huggins model, the micelle size and composition distribution equation is:

$$\phi_{gj} = \phi_1{}^g\, \phi_{1J}{}^j \exp(g+j-1) \exp\left[-\frac{\mu^0{}_{gj}-g\mu^0{}_1-j\mu^0{}_{1J}}{kT}\right] \tag{1.5}$$

The volume fractions of the micelles, the singly dispersed copolymer, and the singly dispersed solute in solution are denoted as ϕ_{gj}, ϕ_1 and ϕ_{1J}, respectively. Again, this equation does not account for interactions between micelles and is thus valid for dilute solutions.

Only the CMC depends on the choice of model for the system entropy. The micellar size parameters do not and can thus be derived from either equation. A convenient simplification that is often used is the "pseudo-phase" approximation. This approximation presents the solute encapsulating micelle as a pseudo-phase in equilibrium with the singly dispersed solute and copolymer molecules. For systems with a narrow dispersity, this simplification gives practically the same results as the detailed size distribution equations. Following the pseudo-phase approximation, the equilibrium characteristics are obtained from two conditions:

$$\frac{\partial}{\partial g}\left(\frac{\frac{\mu^0{}_{gj}}{g}-\mu^0{}_1-\frac{j}{g}\,\mu^*{}_{1J}}{kT}\right) = \frac{\partial}{\partial g}\left(\frac{\Delta\mu^0{}_g}{kT}\right) = 0 \tag{1.6}$$

$$\frac{\partial}{\partial j}\left(\frac{\Delta\mu^0{}_g}{kT}\right) = 0 \tag{1.7}$$

The term $\Delta\mu^0{}_g$ represents the free energy of solubilization, i.e. the change in the reference state free energy when a singly dispersed block copolymer in solution and j/g solute molecules in their pure phase are transferred into a micelle in the solution. The structural properties of the micelle are determined by the dependence of this free energy difference on the variables j and g.

The free energy of solubilization $\Delta\mu^\circ{}_g$ consists of several contributions: the change in state of dilution $(\mu^\circ{}_g)_{dil}$ and the change in state of deformation $(\mu^\circ{}_g)_{def}$ of both blocks, the localization of the copolymer molecule $(\mu^\circ{}_g)_{loc}$, and the free energy of formation of the micellar core-solvent interface $(\mu^\circ{}_g)_{int}$:

$$\Delta\mu^0{}_g = \left(\Delta\mu^0{}_g\right)_{A,dil} + \left(\Delta\mu^0{}_g\right)_{B,dil} + \left(\Delta\mu^0{}_g\right)_{A,def} + \left(\Delta\mu^0{}_g\right)_{B,def} + \left(\Delta\mu^0{}_g\right)_{loc} + \left(\Delta\mu^0{}_g\right)_{int} \tag{1.8}$$

A concise explanation of the meaning of the different contributions to the free energy of solubilization is introduced here. No equations will be given, as they can be found in Nagarajan and Ganesh's work.[17] It is assumed that the concentrations in the core and in the shell of the micelle are uniform and that the deformation of the chains are characterized by uniform stretching along the length of the chain.

The free energy of mixing or dilution of the A block $(\mu^\circ{}_g)_{A,dil}$ is due to the change in state of the A block when transferred from the solvent into the micelle core. In the singly dispersed state, the A block is insoluble and therefore in a collapsed state, with some entrapped solvent molecules, so its interactions with the solvent are minimized. When the micelle is formed, the A block is confined to the micellar core, swollen by the solute. Similarly, the change in state of dilution of the soluble B block $(\mu^\circ{}_g)_{B,dil}$ is due to the B block being transferred from the singly dispersed state in solution into the corona or shell of the micelle.

The free energy of deformation of block A, $(\mu^{\circ}_g)_{A,\,def}$ is the change in state of chain deformation (or packing) of the A block when transferred from the singly dispersed state in solution to the micelle core. The initially unperturbed end-to-end distance of the A block changes when the A block is transferred into the micelle core, where it is stretched over a length equal to the core radius R of the micelle. The free energy of chain deformation (or packing) of the B block in the micelle corona, $(\mu^{\circ}_g)_{B,\,def}$, is almost completely analogous to the change in state of deformation of block A, with the exception that the B block is stretched over a length equal to the shell thickness D of the micelle.

In the micelle, an interfacial region exists between the core, consisting of A block and solute molecules, and the corona, consisting of B block and solvent molecules. The free energy of the formation of this micellar core – solvent interface is denoted by $(\mu^{\circ}_g)_{int}$. When block copolymer molecules are arranged into micelles, the bond between both blocks of the copolymer can now only be localized in the interfacial region. A reduction in conformational entropy ensues, which results in the localization free energy, $(\mu^{\circ}_g)_{loc}$.

The free energy calculations show that solute molecules are fully dispersed within the micelle core where all solute molecules interact with the insoluble core blocks, rather than micelles with a "solute pool" in their core. It is for this type of system that Nagarajan and Ganesh developed their theory of solubilization of low molecular weight compounds in spherical micelles and the subsequent equations leading to the structural properties of the micelle.

1.2.3 Advantage of block copolymer micelles for drug delivery

Many different systems have been developed for use in drug delivery, such as liposomes, nanogels, nanoparticles, and polymeric micelles.[23] Liposomes are the most well-characterized and well-established drug delivery vehicles.[24] Liposomes are known to be the most effective for the delivery of amphiphilic molecules.[24] Even though they are also capable of solubilizing highly hydrophobic compounds, the release of these compounds is quite fast after administration because they tend to be incorporated within the lipid bilayer of the liposome vesicles.[6] Amphiphilic block copolymers that form micelles in water are thus one of the most promising materials for the delivery of hydrophobic drugs.[6] They have a unique core-shell structure; the hydrophobic chains make up the core and the hydrophilic segments make up the corona or shell.

As discussed earlier, the hydrophobic core can encapsulate hydrophobic molecules like drugs.[7,23] This solubilization effect can increase the solubility of drugs significantly, even up to 30,000-fold.[5-8] Solubilization of drugs can also offer control over the release rate and allow sustained release over a prolonged time, which is useful when the drug is rapidly metabolized.[7]

The hydrophilic corona acts like a tight protective shell by forming hydrogen bonds with its aqueous surroundings.[7,23] The corona protects the solubilized compounds against adverse external environments like hydrolysis and enzymatic degradation.[7,23] Hydrolysis or enzymatic degradation need to be avoided because it they pose problems with respect to the storage and *in vivo* stability of the drug-loaded micelle solution.[7] Also, the degradation products may not be well tolerated or even toxic.[7] On top of the protective property of the hydrophilic corona, it can also avoid

recognition by the reticuloendothelial systems (RES) to achieve long blood circulation of the drug-loaded micelles.[25]

The previous advantages are due to general properties of micellar systems. The use of block copolymers for drug delivery also has some specific advantages compared to micellar systems made up of molecular weight surfactants. Block copolymer micelles have tailorable sizes ranging from 10 to 100 nm.[1] The CMC of block copolymers is also much lower compared to low molecular weight surfactants:[1,4] while the CMC is 10^{-2} M to 10^{-5} M for C_{12} to C_{16} surfactants, the CMC is usually smaller than 10^{-5} M for block copolymers.[26,27] Due to this lower CMC no dissociation of micelles into unimers (micelle break-up) will occur when a formulation is diluted, such as during administration into the blood stream.[1,4] Block copolymer micelles are highly stable and durable due to their mechanical and physical properties.[2] A possibility exists to modify the chemical nature of block copolymers by end-group functionalization to increase the targeting efficiency of the nanocarriers.[1] Kinetically frozen micelles can result in longer drug retention and higher drug concentrations at the target site because these frozen micelles may stay intact, and will dissociate into unimers only slowly even when the concentration is lower than the CMC.[28] By using block copolymers, the partition coefficient and the total solubilized amount of the drug can be adjusted because these parameters are dependent upon the micelle characteristics.[17]

1.3 Drug release from micelles

Different ways exist for a drug to be released from micelles: immediate release, delayed release or drug retainment until target site is reached.[6] "Burst release" or immediate release following administration is typically not desirable. For a micelle

system to act as a drug delivery vehicle, prolonged retention of the drug inside the micelle is needed.[6] According to Lim Soo et al. the burst release effect is due to release of molecules for which the site of solubilization is the corona or the core-corona interface.[29] Usually, (non-polar) hydrophobic molecules are solubilized within the core as determined by the thermodynamic theory of solubilization of Nagarajan and Ganesh.[17] The primary site of solubilization of polar amphiphilic molecules, however, may be at the interface.[6] When block copolymers act solely as solubilizers, drug release *in vivo* might be quite rapid.[6] When block copolymer micelles retain the drug until the target site is reached, they function as true drug carriers.[6]

In vitro drug release experiments are often carried out with the dialysis method.[6] Solutions of nanocarriers loaded with drugs are dialyzed against a buffer, possibly with added components like proteins.[6] Block copolymer molecules (as unimers and micelles) are retained inside the dialysis bag, while drug molecules equilibrate with the external buffer solution.[6] During the experiment, perfect sink conditions should ideally be maintained by changing the buffer solution frequently.[6] The multilamellar vesicle (MLV)–based method is developed by Shabbits et al. to achieve a more accurate prediction of the *in vivo* drug retention properties than the dialysis method.[30] Multilamellar vesicles (MLV) are used to simulate the membrane pools found in blood cells and tissues, into which drug molecules can distribute.[30]

Release kinetics *in vitro* and *in vivo* are often drastically different.[31] In general, *in vitro* experiment are often not good enough to recreate the dynamic release mechanisms that exist *in vivo*.[31] For example, the rate of drug release is underestimated and the stability of the formulation is overestimated by *in vitro* studies using the dialysis approach.[30] *In vitro* experiments are still very useful because they

are much easier and cheaper to carry out than the financially and practically challenging *in vivo* experiments.[31] *In vitro* experiments can be a first step to obtain some initial information before moving on to more advanced experiments with *in vivo* methods.[31]

The *in vivo* fate of nanocarriers is often dependent upon proteins.[6] A process called "opsonization" can occur: proteins adsorb to surface of the drug delivery vehicle which is then cleared from the bloodstream by the RES, i.e. by macrophages.[6,32] Proteins may also extract the drug out of the nanocarrier. This protein extraction happens primarily if the drug has a high binding affinity for serum (blood) protein.[6] When the nanocarrier is delivered to the site of interest (target site), it acts as a true drug carrier.[6] Protein adsorption to the surface of the nanocarrier can occur within a few minutes following administration and especially happens if the nanocarrier has a charged or hydrophobic surface.[6,33]

Different techniques exist for controlled release of drugs from nanocarriers: ultrasound-triggered[34], pH-triggered[35], and photo/temperature-triggered[36] drug release have been reported.

1.4 Exchange of solubilized molecules between micelles

Not only drug loading (solubilization) in micelles and drug release from micelles are crucial processes, drug exchange between micelles is also an important factor. This cargo exchange, or guest exchange, is the most direct and rigorous indicator of encapsulation stability, according to Li and Thayumanavan.[10] The encapsulation stability is a critical parameter for the design of nanocontainers, as a drug delivery vehicle ideally has to encapsulate the drug until it is released at its target site.[10]

Three different mechanisms for guest exchange exist: collision-based, diffusion-based, and fission-based (Figure 1.3).
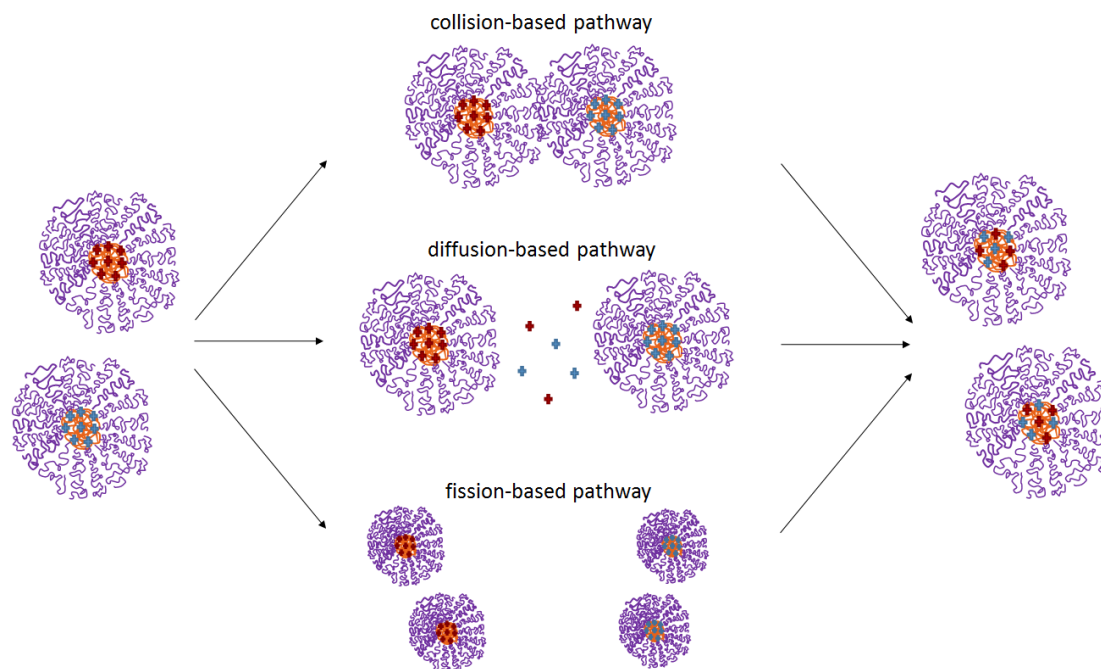
Figure 1.3: Exchange of solubilized molecules between micelles can occur through different mechanisms: collision-based, diffusion-based or fission-based pathways.

1.4.1 Collision-based pathway

In the collision-based mechanism (collision-exchange-separation mechanism) exchange will only happen due to collision between micelles, and the rate of this process depends mostly on the effective collision frequency.[10] A strong positive correlation between micelle concentration and collision frequency is expected.[10] The collision frequency will also be dependent upon the size of the micelles: following the

Einstein-Stokes equation, it usually decreases with increasing size due to slower diffusion.[10]
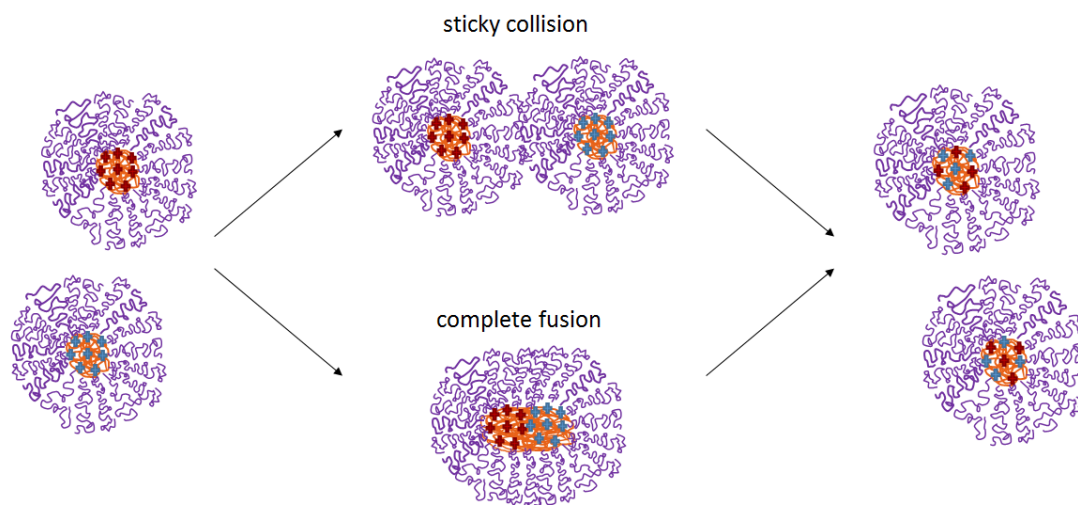
Figure 1.4: The collision-based pathway for guest exchange can occur through two different mechanisms: sticky collision or complete fusion.

Two separate mechanism have been proposed for the collision-based guest exchange pathway (Figure 1.4).[37] The first mechanism involves "sticky collision" between micelles. In this mechanism, two micelles collide and are temporarily adhered to one another. During this short time of adhesion, guest molecules are exchanged through the hydrophilic corona layer without becoming free in the solution. Whether or not the guest exchange happens through the sticky collision mechanism will depend on the adhesion ability of the micelles and the solubility of the solute in the hydrophilic block of the block copolymer. The second collision-based mechanism involves complete fusion of the two micelles. Micelles undergo fusion to form a short-lived "super-micelle" with subsequent fragmentation of the super-micelle into two

23

normal (or "proper") micelles. The super-micelle is made up of twice the number of block copolymer molecules. In this super-micelle, guest exchange happens by diffusion of the guest molecules inside the super-micelle core. The super-micelle then transforms into two normal-sized micelles through the process of fission (fragmentation).[37]

The energy barrier of the complete fusion mechanism process has at least four contributions.[37] The first contribution is the steric interaction between the hydrophilic chains: two micelle cores cannot closely approach one another due to an entropic as well as a hydration barrier provided by these hydrophilic chains. The second contribution involves energy changes within the super-micelle because it consists of twice as many block copolymer chains. The third contribution is the activation energy of the rearrangement of block copolymer chains during fusion of micelles. The fourth contribution is the barrier to diffusion of the solute throughout the core.[37] According to Rharbi and Winnik, the steric and hydration barriers (first contribution) and the barrier to accommodate twice as many block copolymer molecules in the super-micelle (second contribution) are likely the rate-limiting steps of the fusion mechanism.[37] The rates of these two processes should be independent of the solute.[37] On the contrary, the sticky collision mechanism will be dependent upon the nature of the solute due to the necessary transfer of these guest molecules across the (hydrophilic) coronas.[37] The complete fusion mechanism will not occur for strictly monodisperse micelles, because the second contribution to the energy barrier is related to the extent of micelle polydispersity.[38]

Both of the collision-based guest exchange processes exhibit second order kinetics due to two-body collision arguments.[27,37] The guest exchange rate will increase with increasing concentration of micelles.[27,37,39]

1.4.2   Diffusion-based pathway

As shown in Figure 1.3, a second possible pathway for guest exchange is the diffusion-based mechanism (exit – re-entry mechanism). A guest molecule exits the nanocarrier, diffuses through the solvent, and re-enters another nanocarrier.[10,37]

This pathway depends on ability of guest molecules to exit and enter the micelles. Diffusion-based guest exchange is a first order process: exit of the guest molecules from the micelle is rate-limiting, whereas re-entry into a micelle occurs at the diffusion–controlled rate.[37] The guest exchange rate decreases with decreasing solubility of guest molecules in the solvent, as it is less likely the guest molecules will diffuse out of the nanocarrier and into the solvent.[37] As a result, the diffusion-based pathway is unlikely when the guest molecules are very insoluble in the solvent.[37]

A less hydrophobic core can considerably decrease the ability of nanocarriers to encapsulate hydrophobic molecules. The (hydrophobic) guest molecules will thus exit nanocarriers more easily, diffuse through the solvent and be taken up by another nanocarrier. As a result, the guest exchange involving nanocarriers with less hydrophobic cores will follow the diffusion-based pathway.[10]

1.4.3   Fission-based pathway

The fission-based mechanism (fission – recombination or fragmentation – growth mechanism) is the third possible guest exchange pathway (Figure 1.3). Nanocarriers are fragmented into two smaller "sub-micelles'" and the nanocarrier

returns to its original size by fusion of different sub-micelles or by uptake of block copolymer chains.[10,37]

The fission-based pathway exhibits first order kinetics.[37] The rate-limiting step of the process is the fragmentation, due to the fast exit and entry rates of block copolymer chains from and into micelles and the usually low concentration of sub-micelles (for micelles with a low polydispersity).[37]

1.4.4 Determination of dominant pathway

As mentioned before, the collision-based mechanism is dependent upon the concentration of micelles because the concentration influences the collision frequency.[10] When experiments with different concentrations of nanocarrier are set up, the rate of guest exchange should increase with increasing concentration. The guest exchange rate would decrease with increasing micelle concentration for the diffusion-based mechanism, due to a decrease in concentration of guest molecules and, as a result, a decrease in the driving force for guest molecules to diffuse out of the micelles.[10] By conducting experiments for which the guest exchange rate can be determined for samples with different micelle concentrations, one can distinguish between a collision-based and diffusion-based mechanism. Collision-based and diffusion-based pathways also have different kinetics: the collision-based mechanism exhibits second order kinetics, while the diffusion-based mechanism is a first order process.[37]

The rate of exchange in the collision-based mechanism is also dependent upon the micelle size.[10] Experiments can be set up to determine if the collision-based mechanism is the dominant pathway for guest exchange if micelles (made up of the

same block copolymer) can be obtained with different sizes by, for example, a dependency of micelle size on the pH of the solution.[10]

Two different collision-based mechanisms have been described before: sticky collision and complete fusion (Figure 1.4).[37] In the sticky collision mechanism, the rate is dependent upon the nature of the guest molecules because these molecules have to move across the hydrophilic coronas of the two colliding micelles.[37] For the complete fusion mechanism, the rate is not dependent upon the nature of guest molecules.[37]

The diffusion-based and fission-based mechanisms both exhibit first order kinetics.[37] One can distinguish between the two pathways by comparing the observed kinetics (k_{obs}) with the expected exchange rates of these mechanisms ($k_{diffusion}$ and $k_{fission}$) for different types of guest molecules, as described by Rharbi and Winnik.[37] The exit of guest molecules from the micelles is the rate-limiting step of the diffusion-based mechanism and depends on the solubility of the guest molecules in the solvent.[37] These exit rates ($k_{diffusion}$) are much lower than the rates obtained if the dominant pathway is fission-based ($k_{fission}$).[37]

1.4.5 Relation to micelle relaxation kinetics and air-water interface

The collision-based and fission-based mechanisms are related to micelle relaxation kinetics. Usually two different relaxation times are determined in micelle relaxation experiments: fast and slow relaxation times. The fast relaxation time, which is on the order of microseconds, is associated with single chain exchange, i.e. the exit and entry of individual block copolymer chains from the micelle. The slow relaxation time for dilute solutions is associated with the overall formation (association of chains) and breakdown (dissociation of chains) of micelles.[37]

27

No chain exchange occurs for block copolymer micelles in highly selective solvents under quiescent conditions.[11] However, it has been reported that rapid vortex mixing can induce chain exchange between micelles within minutes.[11] Murphy and co-workers have demonstrated that the mixing time to achieve complete chain exchange is dependent on the polymer concentration.[11] Also, the fraction of exchanged chains varied linearly with mixing time. It was concluded from this linear relationship that the chain exchange mechanism was dependent upon the air-water interface regeneration rate and that the chain exchange rate was surface-limited. A hypothesis was proposed that chain exchange of block copolymer micelles in a highly selective solvent needed deformation and regeneration of the air-water interface. The high pressures due to the collapse of the interface would result in desorption of the block copolymer micelles from the interface. The following mechanism of chain exchange mediated by the air-water interface was proposed: block copolymer micelles adsorb to the interface, where they exchange chains and when the interface collapses they desorb from the interface into the bulk solution.[11]

1.5   Thesis overview

In this thesis, the exchange of hydrophobic dyes between polybutadiene-*b*-poly(ethylene oxide) (PB-PEO) micelles during agitation is examined. It is assumed that a type of collision-based pathway is followed as the guest exchange mechanism. A diffusion-based pathway is determined to be unlikely due to the very hydrophobic core of PB-PEO micelles. The collision-based pathway is related to chain exchange.[37] Chain exchange in PB-PEO micelles in aqueous solution under rapid vortex mixing is associated with a surface-limited process with chain exchange happening through the air-water interface.[11] Therefore, the hypothesis presented here is that exchange of the

dye molecules between PB-PEO micelles in aqueous solution during vortex mixing is also mediated through the collapse and regeneration of the air-water interface.

Chapter 2 discusses the materials and methods that are used. The properties of the polymer (PB-PEO) and dye molecules (Cy3 alkyne and BHQ-2 amidite) are introduced. Also, the different ways to prepare solutions of polymer micelles, with and without encapsulated dye molecules, are discussed. Dynamic light scattering is reviewed as a solution characterization method to obtain micelle sizes. Fluorescence resonance energy transfer (FRET) is examined as a way to characterize the guest exchange of dye molecules. Determination of the concentrations of dye molecules and polymer is done by UV-Vis absorbance.

Chapter 3 explores the encapsulation of dyes in micelles and the dye exchange between micelles. Several experimental methods were used to obtain insights in the encapsulation of dyes. Dye exchange between micelles during quiescent conditions, magnetic stirring and vortex mixing is investigated. Self-quenching of cyanine3 alkyne was observed in experiments, discussed and compared to previous experimental results.

Chapter 4 gives a summary to the results obtained in chapter 3 and suggests some possible routes for improvements of the current experiments and future work in the area of encapsulation and exchange of dyes in polymer micelles.

REFERENCES

1. Riess, G. Micellization of block copolymers. *Progress in Polymer Science*, **2003**, *28*, 1107-1170.

2. Mai, Y. Y.; Eisenberg, A. Self-assembly of block copolymers. *Chemical Society Reviews*, **2012**, *41*, 5969-5985.

3. Karayianni, M.; Pispas, S. *Self-Assembly of Amphiphilic Block Copolymers in Selective Solvents*. In *Fluorescence Studies of Polymer Containing Systems*; Prochàzka, K., Ed.; Springer Series on Fluorescence 16; Springer International Publishing: Switzerland, 2016; pp 27-63.

4. Gohy, J. F. Block Copolymer Micelles. *Advances in Polymer Science*, **2005**, *190*, 65-136.

5. Adams, M. L.; Lavasanifar, A.; Kwon, G. S. Amphiphilic block copolymers for drug delivery. *Journal of Pharmaceutical Sciences*, **2003**, *92*, 1343–1355.

6. Liu, J.; Lee, H.; Allen, C. Formulation of drugs in block copolymer micelles: drug loading and release. *Current Pharmaceutical Design*, **2006**, *12*, 4685-4701.

7. dos Santos, S.; Medronho, B.; dos Santos, T.; Antunes, F. Amphiphilic Molecules in Drug Delivery Systems. In *Drug Delivery Systems: Advanced Technologies Potentially Applicable in Personalised Treatment*; Coelho, J., Ed; Springer: Netherlands, 2013; Vol. 4, pp 35-85.

8. Nagarajan, R. Solubilization in aqueous solutions of amphiphiles. *Current Opinion in Colloid & Interface Science*, **1996**, *1*, 391–401.

9. Kalepu, S.; Nekkanti, V. Insoluble drug delivery strategies: review of recent advances and business prospects. *Acta Pharmaceutica Sinica B*, **2016**, *5*, 442–453.

10. Li, L.; Thayumanavan, S. Environment-Dependent Guest Exchange in Supramolecular Hosts. *Langmuir*, **2014**, *30*, 12384–12390.

11. Murphy, R. P.; Kelley, E. G.; Rogers, S. A.; Sullivan, M. O.; Epps, T. H. Unlocking Chain Exchange in Highly Amphiphilic Block Polymer Micellar Systems: Influence of Agitation. *ACS Macro Letters*, **2014**, *3*, 1106–1111.

12. Quémener, D.; Deratani, A.; Lecommandoux, S. Dynamic Assembly of Block-Copolymers. In *Constitutional Dynamic Chemisty.* Barboiu, M., Ed.; Topics in Current Chemistry 322; Springer-Verlag: Berlin Heidelberg, 2012; pp 165–192.

13. Bhattacharjee, S. DLS and zeta potential – What they are and what they are not? *Journal of Controlled Release*, **2016**, *235*, 337–351.

14. Lund, R.; Willner, L.; Richter, D. Kinetics of Block Copolymer Micelles Studied by Small-Angle Scattering Methods. *Advances in Polymer Science*, **2013**, *259*, 51–158.

15. Noolandi, J.; Hong, K. M. Theory of block copolymer micelles in solution. *Macromolecules*, **1983**, *16*, 1443–1448.

16. Leibler, L.; Orland, H.; Wheeler, J. C. Theory of critical micelle concentration of solutions of block copolymers. *The Journal of Chemical Physics*, **1983**, *79*, 3550–3557.

17. Nagarajan, R.; Ganesh, K. Block Copolymer Self-Assembly in Selective Solvents: Theory of Solubilization in Spherical Micelles. *Macromolecules*, **1989**, *22*, 4312–4325.

18. Hurter, P. N.; Scheutjens, J. M. H. M.; Hatton, T. A. Molecular modelling of micelle formation and solubilization in block copolymer micelles. *Macromolecules*, **1993**, *26*, 5592–5601.

19. Kipp, J. E. The role of solid nanoparticle technology in the parenteral delivery of poorly water-soluble drugs. *International Journal of Pharmaceutics*, **2004**, *284*, 109–122.

20. Prentis, R. A.; Lis, Y.; Walker, S. R. Pharmaceutical inno- vation by the seven U.K.-owned pharmaceutical companies (1964–1984). *British Journal of Clinical Pharmacology*, **1998**, *25*, 387–396.

21. Everett, D.H. Manual of Symbols and Terminology for Physicochemical Quantities and Units, Appendix II: Definitions, Terminology and Symbols in Colloid and Surface Chemistry. *Pure Appl. Chem.*, **1972**, *31*, 577-638

22. Nagarajan, R. Solubilization in aqueous solutions of amphiphiles. *Current Opinion in Colloid & Interface Science*, **1996**, *1*, 391–401.

23. Zhang, H.; Xu, J.; Xing, L.; Ji, J.; Yu, A.; Zhai, G. Self-assembled micelles based on Chondroitin sulfate/poly (d,l-lactideco-glycolide) block copolymers for doxorubicin delivery. *Journal of Colloid and Interface Science,* **2017**, *492*, 101–111.

24. Drummond D. C.; Meyer, O.; Hong, K.; Kirpotin, D. B.; Papahadjopoulos, D. Optimizing liposomes for delivery of chemotherapeutic agents to solid tumors. *Pharmacological Reviews*, **1999**, *51*, 691-743

25. Duncan, R. The dawning era of polymer therapeutics. *Nature Reviews Drug Discovery*, **2003**, *2*, 347-360.

26. Israelachvili, J. N. *Intermolecular and Surface Forces*, 3rd ed.; Academic Press: Burlington, MA, 2011

27. Murphy, R. P., Chain Exchange in Aqueous Solutions of Block Polymer Micelles. M.S. Thesis, University of Delaware, Newark, DE, 2014.

28. Kwon, G. S.; Okano, T. Polymeric micelles as new drug carriers. *Advanced Drug Delivery Reviews*, **1996**, *21*, 107–116.

29. Soo, P. L.; Luo, L., Maysinger, D.; Eisenberg, A. Incorporation and Release of Hydrophobic Probes in Biocompatible Polycaprolactone-block-poly(ethylene oxide) Micelles: Implications for Drug Delivery. *Langmuir*, **2002**, *18*, 9996–10004.

30. Shabbits, J. A.; Chiu, G. N. C.; Mayer, L. D. Development of an in vitro drug release assay that accurately predicts in vivo drug retention for liposome-based delivery systems. *Journal of Controlled Release*, **2002**, *84*, 161–170.

31. Bains, A.; Wulff, J. E.; Moffitt, M. G.; Moffitt, M. G. Microfluidic synthesis of dye-loaded polycaprolactone-block-poly (ethylene oxide) nanoparticles: Insights into flow-directed loading and in vitro release for drug delivery. *Journal of Colloid And Interface Science*, **2016**, *475*, 136–148.

32. Patel, H. M.; Moghimi, S. M. Serum-mediated recognition of liposomes by phagocytic cells of the reticuloendothelial system - The concept of tissue specificity. *Advanced Drug Delivery Reviews*, **1998**, *32*, 45-60

33. Ishihara, K.; Nomura, H.; Mihara, T.; Kurita, K.; Iwasaki, Y.; Nakabayashi, N. Why do phospholipid polymers reduce protein adsorption? *Journal of Biomedical Materials Research*, **1998**, *39*, 323–330.

34. Rapoport, N. Ultrasound-mediated micellar drug delivery. *International Journal of Hyperthermia*, **2012**, *28*, 374–385.

35. Wang, L.; Liu, G.; Wang, X.; Hu, J.; Zhang, G.; Liu, S. (). Acid-Disintegratable Polymersomes of pH-Responsive Amphiphilic Diblock Copolymers for Intracellular Drug Delivery. *Macromolecules*, **2015**, *48*, 7262–7272.

36. Yan, K.; Chen, M.; Zhou, S.; Wu, L. Self-assembly of upconversion nanoclusters with an amphiphilic copolymer for near-infrared-and temperature-triggered drug release. *RSC Advances*, **2016**, *6*, 85293–85302.

37. Rharbi, Y.; Winnik, M. A. Solute exchange between surfactant micelles by micelle fragmentation and fusion. *Advances in Colloid and Interface Science*, **2001**, *89–90*, 25–46.

38. Hall, D. G. Polydispersity of Sodium Dodecyl Sulfate (SDS) Micelles. *Langmuir*, **1999**, *15*, 3483–3485.

39. Li, Z. L.; Dormidontova, E. E. Equilibrium chain exchange kinetics in block copolymer micelle solutions by dissipative particle dynamics simulations. *Soft Matter*, **2011**, *7*, 4179-4188.

Chapter 2

MATERIALS AND METHODS

This chapter explains the materials and experimental methods used for characterizing the dye-loaded micelles and for investigating dye exchange between micelles. Section 2.1 describes the material properties of the polymer. In section 2.2 the procedure for fractionation and the polymer properties after fractionation are described, as well as the solution preparation methods for micelle and dye-loaded micelle solutions. Section 2.3 describes the characterization methods, including dynamic light scattering (DLS) to obtain the micelle sizes, fluorescence resonance energy transfer (FRET) to characterize the dye exchange process and UV-Vis spectroscopy for solution concentration determination.

2.1 Material selection and properties

The block copolymer which is used in this work is poly(butadiene-*b*-ethylene oxide) or simply PB-PEO. PB-PEO is highly amphiphilic due to the high interaction parameter of the hydrophobic polybutadiene block with water ($\chi \sim 3.5$), while the poly(ethylene oxide) block is hydrophilic.[1]

Chain exchange can be significantly influenced by glassy core dynamics.[1,2] The polybutadiene block is a 1,4-PB isomer and has a low glass transition temperature, reported to be around -77 °C or even lower.[3,4] As a result, PB-PEO micelles will have a non-glassy core.[5] Similarly, chain exchange is also significantly influenced by the core entanglements because they have an effect on the core chain

mobility.[2] The molecular weight of entanglements of 1,4-polybutadiene is predicted by calculations to be 2254 g/mol, while a value of 1815 g/mol was obtained from measurements.[6] These entanglement molecular weights are relatively low, so core entanglements should not significantly influence the chain dynamics.[1,2]

PB-PEO (P10599-BdEO) was purchased from Polymer Source Inc. (Dorval, Québec, Canada) with number-average molecular weights of 4.5 and 12.5 x 10^3 g/mol for polybutadiene and poly(ethylene oxide) blocks, respectively.[7] The dispersity (Đ) of the block copolymer was reported by Polymer Source to be equal to 1.09.[7] The degree of polymerization (N) of both blocks can be obtained from the reported molecular weights and monomer repeat unit masses (54 g/mol for PB and 44 g/mol for PEO) and is equal to 83 and 284 for the PB and the PEO blocks, respectively.

Proton nuclear magnetic resonance (^{1}H NMR) spectroscopy and size exclusion chromatography (SEC) were used to verify the structure and PDI of the block copolymer.

Ideally, the dispersity of the block copolymer is low (Đ < 1.1) such that the micelle sizes have a low polydispersity and uniform morphologies are obtained (spherical micelles).[8,9] A low dispersity (Đ = 1.09) of the PB-PEO block copolymer (P10599-BdEO) is reported by Polymer Source. However, SEC analysis of the sample indicates a severely higher value for the PDI. From the chromatograph in Figure 2.1, a dispersity Đ of 1.35 is obtained when including the tail. The long tail visible in the chromatograph is due to the presence of polybutadiene homopolymer. The PB homopolymer is (partially) removed by fractionation (see section 2.2.1). A number average molecular weight M_n of 17 x 10^3 g/mol for the block copolymer is obtained, which is the same as Polymer Source reports.
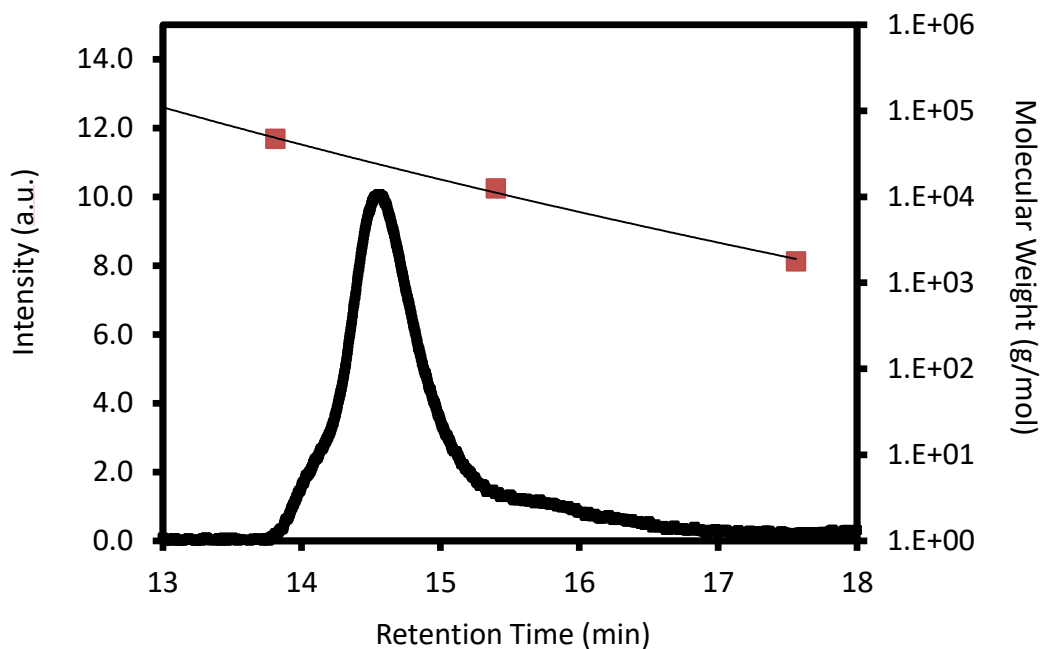
Figure 2.1:   Chromatogram of poly(butadiene-*b*-ethylene oxide), obtained with size exclusion chromatography (SEC).

The ^{1}H NMR spectrum of the PB-PEO sample is shown in Figure 2.2. As peaks due to 1,2-PB and 1,4-PB are overlapping at around 5.5 ppm and 2.0 ppm (b, e), the integral of the peak due to 1,2-PB at 5.0 ppm (a) is needed as well. Calculations based on the integration of peaks gives a PB/PEO-ratio of 25%, which is close to the 29% PB/PEO-ratio calculated based on the NMR spectrum reported by Polymer Source. The amount of 1,4-isomer in the polybutadiene is about 94%, while the Polymer Source ^{1}H NMR data indicates about 91% of the polybutadiene consists of the 1,4-isomer. Considering the uncertainty due to the manual phase and baseline correction, and the choice of integration interval, these results are fairly consistent with the characterization done by Polymer Source.
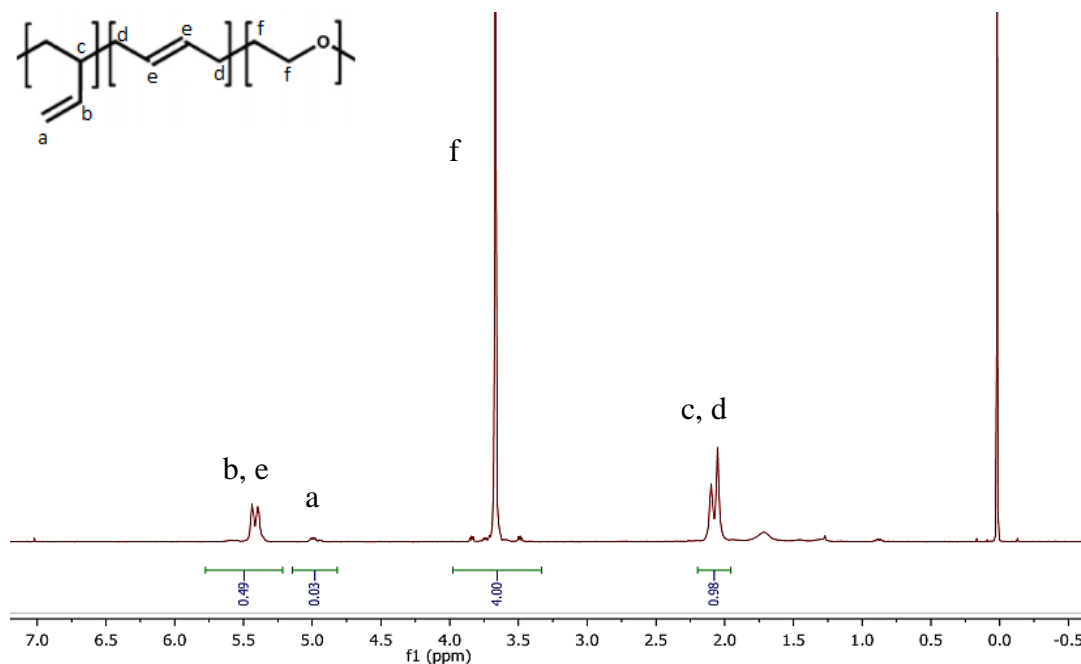
Figure 2.2:   NMR spectrum of poly(butadiene-*b*-ethylene oxide), obtained with proton nuclear magnetic resonance (^{1}H NMR) spectroscopy.

PB-PEO forms nanostructures in aqueous solution, as reported by Jain and Bates.[10] For dilute solutions (1%) of PB-PEO in water, Jain and Bates produced a phase diagram of possible morphologies for the PB-PEO nanostructures. This phase diagram (Figure 2.3, reprinted with permission from AAAS) illustrates that the morphology, including bilayer vesicles (B), networks (N), or cylindrical (C) or spherical (S) micelles, depends on the weight fraction of the hydrophilic block (w_{PEO}) and the degree of polymerization of the hydrophobic block (N_{PB}) in the block copolymer.
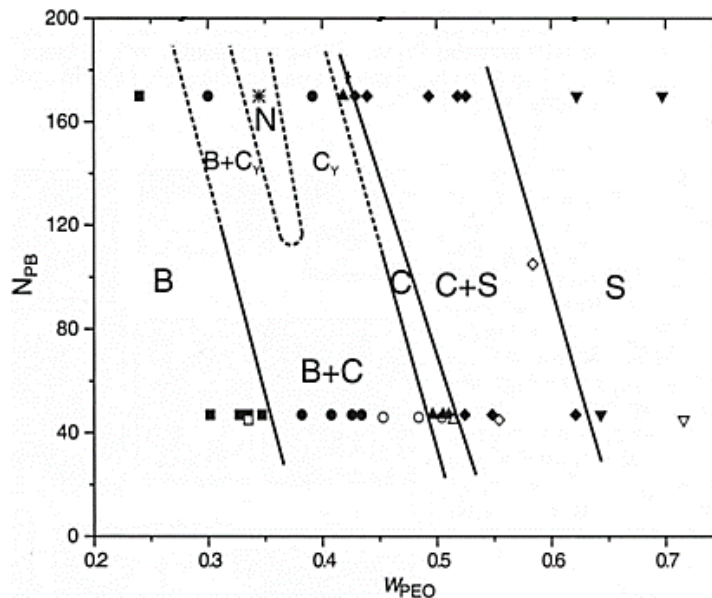
Figure 2.3:   Phase diagram for dilute (1 wt%) aqueous solutions of poly(butadiene-*b*-ethylene oxide). In solution, PB-PEO forms various morphologies including bilayer vesicles (B), cylindrical micelles (C), networks (N) and spherical micelles (S). The morphology can be controlled by the weight fraction of PEO (w_{PEO}) and the degree of polymerization of PB (N_{PB}). The figure was reproduced from Jain and Bates, *Science,* **2003**, *300*, 460–464. The figure was reprinted with permission from AAAS.

The PB-PEO block copolymer purchased from Polymer Source was chosen such that the weight fraction of PEO (w_{PEO}) and the degree of polymerization of PB (N_{PB}) would lead to the formation of spherical micelles. The combination of these two parameters ($w_{PEO} = 0.74$ and $N_{PB} = 83$) lies deeply into the region of the phase diagram where spherical micelles are obtained (Figure 2.3).

The CMC of PB-PEO is, like most block copolymers, much lower than conventional low molecular weight surfactants. Topel et al. measured the CMC of PB(1800)-*b*-PEO(4000) by fluorescence spectroscopy and dynamic light scattering (DLS) and obtained CMC values on the order of 10^{-7} mol/L (i.e. $3 \pm 1 \times 10^{-7}$ and 6 ± 2

$\times 10^{-7}$ mol/L, respectively).[11] As a comparison, a commonly used surfactant for micelle experiments is Triton X-100 and has a CMC of 0.22 x 10^{-3} mol/L, which is many orders of magnitude higher than the CMC of PB-PEO.[12]

To investigate the cargo exchange between micelles, the PB-PEO micelles are loaded with a hydrophobic fluorescent probe (Cyanine3 alkyne) and a (non-fluorescent) hydrophobic dye (BHQ-2 amidite), which acts as a quencher. Fluorescent dyes are used often as model hydrophobic probes or "drug surrogates" for block copolymer nanocarrier development.[13-17] Using fluorescent probes has several advantages. Fluorescent dye experiments can give some important *a priori* information so studies with drugs can be done with an increased time efficiency.[18] Fluorescent dyes are also available at a lower cost than some therapeutics used for drug delivery applications which increases the cost efficiency.[18] The hydrophobic dyes used are Cyanine3 alkyne, purchased from Lumiprobe Corporation (Hallandale Beach, FL, USA), and BHQ-2 amidite, purchased from LGC Biosearch Technologies (Petaluma, CA, USA). This choice of dyes will be elaborated on later (section 2.3.2.2).

Deionized water (H_2O, 18.2 MΩ resistance), purified using a Milli-Q Biocel system (Millipore), is used in all experiments requiring aqueous solutions. Other solvents used are chloroform (Fisher Scientific, Certified ACS Reagent Grade, ≥ 99.8%), tetrahydrofuran (THF, Fisher Chemical, Optima® (chromatography grade), ≥ 99.9%) , petroleum ether (Fisher Scientific, Certified ACS Reagent Grade), N,N-dimethylformamide (DMF, ACROS, chromatography grade, ≥ 99.5%), hexanes (Fisher Chemical, Certified ACS Reagent Grade, Various Methylpentanes 4.2%, ≥ 98.5%), and 1-octanol (Aldrich, chromatography grade, ≥ 99%).

2.2 Solution preparation

The different possible techniques for preparation of micelle solutions from a bulk block copolymer sample are covered in this section. Methods for loading (drug) molecules into block copolymer micelles are also discussed. Finally, the practical procedures used for the solutions employed in further experiments are provided.

2.2.1 Fractionation

Before solution preparation the polymer as received by Polymer Source is fractionated. The motivation for fractionation, the practical procedure and the resulting polymer properties after fractionation are detailed in this section.

2.2.1.1 Motivation

Size exclusion chromatography (SEC) of the PB-PEO block copolymer purchased from Polymer Source indicated that the dispersity was higher (1.35) than the value reported by Polymer Source (1.09). This higher dispersity was mainly due to a long tail visible in the chromatogram (Figure 2.1), with a molecular weight corresponding to polybutadiene (PB) homopolymer. Hydrophobic impurities, like trace amounts of initiator or homopolymer, could have a strong influence on the micellization process.[19] The PB homopolymer can therefore have unwanted effects on experiments involving micelles. Most importantly for experiments involving solubilization of compounds and cargo exchange of these compounds between micelles, is the possibility of homopolymers to be solubilized to some extent.[20,21] Because PB is hydrophobic, it will be captured in the hydrophobic PB cores of the micelles and could interact with other solubilized compounds in the core. Additionally, homopolymer solubilization can also affect the size of the block copolymer micelles.[21] It has been demonstrated that the presence of homopolymer,

albeit the soluble block homopolymer, has an effect on the chain exchange kinetics: corona block homopolymer retards this process.[22] It is obvious that the amount of PB homopolymer present in the sample should be minimized. The removal of PB homopolymer can be done by fractionation of the block copolymer sample.

2.2.1.2 Procedure

The first step in the fractionation process was making a concentrated solution of the polymer. PB-PEO was dissolved in THF (223 mg/mL) because it is a good solvent for the polymer.[23] This solution was added drop-wise to a large excess volume (about 5:1 ratio) of petroleum ether. Petroleum ether was chosen due to the limited solubility of PB-PEO and good solubility of PB in this solvent. Hexanes solvent did not produce as much precipitation and was therefore discarded after an initial test run. PB-PEO precipitated in the petroleum ether, while the PB homopolymer dissolved and thus separated from the PB-PEO block copolymer. The solution was centrifuged and the supernatant was decanted off to obtain a semi-dry sample. Finally, the polymer was dried using vacuum to remove all remaining petroleum ether solvent.

2.2.1.3 Polymer properties after fractionation

A yield of 71% PB-PEO was obtained after the fractionation procedure. Due to the removal of PB homopolymer, the material properties of the polymer changed. A new SEC and ^{1}H NMR analysis on the fractionated polymer sample resulted in the chromatograph of Figure 2.4 and the ^{1}H NMR spectrum of Figure 2.5.

From the chromatogram (Figure 2.4), it is clear that the tail due to the presence of the PB homopolymer has been almost completely removed. A small shoulder to the right of the main peak indicates some additional high molecular weight compounds

41

are present in the sample after fractionation. Most likely, this high molecular weight compound consists of cross-linked PB-PEO chains. The number average molecular weight increased to 24 x 10^3 g/mol, due to the removal of the low molecular weight PB homopolymer and the increased amount of cross-linked chains. The dispersity Đ of the fractionated sample decreased from 1.35 to 1.30.
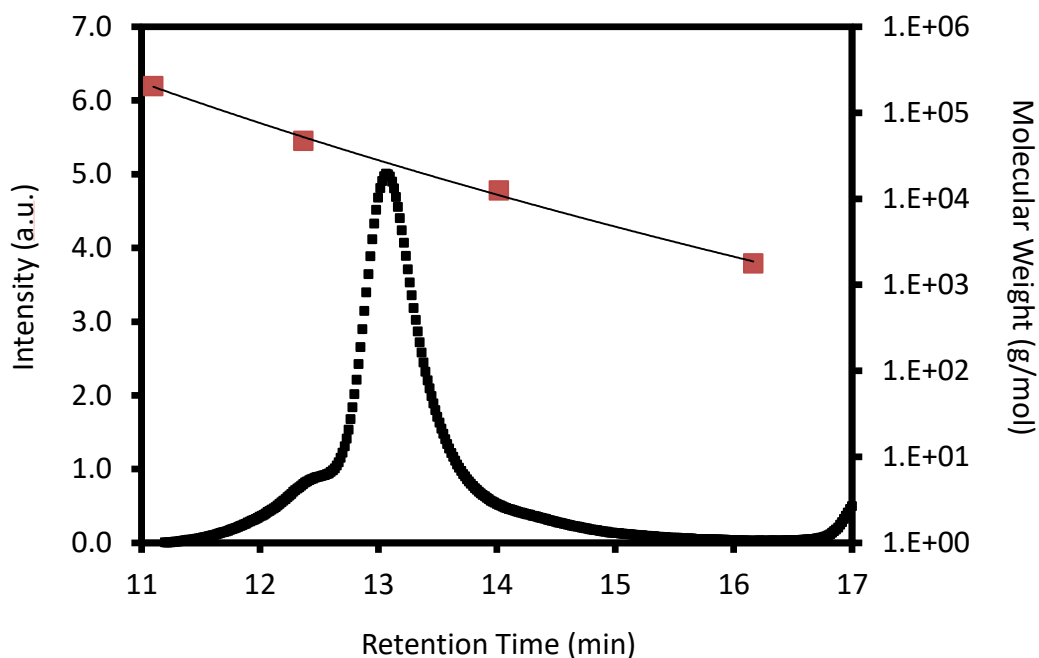
Figure 2.4:   Chromatogram of fractionated poly(butadiene-*b*-ethylene oxide), obtained with size exclusion chromatography (SEC).

The ^{1}H NMR spectrum (Figure 2.5) confirms that the amount of polybutadiene in the sample has decreased. The ratio of PB to PEO is 22% compared to 25% before fractionation and 29% PB/PEO-ratio obtained from the ^{1}H NMR spectrum reported by

Polymer Source. The 1,4-isomer accounts for 93% of the polybutadiene, compared to 94% before fractionation and 91% based on Polymer Source data.
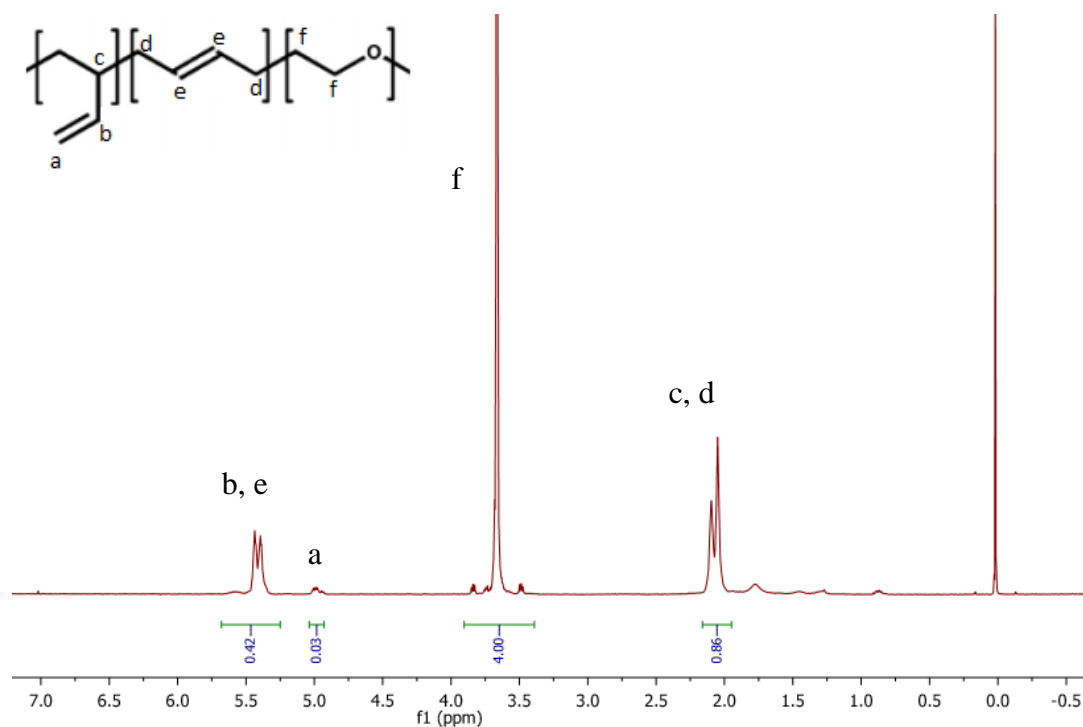

Figure 2.5:   NMR spectrum of fractionated poly(butadiene-*b*-ethylene oxide), obtained with proton nuclear magnetic resonance (^{1}H NMR) spectroscopy.

2.2.2   Micelle preparation techniques

Several different methods exist for the preparation of block copolymer micelles. The first and most direct way is direct dissolution of solid bulk polymer in a selective solvent.[20,24] This method is only suitable for block copolymers with low molecular weight and insoluble blocks with a short enough length.[24,25] The solution is "annealed," i.e. the solubility is increased, by standing or by an annealing process like

prolonged stirring, thermal treatment or ultrasonic agitation.[20,24,25] It is possible that non-equilibrium (or "frozen") micelles are formed, especially for block copolymer with an insoluble block with a high glass transition temperature (T_g).[20,24,25] In general, direct dissolution in a selective solvent is not a very suitable method for micelle formation.[20] To obtain equilibrium micelles within a reasonable time frame, the selective solvent would have to swell the insoluble blocks quite extensively.[20]

The co-solvent (or solvent switch) method is a regularly used alternative: the bulk copolymer is first dissolved in a common solvent for both blocks and then conditions of the solvent are changed such that micelles are formed.[20,24] Usually, this change in conditions is brought about by gradually adding a solvent which is a selective solvent for one of the blocks and a precipitant for the other blocks.[20,24,25] Altering the solvent conditions is also possible via concentration, temperature or pH changes.[20,24,25] Eventually, the common solvent can be stripped by evaporation.[24,25] (Step-wise) dialysis is often used as an alternative to evaporation: the common solvent is gradually replaced by the selective solvent.[20,24-26] The dialysis technique is the preferred preparation method for micellar systems in aqueous solution.[20,24] It avoids the formation of large aggregates which are a problem when preparing micelles using the direct dissolution approach.[24,25] Also, crew-cut micelles, which consist of block copolymer chains with very short soluble blocks, can be obtained using the dialysis technique.[24,25] Despite these advantages, "frozen" micelles with a "glassy" micellar core (at room temperature) are not avoided by using the dialysis method.[20,24,25] Also, in the case of polydispersity of the composition or molecular weight of the block copolymer, this preparation technique can lead to micelles with a large distribution in size.[20,24,25]

Obtaining micelles from amphiphilic block copolymer is usually done with the direct dissolution approach or the co-solvent method.[25] However, a third method called the (thin) film rehydration or dry-down method exists.[26] A dry block copolymer film is rehydrated in a selective solvent, possibly with the help of mechanical mixing, sonication, extrusion or electrical fields.[26,27] Like for the direct dissolution technique, this method is used for block copolymers with an insoluble block that is relatively flexible, i.e. has a low glass transition temperature.[26]

Several other, less common, techniques are also used to obtain polymer nanostructures in a selective solvent. The emulsion method[28], electroformation[29], layer-by-layer deposition process[30], and microfluidic technique[31] are a few examples.

The method used for preparation of block copolymer micelles strongly influences the micellar characteristic features.[24]

2.2.3 Preparation techniques for loading micelles with hydrophobic molecules

The preparation of drug loaded block copolymer micelles can be done using several different methods, many of which are similar to the preparation of "empty" micelles. Again, the choice of preparation method is usually dictated by the solubility of the block copolymer in the solvent.[32]

In the direct dissolution method, used for quite soluble copolymers, the drug and the block copolymers are dissolved in the preferred solvent.[32,33] Drug loading into the micelles occurs by use of stirring, heating and/or sonication of the solution.[32] Aqueous solutions of micelles of for example Pluronic® block copolymer loaded with several different drugs (e.g. DOX) have been prepared before.[34,35]

The dialysis method is one of the most used methods for preparation of drug-loaded micelles and many different drug-loaded systems have been successfully

prepared using this method.[36-38] The copolymer and drug are dissolved in a common solvent and by addition of the selective solvent to this solution, micelle formation is induced.[32] The common solvent is then removed by dialysis against a large excess of selective solvent (water).[32] The choice of common solvent can affect the physical and drug loading properties of the micelles.[39] Also, an optimal ratio of water (selective solvent) to common solvent has been found that leads to the ideal properties concerning size, stability and drug loading level of the micelles.[40-43]

Even though the (thin) film rehydration approach is not widely used for the preparation of 'empty' micelles, it is common for the preparation of drug-loaded micelles.[32] The film rehydration approach is also referred to as the dry-down, evaporation or solution-casting method.[32,33] With the film rehydration method, the copolymer and drug are first dissolved in a common solvent or mixture of miscible solvents.[32] After stirring, this mixture is dried, for example by evaporation, to form a copolymer-drug film.[32] The film is reconstituted in warm water or buffer, i.e. the selective solvent.[32,33] Sometimes these samples are then sonicated or passed through a high-pressure extruder to obtain a monomodal size distribution.[32] The extent of drug loading when using the film rehydration approach depends heavily on which common solvent is used.[32] Liu et al. hypothesize that it is likely most favorable if the copolymer and the drug are equally soluble in the common solvent.[32] Phase separation during the evaporation process would then be avoided.[32] During the dry-down method, favorable interactions between the copolymer and drug due to similar solubility should encourage loading of the micelles with the drug during reconstitution of the film.[32,33]

A study by Yokoyama et al. showed that by using the dry-down method to load an anticancer drug, camptothecin, into a block copolymer, poly(ethylene glycol)-

b-poly(aspartate), much higher loading efficiencies and less aggregation was obtained compared to the dialysis method or the emulsion method.[44] This result was corroborated by Parnell et al., who found that for polymersomes (vesicles), the encapsulation efficiency is higher for the thin film rehydration method than other preparation methods because the block copolymer can be mixed with a molecule prior to self-assembly.[45]

Using the film rehydration technique, many different authors like. Binder et al.[46], Lee et al.[47], Mueller et al.[48], Li et al.[49], and Henderson et al.[50] have prepared PB-PEO polymersomes, often loaded with drug or dye molecules. The specific procedure used varies greatly: different common solvents are used, different drying techniques, the solutions are not heated at all or heated to 60 °C, etc.

Other methods for drug loading in polymeric micelles include an oil-in-water emulsion method[33,51] or an approach using freeze-drying and rehydration of the resulting powder developed by the Leroux group.[43] According to the Leroux group, the direct dissolution, dialysis, film rehydration, and emulsion methods all require sterilization and freeze-drying steps to produce injectable formulations with an adequate shelf-life.[43]

As was the case for "empty" micelles, the method of preparation of the drug-loaded micelles does influence the physicochemical properties and, in this case, the drug loading properties of the micelles.[24,32]

2.2.4 Practical procedures for micelle preparation

Previous work from our research group has demonstrated that, due to the low glass transition temperature (T_g) and low entanglements of PB-PEO, reproducible sizes and structures could be obtained by direct dissolution.[2] Therefore, the "empty"

PB-PEO micelles were prepared using the direct dissolution method. The solid block copolymer sample was first dissolved in water and this mixture was magnetically stirred at 200 rpm for 3 days. Afterwards, the sample was sonicated using an ultrasonic bath (Fisher Scientific Ultrasonic Cleaner FS20, 42 kHz ± 6%) for 1 h. To avoid significant sample heating, sonication was halted after 30 min to let the water cool down before continuing. Sonication was necessary due to large (> 150 nm) aggregates being present which resulted in a cloudy solution before sonication.
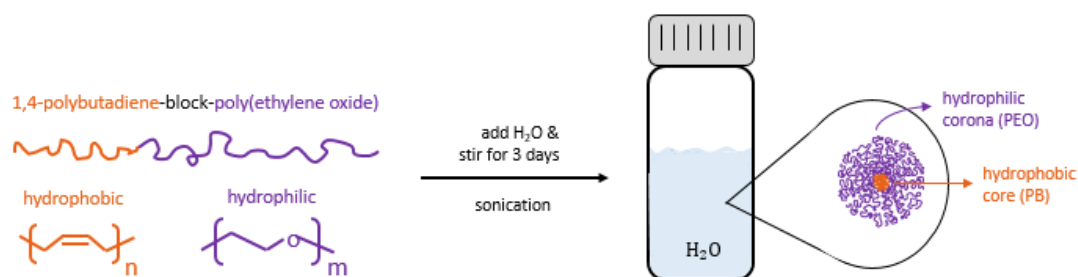
Figure 2.6:   Schematic representation of the direct dissolution process for preparation of poly(butadiene-*b*-ethylene oxide) micelles in aqueous solution. This figure was used with permission from Laurens Heusele.

For preparation of the micelles loaded with hydrophobic dyes, the film rehydration (dry-down) method was used. Concern was that the direct dissolution method would not give reproducible encapsulation of the hydrophobic particles. The dyes are insoluble in water, so it is unlikely that these molecules would be encapsulated homogeneously by the block copolymer micelles.

To prepare the PB-PEO micelles loaded with hydrophobic dyes, dilutions of the dyes were first made by dissolving the dyes in chloroform. These dilutions were stored at − 20 °C due to storage requirements and to diminish the effect of evaporation

of chloroform on the concentration. Using these dilutions, the dyes were then independently added to solutions of PB-PEO in 1 mL chloroform (in 20 mL scintillation vials). No stirring or mixing was required, as all components readily dissolved in chloroform. Thin films were formed by removal of chloroform from the samples by rotary evaporation for about 15 min at a fixed temperature of 22 °C (due to submersion of the sample in a temperature bath). These films were further dried by vacuum at room temperature so no chloroform was left in the films before rehydration. DI water was added to the films to obtain 2.5 mg/mL PB-PEO concentrations and the samples were stirred overnight at 200 rpm. Due to solutions often being slightly turbid, the samples were sonicated using an ultrasonic bath (Fisher Scientific Ultrasonic Cleaner FS20, 42 kHz ± 6%) for 1 h so no micelle aggregates would be present. To avoid significant sample heating, sonication was halted after 30 min to let the water cool down before continuing.

All samples ("empty" and loaded micelle solutions, films, etc.) were covered or handled with dim lighting as much as possible during storing and preparation to avoid photo-induced cross-linking of PB or photodegradation of the dyes. To avoid changes in polymer concentration and disruption of the micelle structure, samples were not filtered. Instead, dust was removed from all vials before use. All sample preparations and experiments were carried out at ambient temperature (fluctuating, $T_{avg} \sim 22$ °C).
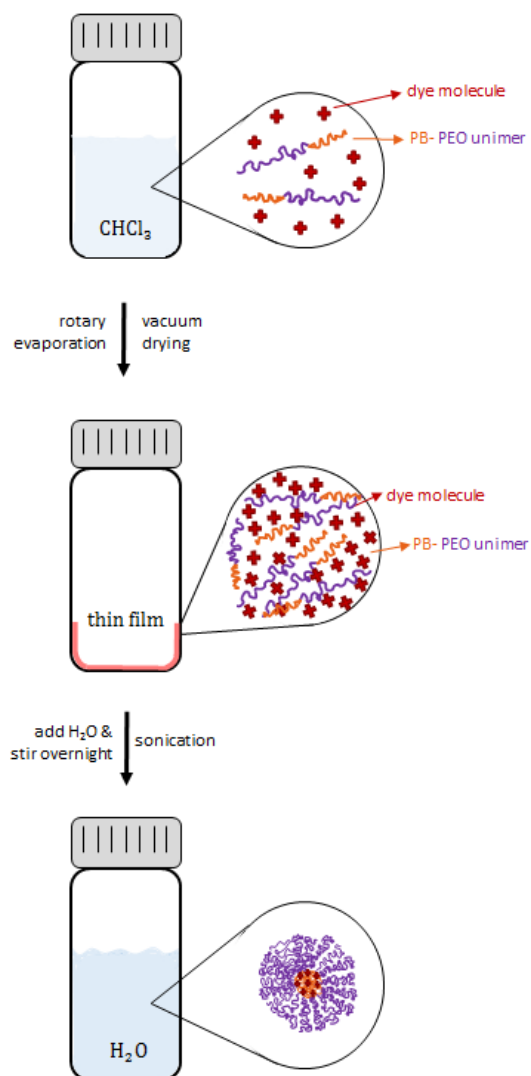
Figure 2.7: Schematic representation of the film rehydration (or dry-down) process for the preparation of poly(butadiene-*b*-ethylene oxide) micelles, loaded with dye molecules, in aqueous solution.

2.3   Solution characterization

The solution characterization is performed using dynamic light scattering (section 2.3.1), fluorescence resonance energy transfer (section 2.3.2), and UV-Vis spectroscopy (section 2.3.3) methods.

2.3.1 Dynamic Light Scattering (DLS)

2.3.1.1 DLS background

Dynamic Light Scattering (DLS) can be used to determine the particle size and its distribution in dilute colloidal dispersions.[2,52] The colloidal particles will scatter incident light and this scattered light is time dependent due to the continuous (Brownian) motion of the particles.[52,53] This time dependency of the intensity of scattered light is used to obtain the diffusion coefficient of the particles, which is related to the particle size.[52] More rapid fluctuations in light intensity indicates larger diffusion coefficients and are thus a result of smaller particles.[2]

In the DLS technique, a detector measures the intensity of the scattered light over time.[52] The time dependence of the fluctuations of this intensity is captured in the autocorrelation function $C(q, \tau)$ by correlating the fluctuations in intensity against short decay time intervals τ, also known as the delay time.[52,53] This autocorrelation function also depends on the scattering vector q, defined as:[2,52]

$$q = \frac{4\pi n}{\lambda} \sin\left(\frac{\theta}{2}\right) \tag{2.1}$$

The refractive index of the solvent is denoted by n, λ is the light wavelength and θ is the scattering angle. The scattering vector q has units of "1/length" and is a measure of the distance between the scattering centers, when the intensity of the scattered light at wavelength λ is measured at angle θ.[52] If the scattering vector q is small compared to the characteristic length of the particles compares, the scattering centers are located within the same particle.[52] The intensity of scattered light will then contain information on this intraparticle interference of scattering centers and thus on the structural parameters of the particle.[52] For dilute solutions, interparticle spacing is so large that no interparticle interference of scattering centers exists and thus the intensity

fluctuations that are measured are only due to single-particle motion, i.e. no interparticle interference exists.[52] For a scattering angle θ of 90°, water with a refractive index of $n = 1.336$, and light with a wavelength $\lambda = 532$ nm, the scattering vector q is about 0.0022 Å^{-1}.

The autocorrelation function $C(q, \tau)$ is described by the following equation:[52]

$$C(q,\tau) = \lim_{t_n \to \infty} \frac{1}{t_n} \int_0^{t_n} I(q,t)\, I(q,t+\tau)\, dt \qquad (2.2)$$

in which t_n is the period of time over which the intensity was recorded. For infintitely short time periods ($t_n = 0$), the autocorrelation function has a maximum value because the intensity is highly correlated.[2,52] For infinitely long times ($t_n = \infty$), the intensity becomes uncorrelated and the autocorrelation function is equal to the square of the average intensity over time, $[\bar{I}(q)]^2$.[2,52] The autocorrelation function $C(q, \tau)$ follows a monotonic decrease between these two extremes and this decay contains information about the diffusion coefficient (and thus the size) of the particles in the solvent.[2,52]

Alternatively, this decay can be captured by the Siegert relation, which is effectively the autocorrelation function normalized to its asymptotic minimum value:[52]

$$g_2(q,\tau) = \frac{C(q,\tau)}{[\bar{I}(q)]^2} = 1 + \xi\, |g_1(q,\tau)|^2 \qquad (2.3)$$

in which ξ is an instrumental constant approximately equal to unity.[52]

For monodisperse, spherical particles, the field correlation function $g_1(q,\tau)$ is related to the (translational) diffusion coefficient of the particle D according to the equation:[52,53]

$$|g_1(q,\tau)| = \exp(-q^2 D\, \tau) \qquad (2.4)$$

The cumulant method or also referred to as the method of moments can account for some polydispersity by defining an average decay rate and some variance in the decay rate.[2] A polydispersity coefficient $\sigma = \mu/(q^2 D)^2$ describes the width of the diffusivity distribution in the quadratic cumulant (QC) fit expression:[2]

$$|g_1(q,\tau)| = \exp(-q^2 D\,\tau)\;(1 + \tfrac{\mu}{2}\tau^2 + \cdots) \qquad (2.5)$$

The polydispersity index (PDI) of the particles in solution can be determined by the QC fit. A PDI smaller than 0.1 indicates a highly monodisperse sample, values between 0.1 and 0.4 are considered moderately polydisperse, while a PDI higher than 0.4 indicates a highly polydisperse sample.[53]

Other methods to fit the correlation data exist, like the double exponential (DE) fit or the polydisperse double exponential (PDE) fit, but these fits are not used in this thesis.[2]

From the fits of the decay rate, $|g_1(q,\tau)|$ the diffusivity of the particle can be obtained and with the Stokes-Einstein equation, the hydrodynamic radius R_h can be calculated from the diffusion coefficient D:[52]

$$D = \frac{k_B\,T}{6\,\pi\,\eta\,R_h} \qquad (2.6)$$

where k_B is the Boltzmann constant, T is the temperature, and η is the viscosity of the solvent.

Due to the effective hydrodynamic radius being determined from an intensity-weighted decay constant, which scales with R^6 ($I \sim M_i^2 \sim R_i^6$), a bias towards large sizes exist, i.e. a small number of large particles can shift the effective R_H significantly.[54] This intrinsic bias towards larger particles is the major drawback of DLS.[2] Small particles can be difficult or impossible to detect if in presence of much larger particles. Another drawback of DLS is its low resolution and its limited

capability to resolve particles with different sizes within a sample.[55] As a result, a sample may appear to consist of particles with one broad size distribution, while in reality it consists of particles of two different sizes. An advantage of DLS is that measurements only takes a few minutes. Also, DLS provides good sampling statistics because light scatters off a large portion of the solution.[2]

2.3.1.2   Practical procedure

Experiments were conducted on a Brookhaven Instruments Light Scattering System (BI-200SM, Brookhaven Instruments Corporation, BIC) equipped with a CNI Laser, which has a wavelength of 532 nm. The scattering angle, controlled with a goniometer, was 90° for all data used in this thesis. All DLS experiments were performed at 25.0 ± 0.1 °C. The solutions were pipetted into a glass culture tubes (Fisherbrand disposable culture tubes, borosilicate glass, 10 x 75 mm) at a minimum volume of 300 μL, covered with parafilm and placed into the temperature controlled decalin bath. Decalin is used to match the refractive index of glass, so the refraction of light due to the glass vial is accounted for. To remove dust, the decalin bath was filtered for 5 min prior to experiments, and polymer solutions were equilibrated within the temperature bath ($\sim$ 3 min) prior to recording data. The count rate was between $\sim$ 50 and 500 kcps. Data were analyzed and fit with the instrument software supplied by BIC, using the quadratic cumulant (QC) fit. Measurements were carried out in triplicate form for each sample.

2.3.2 Fluorescence Resonance Energy Transfer (FRET)

2.3.2.1 FRET background

Fluorescence, or sometimes called Förster, Resonance Energy Transfer (FRET) is the radiationless transfer of energy between two molecules.[56] The FRET technique can be used to determine the distance and changes in distance between these two molecules within several nanometers.[56] The distance sensitivity of the FRET technique is often used to investigate molecular interactions.[56] The structure and conformations of proteins and nucleic acids can be elucidated by use of the FRET technique[57,58], as well as receptor/ligand interactions[59], and many other biological processes.[60]

FRET is the radiationless transfer of energy between two fluorophore molecules, with one fluorophore being the donor, the other the acceptor of the transferred energy (Figure 2.8).[56] When the donor fluorophore is excited by incident light, its electrons will go from the ground state into a higher vibrational state, which takes about one femtosecond.[60,61] Within picoseconds, the electrons will decay to the lowest vibrational state, because some energy is lost as heat, before returning to their ground state (within nanoseconds).[60,61] This return to the ground state is usually accompanied by the emission of a photon, i.e. fluorescent light of a longer wavelength due to the energy loss.[60,61] The change in absorption and emission spectrum due to the energy loss is called the "Stokes shift".[61] If FRET occurs, however, the photon is not emitted: the energy is transferred in a non-radiative manner to the acceptor molecule through long-range dipole-dipole interactions.[56,60] The acceptor's electrons will then be excited in the same way as the donor.[60] Possibly, a photon (fluorescent light) can then be emitted once the electrons of the acceptor molecule return to their ground

state.[60] However, the acceptor chromophore does not necessarily have to be a fluorescent molecule.[56,60] "Dark quenchers" (non-fluorescent quencher) can be used as acceptor molecules, for example. In this case, the transferred energy does not cause emission of a photon and acceptor fluorescence.[61,62] Rather, the energy is dissipated through the quencher and (partially) lost as heat.[61,62]
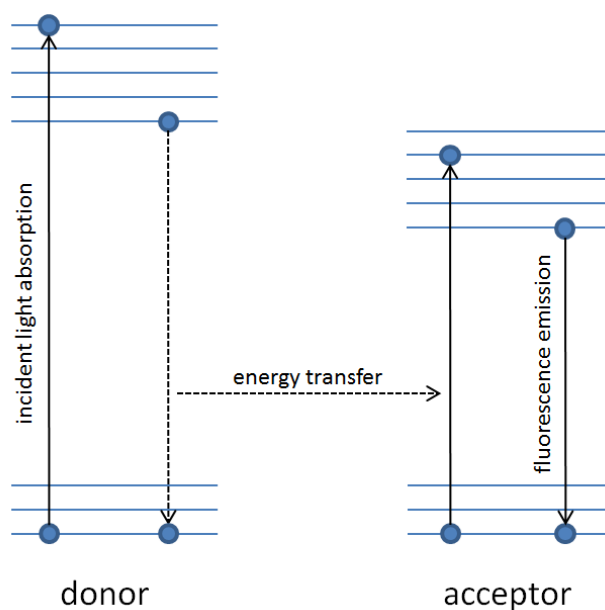
Figure 2.8:   A schematic overview of the FRET process and the energy state transitions of the donor and acceptor molecules accompanying this process.

The energy transfer from donor to acceptor is accompanied by several different effects. For donor-acceptor pairs that are both fluorophores, an increase of acceptor fluorescence and a decrease in the donor fluorescence is present.[56,60] When a dark quencher is used instead of a fluorescent acceptor molecule, only the fluorescence of the donor will be decreased and no acceptor fluorescence is visible because the

absorbed energy is lost as heat instead of emitted as photons.[60,61] A second way in which FRET can be observed is by a reduction of excited state lifetime of the donor.[56] The lifetime of a fluorophore is the time it is in the excited state before returning to the ground state, i.e. the time before a photon is emitted after absorption of one.[63,64]

Several conditions exist that need to be met before the energy transfer can occur. First, both fluorophore molecules need to be in close proximity of each other, within the nanometer range.[56,60,61] Second, the fluorescence emission spectrum of the donor fluorophore has to have significant spectral overlap with the absorption or excitation spectrum of the acceptor fluorophore.[56,60,61] The spectra of the commonly used donor-acceptor pair DiO and DiI is shown in Figure 2.9 as an exemplar. The acceptor excitation or absorption spectrum overlaps the donor's emission spectrum, which is a necessary condition for energy transfer from the donor to the acceptor fluorophore to occur. The degree of overlap between the donor emission spectrum and the acceptor absorption spectrum is called the spectral overlap integral *J*. Another condition for energy transfer to occur is that the transition dipole orientations of the donor and acceptor are approximately parallel.[56,60,61] Finally, the fluorescence lifetime of the donor must be long enough for FRET to occur.[56]
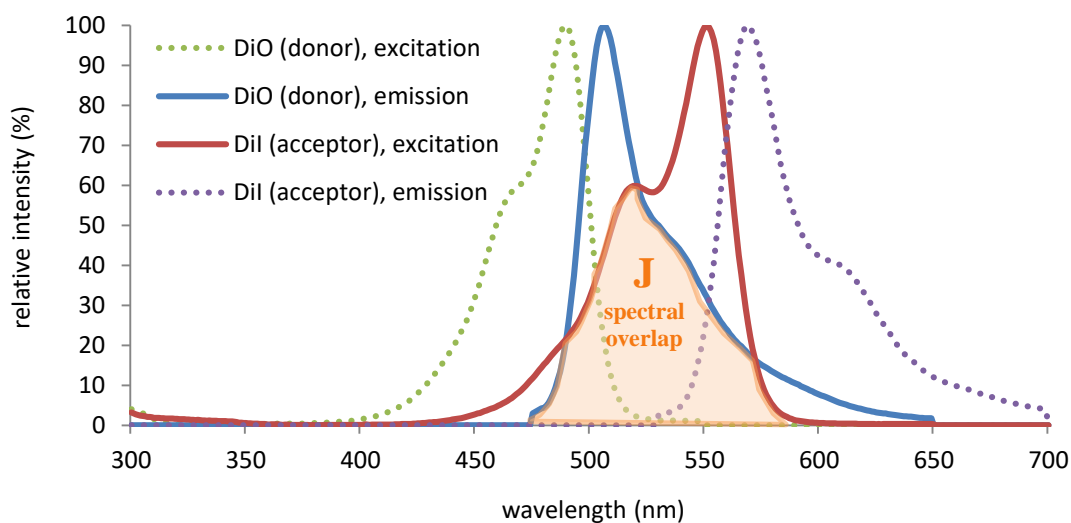
Figure 2.9: The excitation and emission spectra of DiO and DiI as an example of a FRET donor-acceptor pair. The spectal overlap J between the emission spectrum of DiO and the excitation spectrum of DiI is indicated. The Stokes shift between the excitation and emission spectra of both dyes is also clearly visible. The intensity data of DiO and DiI was obtained through ThermoFisher.[65]

The efficiency of the FRET process (E_{FRET}) depends on the distance between the donor and acceptor molecules through an inverse sixth power relation:[66]

$$E_{FRET} = \frac{R_0^6}{R_0^6 + r^6} \tag{2.7}$$

The Förster radius (R_0) is the distance between the donor and the acceptor at which the FRET efficiency is 50%. Typical values of the Förster radius of donor-acceptor pairs are in the range of 5 to 8 nm.[67]

The energy transfer efficiency can also be obtained from the (exited state) lifetime of the donor:[67]

$$E_{FRET} = 1 - \frac{\tau_D(A)}{\tau_D(0)} \tag{2.8}$$

58

The lifetime of the donor when it is in the absence of the acceptor is denoted by $\tau_D(0)$, and when in the presence of the acceptor it is denoted by $\tau_D(A)$.[67]

A non-FRET quenching mechanism, called static quenching or contact quenching, can also occur and results in enhanced quenching.[61,64] The donor and quencher form a ground-state complex by binding together through hydrogen bonds.[61,64] This physical association is presumably controlled by the same forces as dye aggregation, which are electrostatic, steric and hydrophobic forces for dyes in aqueous solutions.[61,64] The complex absorbs incident light, but no fluorescent light is emitted because the excited state immediately returns to the ground state without emitting a photon.[61] A coupling of the excited-state energy levels of the donor and quencher occurs when a complex is formed, which, apart from resulting in no fluorescence emission, creates a unique absorption spectrum.[61,64] In contact quenching, overlap between the emission spectrum of the fluorophore and the absorption spectrum of the quencher is not critical, as it is in the FRET mechanism.[68]

The fluorescence lifetime of the fluorophore can distinguish the two quenching mechanisms.[64] For quenching through FRET, the lifetime and the fluorescence intensity are decreased by the same factor.[64] For contact quenching, a dimer of fluorophore and quencher is created before absorption of a photon, so the fluorophore's lifetime in the quenched state is equal to its lifetime before quenching.[64] Also, the absorption spectrum changes for contact quenching due to the fluorophore-quencher complex formation.[64]

2.3.2.2   Choice of fluorophore and quencher

When using a donor-acceptor pair for which both molecules are fluorophores, a change in the shape of the emission spectrum has to be observed to see if FRET

occurred.[68] However, it is much easier to directly measure the change in fluorescence intensity of the fluorophore as a result of quenching.[68] Therefore, for this project, a fluorescent dye and "dark quencher" are chosen as the donor-acceptor pair. Dark quenchers have the ability to quench the fluorescence of the acceptor molecule without emitting any fluorescence themselves, contrary to donor molecules.

The fluorescent dye needs to meet several criteria. First, the initial brightness needs to be sufficient, to provide a good fluorescence signal strength. Second, the fluorescent dye should be photostable to avoid degradation upon exposure to light. Ideally, the excitation wavelength of the fluorescent dye is located in the visible spectrum between 400 nm and 600 nm. The most important criterion, however, is the hydrophobicity: the fluorescent probe needs to be (very) hydrophobic to ensure encapsulation within the micelle core when in aqueous solution. Many fluorescent dyes adhere to the first three criteria, but only a few are hydrophobic. Based on the information from ThermoFisher, three options, BODIPY® FL, Cy®3 and TRITC, seemed to agree with all criteria involving initial brightness, photostability, excitation wavelength, and hydrophobicity.[69-71] However, information on the hydrophobicity of the molecules was vague, prompting a more extensive comparison to choose the ideal dye from these three options, especially considering the importance of hydrophobicity in this specific application.

Zanetti-Domingues et al. compared the hydrophobicity of several dyes by computing the logarithm of the distribution coefficient (logD) of the dyes based on their chemical structures.[72] The logD is defined as a measure of the ratio of expected dye concentrations in a non-polar solvent (octanol) and water.[72] Molecules with a negative value of logD are thus hydrophilic, while a positive logD indicates

hydrophobicity. Cy3 had the highest positive logD and is therefore hydrophobic.[72] ThermoFisher also reports that Cy®3 dye is the basis for the DiI cell tracing reagents, which are lipophilic.[70] Johansson reports that cyanine dyes are quite planar, hydrophobic molecules.[64] Even though ThermoFisher reports that BODIPY® FL has "unique hydrophobic properties"[69], according to the negative value for the logD as reported by Zanetti-Domingues et al., it would be a (slightly) hydrophilic molecule.[72] No log D value is reported for TRITC, though ThermoFisher mentions that TRITC molecules have a "quite hydrophobic (structure) when compared with their fluorescein counterparts FAM and FITC".[73] Considering the contradicting information on BODIPY® FL and the limited information on TRITC, Cy3 was chosen as the fluorophore.

A dark quencher should be paired with Cy3 fluorophore. The criteria for the selection of this dark quencher are hydrophobicity, a fluorescence absorption range that is compatible with Cy3 and a large efficiency of Cy3 quenching. Black Hole Quencher (BHQ) dyes are a species of hydrophobic dark quencher molecules.[62,64] They can suppress the fluorescence by FRET quenching or contact quenching.[62,64] Because the maximum emission wavelength of Cy3 is at 568 nm, both BHQ-1 or BHQ-2 dye would be a good choice: BHQ-1 should be paired with a dye that emits in the range of 480-580 nm and BHQ-2 with one that emits in the 560-670 nm range, according to Biosearch Technologies, the manufacturer of BHQ dyes.[74] The efficiencies for FRET quenching of Cy3 dye is 92% for BHQ-1 and 97% for BHQ-2 dye.[68] The efficiencies for contact quenching of Cy3 dye are 97% for BHQ-1 and 93% for BHQ-2.[68] For many other donor-quencher pairs, the contact quenching efficiency is higher than the FRET efficiency, but the Cy3 – BHQ-2 pair is an exception.[64,68]

Using the Spectral Overlay Tool provided online by Biosearch Technologies, the spectral overlap of the Cy3 spectrum with the BHQ-1 and BHQ-2 spectra can be compared. BHQ-2 is a slightly better candidate as a dark quencher, because the complete Cy3 emission spectrum is covered by the BHQ-2 adsorption spectrum.[75]

The Förster radius of Cy3 and BHQ-2 is 5.02 nm.[76] Figure 2.10 shows the Cy3 emission spectrum, the BHQ-2 absorption spectrum, and their spectral overlap.
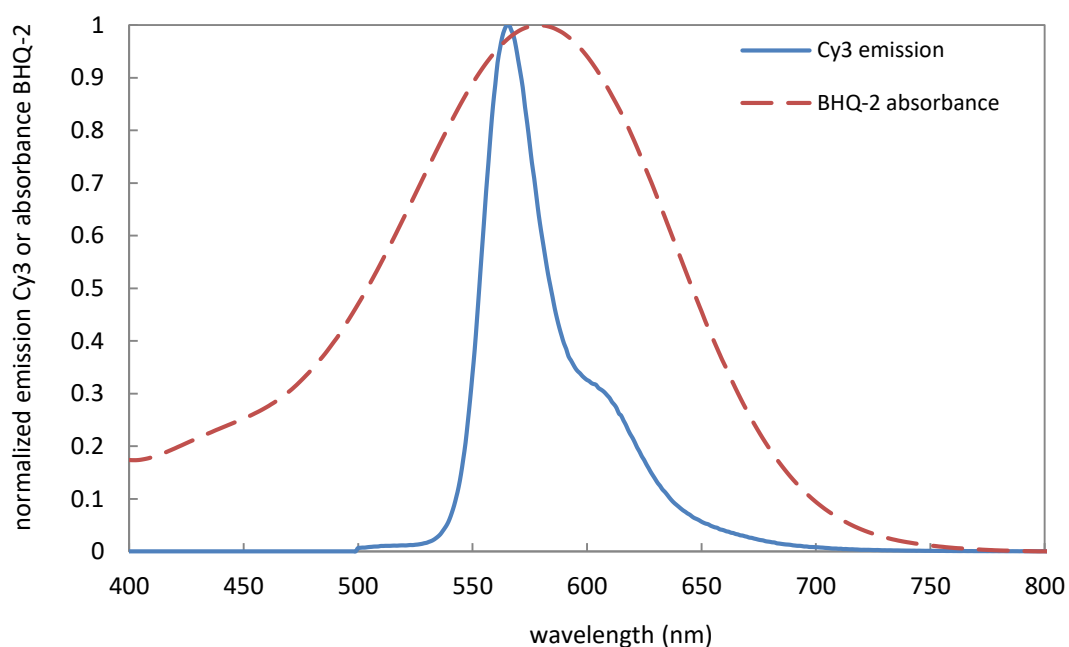
Figure 2.10: The emission spectrum of Cy3 and excitation (absorption) spectrum of BHQ-2 to illustrate the significant spectral overlap between the spectra. The intensity data of Cy3 and BHQ-2 was obtained through ThermoFisher and Biosearch Technologies.[77,78]

Cy3 and BHQ-2 are not available as separate molecules as they are usually attached to oligonucleotides. Lumiprobe offers Cy3 in the form of an alkyne, amine,

azide, carboxylic acid hydrazide, maleimide, and NHS ester. From these options, cyanine3 alkyne was chosen because it is non water-soluble, according to Lumiprobe.[79] BHQ-2 can be purchased from Biosearch Technologies in the form of a DMT amidite, amidite, dT linker amidite, amine, carboxylic acid, and succinimidyl ester. According to Biosearch Technologies, BHQ-2 amidite, amine, carboxylic acid, and succininimidyl ester are hydrophobic.[80] However, BHQ-2 succinimidyl ester contains a reactive group for coupling to primary amines and would have the potential to conjugate to other components in the system.[80] BHQ-2 amidite was chosen as the quencher in combination with cyanine3 alkyne for this application.

2.3.2.3   Practical procedure

For the characterization via FRET of dye exchange between micelles, a Promega GloMax®-Multi Detection System in the fluorometer operation mode, using the green optical kit (excitation peak at 525 nm), was used to read a (black) 96-well plate. For quiescent solutions, 50 µL of each solution was pipetted into a well. For the vortex mixing experiments, 65 µL of each solution was pipetted into a Kimble™ ½ dram borosilicate glass vial and vortex mixed at about 1500 rpm using a Fisher Scientific Analog Vortex Mixer before pipetting 100 µL of this solution into a well. The preparation for the magnetic stirring experiments was analogous to the vortex mixing experiments, except that a Teflon stir bar was added to the vial before the solution was stirred at 200 rpm on a magnetic stir plate.

2.3.3   Determination of concentration

UV-Vis absorption and the spectral properties of the dyes were used to obtain the concentration of dyes in solution. The polymer concentration was determined by

measuring the mass of polymer and mass of water. The polymer concentration after dialysis or in the supernatant of an ultracentrifuged sample was determined by UV-Vis absorption based on an absorbance-concentration calibration curve.

2.3.3.1 Concentration of dyes

UV-Vis experiments were used to determine the concentration of the dyes in the polymer solutions. By using the Beer- Lambert Law and the spectral properties of the dyes, the absorption measured by UV-Vis can be related to the concentration.

The Beer-Lambert Law is represented by the following equation:

$$A_\lambda = \varepsilon_\lambda\, c\, L \qquad (2.9)$$

The absorption and the molar extinction coefficient at a certain wavelength λ are denoted by A and ε, the (molar) concentration is denoted by c and the path length is denoted by L.

For Cyanine3, the extinction coefficient at 552 nm is 150,000 L.mol-1.cm-1.[79] For BHQ-2, the extinction coefficient at 579 nm (maximum absorption) is 38,000 L.mol-1.cm-1 and at 260 nm, it is 8,000 L.mol-1.cm-1.[81] UV-Vis experiments were performed using the NanoDrop® ND-1000 Spectrophotometer, for which the path length was 1.0 mm in this case. Molar concentrations were converted to mass concentrations using the molecular weight of Cyanine3 alkyne and BHQ-2 amidite, which is equal to 530.14 g/mol and 678.72 g/mol, respectively.

To account for the UV-Vis absorption by the PB-PEO polymer, a UV-Vis absorption spectra was obtained for PB-PEO aqueous solutions, with no added dye or quencher. The absorption spectrum did seem to be quite dependent upon the turbidity of the sample. When some aggregates were still present in the sample and the solution would not be completely clear, a different UV-Vis spectra was obtained. Figure 2.11

demonstrates the UV-Vis absorption spectra of two different samples, one clear and one showing slight turbidity, at the same concentration (2.5 mg/mL). Up until a wavelength of about 450 nm, the spectra are distinctly different. However, for wavelengths higher than 500 nm, both spectra are essentially zero (absorbance equal to that of a water sample). Therefore, no correction for the presence of polymer was needed when obtaining the concentration of Cy3 and BHQ-2 at 552 and 579 nm, respectively.

Using the molar extinction coefficient at 260 nm to determine the concentration of BHQ-2 can induce significant errors. First, at this wavelength, it is necessary to correct for the absorption due to the presence of polymer. The BHQ-2 absorption can be obtained by subtracting the absorption of the BHQ-2 loaded micelle samples with its background, i.e. the absorption spectrum of a PB-PEO aqueous solution with equal polymer concentration (2.5 mg/mL). Because the dye-loaded micelle solutions are colored, it is visually more difficult to determine if the sample exhibits any turbidity. Considering turbidity influences the UV-Vis absorbance spectrum of the polymer, the polymer absorbance obtained from a clear sample may be different for other samples. Second, at a wavelength of 260 nm, more background due to the polymer is present, thus making the determination of the absorption due to BHQ-2 more inaccurate than at 579 nm. The choice of determining the concentration of BHQ-2 at 579 nm was validated when comparing the background corrected UV-Vis absorbance of BHQ-2 at 260 nm to the absorbance at 579 nm: the absorbance at 260 nm was higher than at 579 nm for several different batches, which is not a correct result considering the maximum absorbance of BHQ-2 is at 579 nm.
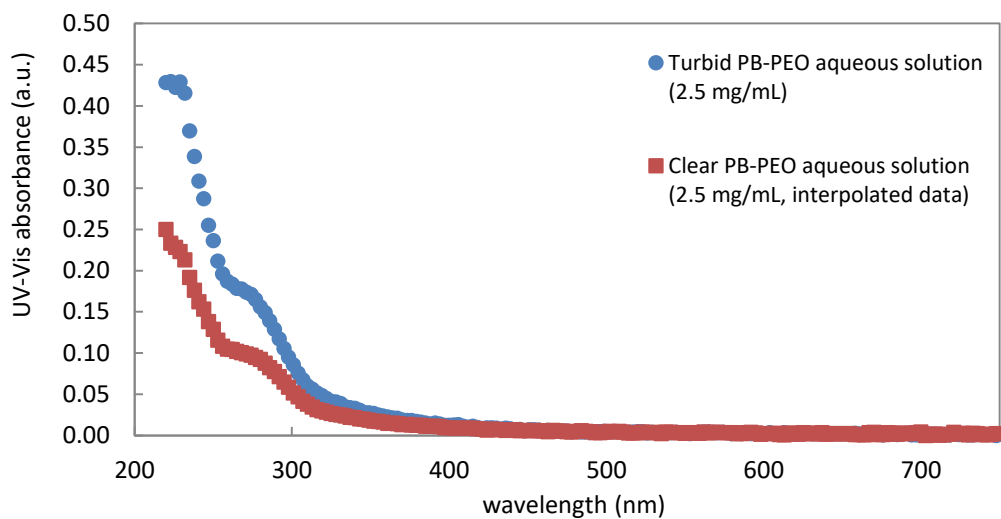
Figure 2.11: UV-Vis absorbance spectra of aqueous solutions of PB-PEO at 2.5 mg/mL to illustrate the difference in UV-Vis absorption for solutions of different turbidity.

In Table 2.1 the concentration of Cy3 and BHQ-2 in the different batches is listed. Even though, the concentration was aimed to be equal for batch 2 through batch 4, the concentration increased for every consecutive batch. This effect was attributed to an increased concentration of the dye dilutions, due to chloroform evaporating with every use. The uncertainties in concentration represent the 95% confidence interval based on three replicate absorbance measurements and the uncertainty due to background noise. The UV-Vis absorption of a water sample can be up to 0.004, even though water is used as a blank for the measurements, creating background noise.

Table 2.1:   Cy3 alkyne and BHQ-2 amidite concentrations in the PB-PEO aqueous solutions for different batches.

Batch		Absorbance at max. absorption wavelength (a.u.)	Concentration (mg/mL)
1	Cy3	0.812 ± 0.030	0.0287 ± 0.0011
	BHQ-2	0.425 ± 0.009	0.0759 ± 0.0010
2	Cy3	0.046 ± 0.014	0.0016 ± 0.0005
	BHQ-2	0.015 ± 0.005	0.0027 ± 0.0004
3	Cy3	0.068 ± 0.006	0.0024 ± 0.0002
	BHQ-2	0.017 ± 0.005	0.0031 ± 0.0003
4	Cy3	0.121 ± 0.005	0.0043 ± 0.0002
	BHQ-2	0.018 ± 0.005	0.0032 ± 0.0003
5	Cy3 (low conc.)	0.044 ± 0.005	0.0016 ± 0.0002
	Cy3 (high conc.)	0.068 ± 0.005	0.0024 ± 0.0002
	BHQ-2	0.021 ± 0.005	0.0038 ± 0.0003
5 (dialyzed)	Cy3 (low conc.)	0.018 ± 0.005	0.0006 ± 0.0002
	BHQ-2	0.021 ± 0.006	0.0038 ± 0.0005
6	Cy3	0.050 ± 0.006	0.0018 ± 0.0002
	BHQ-2	0.022 ± 0.005	0.0039 ± 0.0003
6 (super-natant)	Cy3	0.029 ± 0.005	0.0010 ± 0.0002
	BHQ-2	0.017 ± 0.005	0.0030 ± 0.0002

Initially, determination of the concentration of the dilutions in chloroform was attempted. Chloroform, with a boiling point of 61 °C, was deemed too volatile to produce accurate results with the Nanodrop ® spectrophotometer.[82] Therefore, chloroform was exchanged by DMF, which has a much higher boiling point of 153 °C.[82] Determination of the concentration of the dye dilutions resulted in concentrations which were inconsistent with the initial approximate concentrations and the concentrations of dyes in the polymer solutions. Also, the concentration of the stock solutions did not remain constant over time due to evaporating chloroform. Therefore, it was opted to prepare the samples using an initial guess for the concentration of the dye dilutions and determining the actual obtained concentration once the aqueous solutions were fully prepared.

2.3.3.2 Dialysis

Dye-loaded micelle solutions were independently placed in dialysis tubing (Regenerated Cellulose (RC) pre-treated dialysis tubing, 3.5 kD MWCO). Each dialysis tube was then placed in DI water at a volume ratio of 200:1 for 24 h, with replacement of water after 4 and 8 h.

2.3.3.3 Polymer concentration

The polymer concentration in mg/mL (mass of polymer per volume of solvent) was determined by measuring the mass of polymer and mass of water. In all samples the initial concentration of polymer was 2.5 ± 0.1 mg/mL. However, when performing dialysis, the polymer concentration of the sample decreased as a result of swelling of the dialysis tube by water due to the osmotic pressure. Also, when utilizing ultracentrifugation, the concentration of polymer in the supernatant differs from the

initial concentration. UV-Vis can be used to obtain the concentration of polymer after dialysis or in the supernatant of an ultracentrifugated sample.

A calibration curve for the absorbance at 260 nm of aqueous PB-PEO solutions for concentrations between 1 and 5 mg/mL is shown in Figure 2.12. The calibration curve demonstrates a linear relationship between concentration and absorption, as the Beer-Lambert law dictates. The choice of absorbance characterization at 260 nm was arbitrary, but provided good signal to noise ratio and had been used previously in the group for characterizing the PB-PEO concentration in micelles.[2]

It was determined earlier in this work that the absorption spectrum of PB-PEO micelles in aqueous solution was quite dependent upon the turbidity of the sample. However, all 5 samples used to make the calibration curve abided by the Beer-Lambert law and visibly did not show any turbidity.
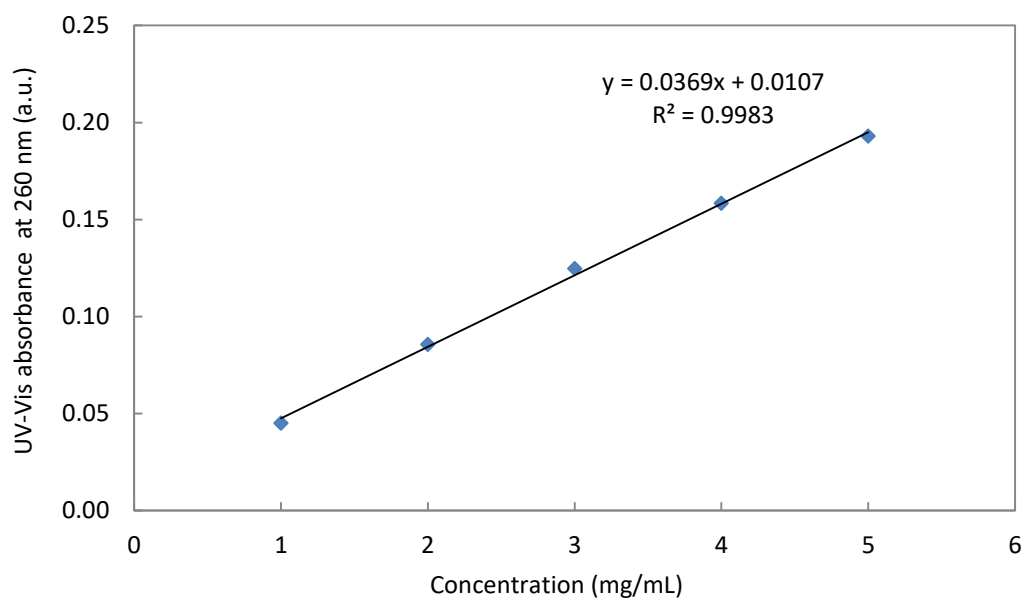
Figure 2.12: UV-Vis calibration curve to determine the PB-PEO concentration from measurements of the UV-Vis absorbance of polymer solutions at 260 nm.

The polymer concentrations of the different batches are listed in Table 2.2. The uncertainties in concentration represent the 95% confidence interval based on three replicate absorbance measurements. However, additional uncertainties exist due to the uncertainty of the initial concentrations of the samples used to obtain the calibration data and due to the interpolation of data while generating the calibration curve.

Table 2.2: Polymer concentrations in the PB-PEO aqueous solution for the dialyzed or ultracentrifuged samples.

Batch		Absorbance at 260 nm (a.u.)	Polymer concentration (mg/mL)
5 (dialyzed)	Cy3 (low conc.)	0.083 ± 0.002	1.97 ± 0.2
	BHQ-2	0.089 ± 0.001	2.12 ± 0.3
6 (centrifuged, supernatant)	Cy3	0.045 ± 0.001	0.94 ± 0.3
	BHQ-2	0.051 ± 0.001	1.09 ± 0.3

2.3.3.4   Determination of octanol-water partition coefficient

The octanol-water partition coefficient K_{ow} or $P_{oct/wat}$ represents the ratio of the concentration of a compound in octanol versus the concentration in water.[83] It is usually expressed as a logarithm, i.e. log K_{ow} or log $P_{oct/wat}$.

To determine the octanol-water partition coefficient, the shake-flask method was used based on work by Oba and Paulson, who determined partition coefficients of (hydrophilic) fluorescent dye tracers.[84] Cyanine3 alkyne and BHQ-2 amidite are

expected to be hydrophobic, which is important for determining the ideal volume ratio of 1-octanol and water. For (very) hydrophobic molecules, relatively small volumes of 1-octanol should be used so that enough material is left in the aqueous phase for analysis.[83] Indeed, when performing an experiment at 0.80:0.20 octanol to water ratio, no measurable quantities of dye in the aqueous phases were present. Experiments were performed in centrifuge tubes, with 200 µL deionized water and 10 µL 1-octanol. Because the amount of dye added to the mixture could not be exactly controlled, dye concentrations in both phases were measured using a UV-Vis spectrophotometer, instead of calculating the dye concentration in one of the phases by mass balance. Tubes were vortex mixed with a Fisher Scientific Analog Vortex Mixer for 10 min at about 1500 rpm and centrifuged at 15,000 rpm for 5 min to separate the 1-octanol and aqueous phases.

REFERENCES

1. Won, Y. Y.; Davis, H. T.; Bates, F. S. Molecular exchange in PEO-PB micelles in water. *Macromolecules*, **2003**, *36*, 953–955.

2. Murphy, R. P., Chain Exchange in Aqueous Solutions of Block Polymer Micelles. M.S. Thesis, University of Delaware, Newark, DE, 2014.

3. Polymer Source Inc. Thermal analysis data for some polymers synthesized at Polymer Source (@10 °C/min). https://www.polymersource.com/Resources/Thermal-analysis.pdf (accessed March 14, 2017)

4. Chemical Data Retrieval on the Web (CROW), http://polymerdatabase.com/polymers/poly14-butadiene.html (accessed March 14, 2017)

5. Won, Y.-Y.; Brannan, A. K.; Davis, H. T.; Bates, F. S. Cryogenic Transmission Electron Microscopy (Cryo-TEM) of Micelles and Vesicles Formed in Water by Poly(ethylene oxide)-Based Block Copolymers. *The Journal of Physical Chemistry B*, **2002**, *106*, 3354-3364.

6. Fetters, L. J., Lohse, D. J., Richter, D., Witten, T. A., and Zirkelt, A. Connection between Polymer Molecular Weight, Density, Chain Dimensions, and Melt Viscoelastic Properties. *Macromolecules*, **1994**, *27*, 4639-4647.

7. Polymer Source Inc. P10599-BdEO data sheet https://www.polymersource.com/dataSheet/P10599--BdEO.pdf (accessed March 14, 2017)

8. Terreau, O.; Luo, L.; Eisenberg, A. Effect of Poly(acrylic acid) Block Length Distribution on Polystyrene-b-Poly(acrylic acid) Aggregates in Solution. 1. Vesicles. *Langmuir*, **2003**, *19*, 5601-5607.

9. Mai, Y. Y.; Eisenberg, A. Self-assembly of block copolymers. *Chemical Society Reviews*, **2012**, 41, 5969-5985.

10. Jain, S.; Bates, F. S. On the Origins of Morphological Complexity in Block Copolymer Surfactants. *Science.,* **2003**, *300*, 460–464.

11.   Topel, Ö.; Çakır, B. A.; Budama, L.; Hoda, N. Determination of critical micelle concentration of polybutadiene-block-poly(ethylene oxide) diblock copolymer by fluorescence spectroscopy and dynamic light scattering. *Journal of Molecular Liquids,* **2013**, *177*, 40-43.

12.   Tiller, G. E., Mueller, T. J., Dockter, M. E., and Struve, W. G. Hydrogenation of Triton X-l 00 Eliminates Its Fluorescence and Ultraviolet Light Absorption while Preserving Its Detergent Properties, *Analytical Biochemistry*, **1984**, *141*, 262-266

13.   Allen, C.; Han, J.; Yu, Y.; Maysinger, D.; Eisenberg, A. Polycaprolactone–b-poly(ethylene oxide) copolymer micelles as a delivery vehicle for dihydrotestosterone. *Journal of Controlled Release*, **2000**, *63*, 275–286.

14.   Soo, P. L.; Luo, L.; Maysinger, D.; Eisenberg, A. Incorporation and Release of Hydrophobic Probes in Biocompatible Polycaprolactone-block-poly(ethylene oxide) Micelles: Implications for Drug Delivery. *Langmuir*, **2002**, *18*, 9996–10004.

15.   Chen, H.; Kim, S.; Li, L.; Wang, S.; Park, K.; Cheng, J.-X. Release of hydrophobic molecules from polymer micelles into cell membranes revealed by Forster resonance energy transfer imaging. *Proceedings of the National Academy of Sciences,* **2008**, *105*, 6596–6601.

16.   Tomcin, S.; Kelsch, A.; Staff, R. H.; Landfester, K.; Zentel, R.; Mailänder, V. HPMA-based block copolymers promote differential drug delivery kinetics for hydrophobic and amphiphilic molecules. *Acta Biomaterialia*, **2016**, *35*, 12–22.

17.   Xie, M.; Wang, S.; Singh, A.; Cooksey, T. J.; Marquez, M. D.; Bhattarai, A.; Kourentzi, K.; Robertson, M. L. Fluorophore exchange kinetics in block copolymer micelles with varying solvent– fluorophore and solvent–polymer interactions. *Soft Matter*, **2016**, *12*, 6196–6205.

18.   Bains, A.; Wulff, J. E.; Moffitt, M. G.; Moffitt, M. G. Microfluidic synthesis of dye-loaded polycaprolactone-block-poly(ethylene oxide) nanoparticles: Insights into flow-directed loading and in vitro release for drug delivery. *Journal of Colloid And Interface Science*, **2016**, *475*, 136–148.

19.   Zana, R. Fluorescence studies of amphiphilic block copolymers in solution. In: *Amphiphilic block copolymers: self assembly and applications*; Alexandridis, P., Lindman, B., Eds.; Elsevier: Amsterdam, 2000; pp 221–52.

20. Riess, G. Micellization of block copolymers. *Progress in Polymer Science*, **2003**, *28*, 1107-1170.

21. Oranli, L.; Bahandur, P.; Riess, G. Hydrodynamic studies on micellar solutions of styrene-butadiene block copolymers in selective solvents. *Canadian Journal of Chemistry*, **1985**, *63*, 2691–2696

22. Lu, J.; Bates, F. S.; Lodge, T. P. Addition of Corona Block Homopolymer Retards Chain Exchange in Solutions of Block Copolymer Micelles. *Macromolecules*, **2016**, *49*, 1405–1413

23. Polymer Source Inc. P10599-BdEO data sheet. https://www.polymersource.com/dataSheet/P10599--BdEO.pdf (accessed March 14, 2017)

24. Gohy, J. F. Block Copolymer Micelles. *Advances in Polymer Science*, **2005**, *190*, 65-136.

25. Karayianni, M.; Pispas, S. *Self-Assembly of Amphiphilic Block Copolymers in Selective Solvents*. In *Fluorescence Studies of Polymer Containing Systems*; Prochàzka, K., Ed.; Springer Series on Fluorescence 16; Springer International Publishing: Switzerland, 2016; pp 27-63.

26. Mai, Y. Y.; Eisenberg, A. Self-assembly of block copolymers. *Chemical Society Reviews*, **2012**, *41*, 5969-5985.

27. LoPresti, C.; Lomas, H.; Massignani, M.; Smart, T.; Battaglia, G. Polymersomes: nature inspired nanometer sized compartments. *Journal of Materials Chemistry*, **2009**, *19*, 3576–3590.

28. Zhu, J.; Hayward, R. C. Spontaneous Generation of Amphiphilic Block Copolymer Micelles with Multiple Morphologies through Interfacial Instabilities. *Journal of the American Chemical Society,* **2008**, *130*, 7496–7502.

29. Menger, F. M.; Angelova, M. I. Giant Vesicles: Imitating the Cytological Processes of Cell Membranes. *Accounts of Chemical Research*, **1998**, *31*, 789–797.

30. Caruso, F. Nanoengineering of Particle Surfaces. *Advanced Materials*, **2001**, *13*, 11–22.

31. Shum, H. C.; Kim, J.-W.; Weitz, D. A. Microfluidic Fabrication of Monodisperse Biocompatible and Biodegradable Polymersomes with Controlled Permeability. *Journal of the American Chemical Society*, **2008**, *130*, 9543–9549.

32. Liu, J.; Lee, H.; Allen, C. Formulation of drugs in block copolymer micelles: drug loading and release. *Current Pharmaceutical Design*, **2006**, *12*, 4685-4701.

33. Gaucher, G.; Dufresne, M. H.; Sant, V. P.; Kang, N.; Maysinger, D.; Leroux, J. C. Block copolymer micelles: Preparation, characterization and application in drug delivery. *Journal of Controllled Release*, **2005**, *109*, 169–188.

34. Croy, S. R.; Kwon, G. S. The effects of Pluronic block copolymers on the aggregation state of nystatin. *Journal of Controllled Release*, **2004**, *95*, 161–171.

35. Batrakova, E. V.; Li, S.; Miller, D. W.; Kabanov, A. V. Pluronic P85 Increases Permeability of a Broad Spectrum of Drugs in Polarized BBMEC and Caco-2 Cell Monolayers. *Pharmaceutical Research,* **1999**, *16*, 1366–1372.

36. Allen, C.; Han, J.; Yu, Y.; Maysinger, D.; Eisenberg, A. Polycaprolactone–b-poly(ethylene oxide) copolymer micelles as a delivery vehicle for dihydrotestosterone. *Journal of Controllled Release*, **2000**, *63*, 275–286.

37. Allen, C.; Yu, Y.; Maysinger, D.; Eisenberg, A. Polycaprolactone-b-poly(ethylene Oxide) Block Copolymer Micelles as a Novel Drug Delivery Vehicle for Neurotrophic Agents FK506 and L-685,818. *Bioconjugate Chemistry*, **1998**, *9*, 564–572.

38. Liu, J.; Xiao, Y.; Allen, C. Polymer–Drug Compatibility: A Guide to the Development of Delivery Systems for the Anticancer Agent, Ellipticine. *Journal of Pharmaceutical Sciences*, **2004**, *93*, 132–143.

39. Yokoyama, M.; Satoh, A.; Sakurai, Y.; Okano, T.; Matsumura, Y.; Kakizoe, T.; Kataoka, K. Incorporation of water-insoluble anticancer drug into polymeric micelles and control of their particle size. *Journal of Controllled Release*, **1998**, *55*, 219–229.

40.   Le Garrec, D.; Gori, S.; Luo, L.; Lessard, D.; Smith, D. C.; Yessine, M.-A.; Ranger, M.; Leroux, J.-C. Poly(N-vinylpyrrolidone)-block-poly(D,L-lactide) as a new polymeric solubilizer for hydrophobic anticancer drugs: in vitro and in vivo evaluation. *Journal of Controlled Release*, **2004**, *99*, 83–101.

41.   Jette, K. K.; Law, D.; Schmitt, E. A.; Kwon, G. S. Preparation and Drug Loading of Poly(Ethylene Glycol)-block- Poly(ε-Caprolactone) Micelles Through the Evaporation of a Cosolvent Azeotrope. *Pharmaceutical Research*, **2004**, *21*, 1184–1191.

42.   Kohori, F.; Yokoyama, M.; Sakai, K.; Okano, T. Process design for efficient and controlled drug incorporation into polymeric micelle carrier systems. *Journal of Controlled Release*, **2002**, *78*, 155–163.

43.   Fournier, E.; Dufresne, M.-H. N.; Smith, D. C.; Ranger, M.; Leroux, J.-C. A Novel One-Step Drug-Loading Procedure for Water-Soluble Amphiphilic Nanocarriers. *Pharmaceutical Research*, **2004**, *21*, 962–968

44.   Yokoyama, M.; Opanasopit, P.; Okano, T.; Kawano, K.; Maitani, Y. Polymer Design and Incorporation Methods for Polymeric Micelle Carrier System Containing Water-insoluble Anti-cancer Agent Camptothecin. *Journal of Drug Targeting*, **2004**, *12*, 373–384.

45.   Parnell, A. J.; Tzokova, N.; Topham, P. D.; Adams, D. J.; Adams,S.; Fernyhough, C. M.; Ryan, A. J.; Jones, R. A. L. The efficiency of encapsulation within surface rehydrated polymersomes. *Faraday Discussions*, **2009**, *143*, 29−46.

46.   Binder, W. H.; Sachsenhofer, R.; Farnik, D.; Blaas, D. Guiding the location of nanoparticles into vesicular structures: a morphological study. *Physical Chemistry Chemical Physics,* **2007**, *9*, 6435–6441.

47.   Lee, J. C-M.; Bermudez, H.; Discher, B. M.; Sheehan, M. A.; Won, Y. Y.; Bates, F. S.; Discher, D. E. Preparation, stability, and in vitro performance of vesicles made with diblock copolymers. *Biotechnology and Bioengineering,* **2001**, *73*, 135–145.]

48.   Mueller, W.; Koynov, K.; Fischer, K.; Hartmann, S.; Pierrat, S.; Basché, T.; Maskos, M. Hydrophobic Shell Loading of PB-b-PEO Vesicles. *Macromolecules,* **2009**, *42*, 357–361.

49.   Li, S.; Byrne, B.; Welsh, J.; Palmer, A. F. Self-Assembled Poly(butadiene)-b-poly(ethylene oxide) Polymersomes as Paclitaxel Carriers. *Biotechnology Progress,* **2007,** *23***,** 278–285.

50.   Henderson, I. M.; Collins, A. M.; Quintana, H. A.; Monta, G. A.; Martinez, J. A.; Paxton, W. F. Lights on: Dye dequenching reveals polymersome fusion with polymer, lipid and stealth lipid vesicles. *Polymer,* **2016**, *83*, 239–245.

51.   Kwon, G. S.; Okano, T. Polymeric micelles as new drug carriers. *Advanced Drug Delivery Reviews,* **1996**, *21*, 107–116.

52.   Hiemenz, P. C.; Rajagopalan, R. *Principles of Colloid and Surface Chemistry*, 3rd ed.; CRC Press Taylor & Francis Group: Boca Raton, FL, 1997.

53.   Bhattacharjee, S. DLS and zeta potential – What they are and what they are not? *Journal of Controlled Release,* **2016**, *235*, 337–351.

54.   Thomas, J. C. The determination of log normal particle size distributions by dynamic light scattering. *Journal of Colloid and Interface Science*, **1987**, *117*, 187- 192.

55.   Kaszuba, M.; Connah, M. T.; McNeil-Watson, F. K.; Nobbmann, U. Resolving Concentrated Particle Size Mixtures Using Dynamic Light Scattering. *Particle and Particle Systems Characterization*, **2007**, *24*, 159–162.

56.   Hussain, S. A. An Introduction to Fluorescence Resonance Energy Transfer (FRET). *Science Journal of Physics,* **2012**, *201*, 1-4.

57.   Jonsson, T.; Waldburger, C. D.; Sauer, R. T. Nonlinear Free Energy Relationships in Arc Repressor Unfolding Imply the Existence of Unstable, Native-like Folding Intermediates. *Biochemistry*, **1996**, *35*, 4795–4802.

58.   Clegg, R. M.; Murchie, A. I. H.; Lilley, D. M. J. The Solution Structure of the Four-Way DNA Junction at Low-Salt Conditions: A Fluorescence Resonance Energy Transfer Analysis. *Biophysical Journal*, **1994**, *66*, 99–109.

59.   Berger, W.; Prinz H.; Striessnig, J.; Kang, H.-C.;, Haugland, R.; Glossmann, H. Complex molecular mechanism for dihydropyridine binding to L-type Ca2+-channels as revealed by fluorescence resonance energy transfer. *Biochemistry*, **1994**, *33*, 11875-11883.

60.   Held, P. An Introduction to Fluorescence Resonance Energy Transfer
       (FRET) Technology and its Application in Bioscience.
       http://www.biotek.com/resources/articles/fluorescence-resonance-energy-
       transfer.html (accessed January 10, 2017).

61.   Marras, S. A. E. Interactive Fluorophore and Quencher Pairs for Labeling
       Fluorescent Nucleic Acid Hybridization Probes. *Molecular Biotechnology*,
       2008, *38*, 247–255.

62.   Biosearch Technologies. http://blog.biosearchtech.com/know-your-oligo-
       mod-bhq-black-hole-quencher-dyes (accessed April 2, 2017)

63.   Weber, G. Polarization of the fluorescence of solutions. In *Fluorescence
       and Phosphorescence Analysis. Principles and Applications*; Hercules, D.
       M., Ed.; Interscience Publishers (J. Wiley & Sons): New York, 1966; pp
       217-240.

64.   Johansson, M. K. Choosing Reporter–Quencher Pairs for Efficient
       Quenching Through Formation of Intramolecular Dimers. In *Fluorescent
       Energy Transfer Nucleic Acid Probes: Designs and Protocols*; Didenko, V.
       V., Ed. Methods in Molecular Biology, vol. 335; Humana Press Inc.:
       Totowa, NJ, 2006; pp 17-29

65.   ThermoFisher Fluorescence SpectraViewer.
       https://www.thermofisher.com/us/en/home/life-science/cell-
       analysis/labeling-chemistry/fluorescence-spectraviewer.html (accessed
       April 2, 2017)

66.   Förster, T. Zwischenmolekulare Energiewanderung und Fluoreszenz.
       (Intermolecular Energy Migration and Fluorescence.) *Annalen Der Physik*,
       1948, *437*, 55–75.

67.   M. Orrit. Leiden Institute of Physics, The Netherlands. Lecture notes for
       Single-Molecule Optics course, 2016. www.single-molecule.nl (accessed
       Jan 10, 2017)

68.   Marras, S. A. E.; Kramer, F. R.; Tyagi, S. Effciencies of fluorescence
       resonance energy transfer and contact-mediated quenching in
       oligonucleotide probes. *Nucleic Acids Research*, **2002**, *30*, e122.

69.   ThermoFisher. https://www.thermofisher.com/us/en/home/life-science/cell-
       analysis/fluorophores/bodipy-fl.html (accessed January 13, 2017)

70. ThermoFisher. https://www.thermofisher.com/us/en/home/life-science/cell-analysis/fluorophores/cy3-dye.html (accessed January 13, 2017)

71. ThermoFisher. https://www.thermofisher.com/us/en/home/life-science/cell-analysis/fluorophores/tritc-dye.html (accessed January 13, 2017)

72. Zanetti-Domingues, L. C.; Tynan, C. J.; Rolfe, D. J.; Clarke, D. T.; Martin-Fernandez, M. Hydrophobic Fluorescent Probes Introduce Artifacts into Single Molecule Tracking Experiments Due to Non- Specific Binding. *PLoS One*, **2013**, *8*, e74200.

73. ThermoFisher. https://www.thermofisher.com/us/en/home/references/molecular-probes-the-handbook/fluorophores-and-their-amine-reactive-derivatives/long-wavelength-rhodamines-texas-red-dyes-and-qsy-quenchers.html (accessed January 13, 2017)

74. Biosearch Technologies. https://www.biosearchtech.com/support/education/fluorophores-and-quenchers/black-hole-quencher-dyes (accessed April 2, 2017)

75. Spectral Overlay Tool by Biosearch Technologies. http://www.qpcrdesign.com/spectral-overlay

76. Schwartz, J. J.; Quake, S. R. Single molecule measurement of the "speed limit" of DNA polymerase. *Proceedings of the National Academy of Sciences*, **2009**, 106, 20294-20299.

77. ThermoFisher Fluorescence SpectraViewer. https://www.thermofisher.com/us/en/home/life-science/cell-analysis/labeling-chemistry/fluorescence-spectraviewer.html (accessed January 26, 2017)

78. O'Hare, S. Product Specialist Biosearch Technologies, Novato, CA. Personal correspondence, 2017.

79. Lumiprobe, Cyanine3 alkyne https://www.lumiprobe.com/p/cy3-alkyne (accessed January 23, 2017)

80. Chen, H.-Y. Product Specialist Biosearch Technologies, Novato, CA. Personal correspondence, 2017.

81. Biosearch Technologies, BHQ-2 amdite. https://www.biosearchtech.com/products/synthesis-reagents/amidites/bhq2-amidite (accessed January 23, 2017)

82. Smallwood, I. M. *Handbook of organic solvent properties*; Arnold (Hodder Headline Group): London, 1996

83. Oba, Y.; Poulson, S. R. Octanol-water partition coefficients (K_{ow}) vs. pH for fluorescent dye tracers (fluorescein, eosin Y), and implications for hydrologic tracer tests. *Geochemical Journal*, **2012**, *46*, 517–520.

84. Leo, A.; Hansch, C.; Elkins, D. Partition Coefficients and Their Uses. *Chemical Reviews*, **1971**, *71*, 525–616.

Chapter 3

RESULTS AND DISCUSSION

Chapter 3 explores the encapsulation of dyes into micelles and the characteristics of these dye-loaded micelles, before the exchange of dyes between micelles is investigated. Section 3.1 gives an introduction into the proposed mechanism for this exchange between micelles. The size of micelles is investigated using DLS in section 3.2. In section 3.3, verification of dye encapsulation is attempted through various experimental methods. Section 3.4 explores the dye exchange between micelles, in quiescent environment, and by vortex mixing. The self-quenching effect and its consequences for the obtained results is also discussed.

3.1 Introduction

As concluded in the first chapter, the diffusion-based pathway is unlikely to be the dominant mechanism for the exchange of dyes between poly(butadiene-*b*-ethylene oxide) micelles, due to the very hydrophobic polybutadiene (PB) core (interaction parameter $\chi \sim 3.5$) and the hydrophobic dyes.[1-3] Because of this high interaction parameter of PB with water, kinetically trapped micelles are obtained in selective solvent (water) under quiescent conditions, with no chain exchange occurring for several days.[4] As a result, dye exchange is expected to occur solely through a collision-based pathway. Amphiphilic block copolymers have a strong affinity for the air-water interface and surfactants based on poly(ethylene oxide) (PEO), specifically, adsorb strongly to the air-water interface.[5-7] Murphy and co-workers demonstrated that

chain exchange is mediated through the air-water interface and is a surface-limited process for which significant interface turnover is necessary for complete chain exchange.[4] Complete chain exchange was observed after about 10 min of vortex mixing at 3200 rpm, for a 2.4 mg/mL PB-PEO sample.[4] The cargo exchange between micelles is expected to follow the same mechanism as described by Murphy et al., considering the collision-based pathway is closely related to chain exchange.[2] Figure 3.1 demonstrates schematically the process of dye exchange between micelles through the air-water interface. Micelles adsorb to newly generated air-water interface, exchange cargo (dyes) and desorb when the air-water interface collapses.
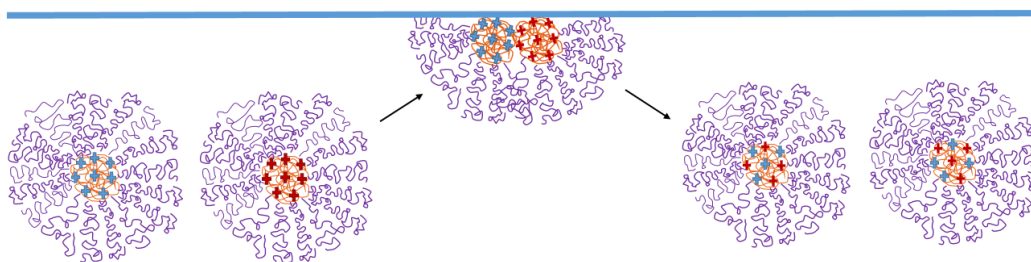
Figure 3.1:   Schematic representation of dye exchange between micelles at the air-water interface.

3.2   Micelle sizes

Using dynamic light scattering (DLS), the size of micelles in a 2.5 mg/mL PB-PEO aqueous solution are obtained. The size of the micelles, further referred to as "empty micelles," was 85.0 ± 1.4 nm, with a polydispersity index (PDI) of 0.194 ± 0.004. Fractionation of the block copolymer did not influence the micelle size: the micelle size before fractionation was 86.2 ± 1.4 nm, while the PDI was slightly higher at 0.212 ± 0.008.

The size of micelles loaded with dye (cyanine3 alkyne and BHQ-2 amidite) in a 2.5 mg/mL PB-PEO aqueous solution can also be obtained. However, results should be interpreted with care, because ideally DLS on colored and fluorescent samples should be avoided.[8] Fluorophores and other dyes can absorb incident light and reduce the intensity of the scattered light, which results in a loss of sensitivity.[9] Fluorophores also emit non-coherent light, which is detected as baseline noise and reduces the data quality.[9] Bhattacharjee reports that the particle sizes obtained by DLS measurements could be lower than in reality due to fluorophores absorbing incident light.[8] Geißler et al. contradict this statement with a study on polymer nanoparticles stained with fluorescent dyes. Comparison of DLS and SAXS measurements on nanoparticles stained with dye and blank samples (non-stained nanoparticles) showed no significant differences in size or distribution.[9]

The wavelength of the laser used in the DLS experiments is 532 nm. The maximum absorption of Cy3 and BHQ-2 is at a wavelength of 552nm and 579 nm, respectively. The dyes thus absorb in the range of the laser wavelength, as is also shown in Figure 3.2. For higher concentrations of dye (∼0.03 mg/mL for cyanine3 alkyne and ∼0.08 mg/mL BHQ-2 amidite), DLS could not be performed because of complete absorption of the laser light by the colored solution. Possibly, artificially smaller particle sizes are obtained with these DLS measurements due to the dyes (partially) absorbing the incident light.[8]
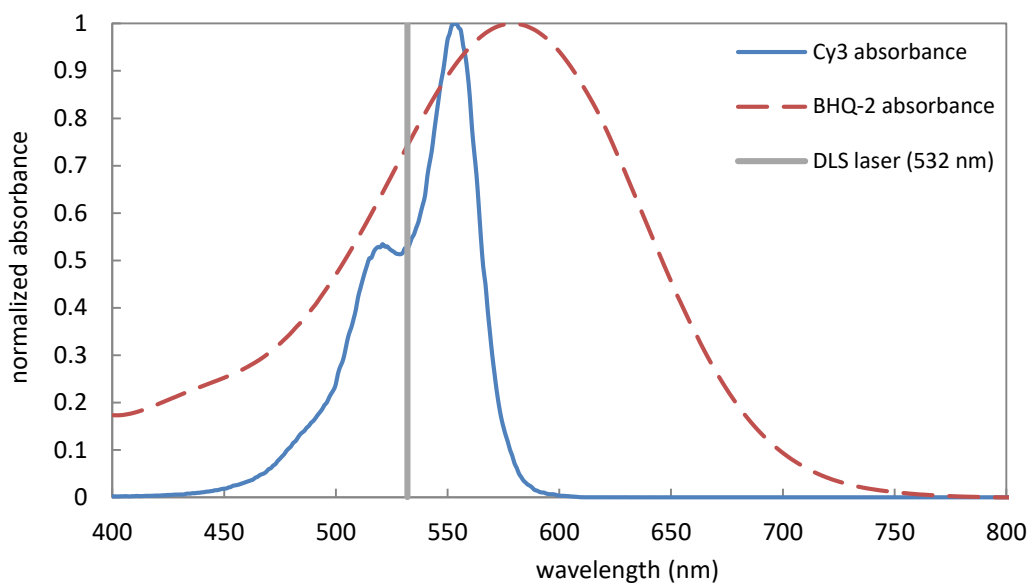
Figure 3.2: Cy3 and BHQ-2 absorption spectra, compared to the DLS laser wavelength. Data for the absorption spectra was obtained from ThermoFisher and Biosearch Technologies.[10,11]

Table 3.1: The hydrodynamic diameter and polydispersity index of PB-PEO micelles, with or without dye loaded inside, obtained with DLS measurements.

	D_h (nm)	PDI
Empty micelles	85.0 ± 1.4	0.194 ± 0.004
Cy3 micelles	87.9 ± 12.6	0.213 ± 0.045
BHQ-2 micelles	83.6 ± 3.7	0.186 ± 0.008
Premixed micelles	84.2 ± 4.2	0.195 ± 0.005

Micelles loaded with cyanine3 alkyne dye, further referred to as "Cy3 micelles", had an average size of 87.9 ± 12.6 nm and average PDI of 0.213 ± 0.045. Micelles loaded with BHQ-2 amidite dye, further referred to as "BHQ-2 micelles," had an average size of 83.6 ± 3.7 nm and PDI of 0.186 ± 0.008. "Premixed micelles," having both dyes loaded in the micelles, had an average size of 84.2 ± 4.2 nm and PDI of 0.195 ± 0.005. Results are summarized in Table 3.1. Loading with dyes does not seem to influence the size of the micelles, when comparing with the previous results for empty micelles. However, due to the solutions being colored, these reported sizes might be smaller than in reality. The sizes of the dye-loaded micelles are also not dependent upon the concentration of dye, as demonstrated in Figure 3.3.
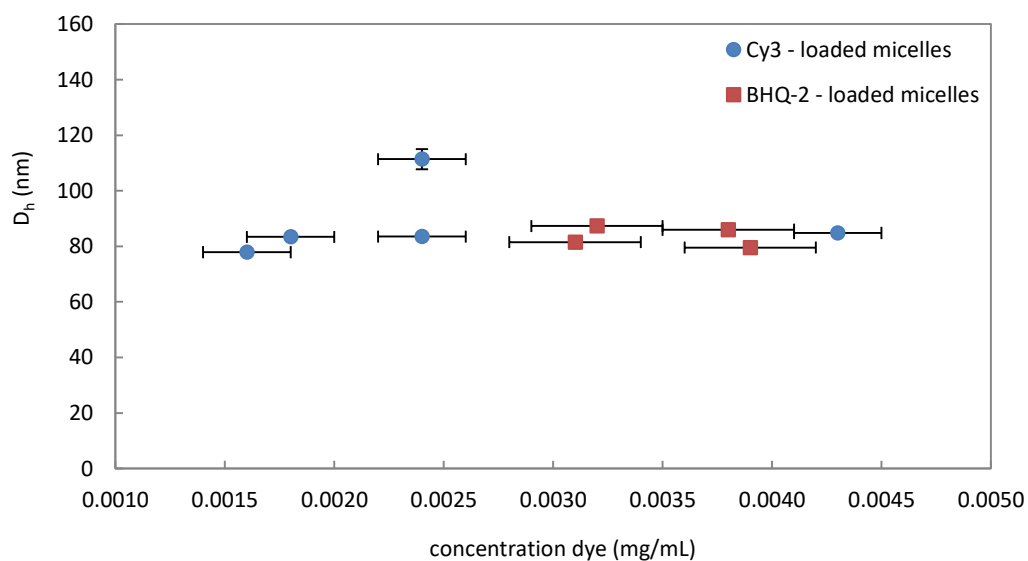
Figure 3.3:   The hydrodynamic diameter of micelles loaded with Cy3 and BHQ-2 for various concentrations of dye. The vertical error bars represent the 95% confidence interval based on three replicate DLS measurements on the same sample. The horizontal error bars represent the error on the concentration (Table 2.1).

3.3   Encapsulation of dyes

Due to the hydrophobic nature of the dyes and the use of the thin film preparation method, it is assumed that dye molecules are encapsulated within the micelles and located in the core. This assumption was tested through various experiments, including UV-Vis spectroscopy, dialysis, ultracentrifugation, and fluorescence spectroscopy. The octanol-water partition coefficient of both dyes was estimated from experimental measurements, to determine a measure for the equilibrium separation between the dye molecules in the core and the molecules in the hydrophilic phases, i.e. the corona and aqueous phase.

3.3.1   UV-Vis spectroscopy

To test the assumption that the hydrophobic dyes are loaded into the micelles during preparation of the micelle solution, a UV-Vis spectroscopy experiment was set up. Solutions were prepared of both dyes, with and without polymer, following the same procedure (thin film rehydration). For the polymer solutions, a film was obtained after evaporation of chloroform, while the dye was unevenly distributed on the bottom of the vial for the other samples. Upon rehydration of the "films," the dyes in the sample which no added polymer did not go completely into solution. Dye adsorbed to the Teflon stir bar and did not fully desorb from the glass vial. These effects did not occur for the polymer solutions, most likely due to the formation of polymer micelles, which solubilized the dye molecules. The UV-Vis spectra of the samples are shown in Figure 3.4. The absorbance is higher for solutions in which polymer was added because the dyes did go completely into solutions whereas this was not the case for the dye solutions without polymer. The polymer background was corrected for the polymer containing samples and the spectra are an average of three UV-Vis

absorbance measurements. Note that the concentration of aqueous dye solutions does not necessarily indicate the solubility of the dyes in water, due to the effects of dye adsorption to the stir bar and glass vial.
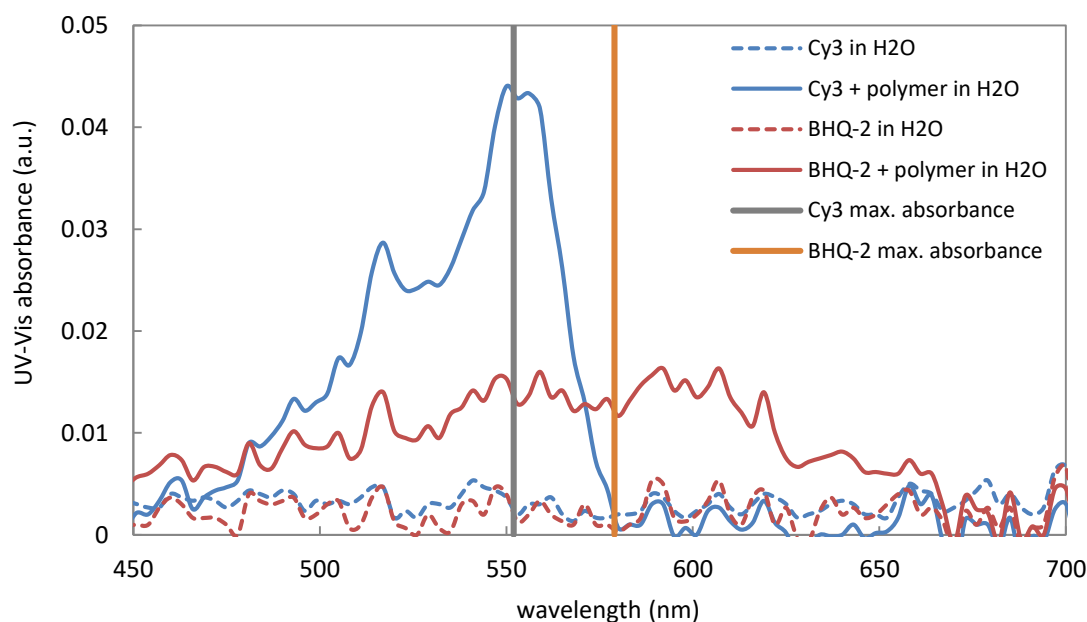
Figure 3.4:   UV-Vis absorption spectra of Cy3 and BHQ-2 in aqueous solution, with and without PB-PEO polymer.

3.3.2   Dialysis

Dialysis was performed on dye-loaded micelle solutions to assess whether dye molecules were loaded in the micelles in a stable manner or if an equilibrium situation existed between the concentration of the dye in the core and in the aqueous phase. Stable loading of dyes in micelles would be expected due to the hydrophobic nature of the dyes, the very hydrophobic PB core, and the kinetically trapped nature of the micelles. If dye molecules migrate in and out of the micelles, an equilibrium situation

would occur between the dye concentration in the micelles and the concentration in the aqueous phase.

Table 3.2 gives the dye and polymer concentrations the Cy3 – loaded and BHQ-2 – loaded micelle solutions before and after dialysis. The concentration of Cy3 decreased by 63% after dialysis. Due to swelling of the dialysis tubing, the polymer concentration decreased as well, by 20%. The ratio of dye per polymer thus decreased, from 0.063 to 0.032 wt% Cy3 dye-to-polymer. The concentration of BHQ-2 did not change after dialysis. The polymer concentration did decrease by 16% due to swelling of the dialysis tubing. The ratio of dye per polymer thus seemed to increase, from 0.150 to 0.178 wt% BHQ-2 dye-to-polymer, which is not a physically possible situation as no dye was added to the system. However, the dye-to-polymer ratio after dialysis was within error of the ratio before dialysis.

Table 3.2: Dye and polymer concentration in solutions of Cy3 and BHQ-2 micelles before and after dialysis.

	before dialysis		after dialysis	
	dye conc. (mg/mL)	polymer conc. (mg/mL)	dye conc. (mg/mL)	polymer conc. (mg/mL)
Cy3 – loaded micelles	0.0016 ± 0.0002	2.5 ± 0.1	0.0006 ± 0.0002	2.0 ± 0.2
BHQ-2 – loaded micelles	0.0038 ± 0.0003	2.5 ± 0.1	0.0038 ± 0.0005	2.1 ± 0.3

The dye-to-polymer ratios are possibly very inaccurate due to the propagation of the errors on the concentration measurement. However, the results do indicate that the Cy3 dye is not encapsulated by the micelles in a stable fashion. The decrease in polymer concentration of 20% is a measure for the dilution of the system due to swelling of the tubing and the decrease in Cy3 concentration (63%) should be compared to this. The concentration of dye thus decreased not only due to the dilution effect, but because Cy3 equilibrated with the external aqueous environment and leached out of the micelles. No decrease in concentration is perceived for BHQ-2, which did seem to contradict the 16% dilution effect, so it is likely stably encapsulated in the micelles. This result also indicates that almost no BHQ-2 dye was free in solution because the free dye molecules would have been removed by dialysis and lowered the concentration. A possible explanation for the different behavior of the two dyes is the hydrophobicity: if BHQ-2 alkyne is more hydrophobic than cyanine3 alkyne, it is less likely to leach out of the hydrophobic polybutadiene core of the micelles into an aqueous environment. The octanol-water partition coefficient can give an indication of the hydrophobicity of a substance.

3.3.3   Octanol-water partition coefficient

The octanol-water partition coefficient K_{ow} or $P_{oct/wat}$ represents the ratio of the concentration of a solute in octanol versus the concentration in water.[12] It is usually expressed as a logarithm, i.e. log K_{ow}. By determining the octanol-water partition coefficient of the dyes, a rough estimate of the equilibrium distribution of dye between the core and the corona or water phase in micelles can be obtained.

The concentrations of the dyes in the 1-octanol and water phases are given in Table 3.3. From these measurements, estimates for the octanol-water partition

coefficients were obtained. The log K_{ow} for cyanine3 alkyne is positive, which indicates a hydrophobic substance. However, because the partition coefficient is relatively small, cyanine3 alkyne is somewhat water soluble, contrary to what was initially reported. BHQ-2 amidite has a log K_{ow} value of 2.30, which indicates it is very hydrophobic, as expected.[12]

Table 3.3:   Concentrations of cyanine3 alkyne and BHQ-2 amidite in the octanol and water phases, and the resulting octanol-water partition coefficient.

	$c_{\text{in octanol}}$ (mg/mL)	$c_{\text{in water}}$ (mg/mL)	log K_{ow}
cyanine3 alkyne	0.0757 ± 0.0172	0.0199 ± 0.0009	0.58
BHQ-2 amidite	0.3120 ± 0.1337	0.0015 ± 0.0003	2.30

3.3.4   Ultracentrifugation

Ultracentrifugation of dye-loaded micelle solutions was performed using a Beckman Coulter Optima L-100 XP Ultracentrifuge at 50,000 rpm and 4 °C. The concentration of dye and polymer in the supernatant can be evaluated by UV-Vis spectroscopy. Initial test runs suggested a minimum polymer concentration in the supernatant was reached after ultracentrifugation for 2.5 h.

Table 3.4 gives the concentrations of dye and polymer in the original micelle solution and in the supernatant after ultracentrifugation for 2.5 h. The concentration of Cy3 was 43% lower and the BHQ-2 concentration was 23% lower in the supernatant after ultracentrifugation compared to the original micelle solutions. The polymer

concentration remaining in the supernatant was about 1 mg/mL, a decrease by approximately 60%. By comparing the ratio of dye versus polymer before and after ultracentrifugation, in theory, an estimate for the encapsulation efficiency is possible. However, due to the propagation of the errors on the concentration determinations of dye and polymer, the calculated efficiencies are extremely imprecise: the encapsulation efficiency ranges from 40% to 97% for Cy3 and 41% to 86% for BHQ-2.

Table 3.4: Dye and polymer concentration in Cy3 and BHQ-2 micelles solutions before ultracentrifugation and in the supernatant after ultracentrifugation.

	before ultracentrifugation		after ultracentrifugation	
	dye conc. (mg/mL)	polymer conc. (mg/mL)	dye conc. (mg/mL)	polymer conc. (mg/mL)
Cy3 – loaded micelles	0.0018 ± 0.0002	2.5 ± 0.1	0.0010 ± 0.0002	0.9 ± 0.3
BHQ-2 – loaded micelles	0.0039 ± 0.0003	2.5 ± 0.1	0.0030 ± 0.0002	1.1 ± 0.3

3.3.5 Fluorescence

Figure 3.5 compares the fluorescence of a solution of Cy3 micelles to the fluorescence of cyanine3 alkyne dissolved in water. Both of these solutions have a Cy3 concentration of 0.0024 mg/mL (0.0024 ± 0.0002 mg/mL and 0.0024 ± 0.0005 mg/mL, respectively). The fluorescence of the free dye solution is about 68% lower

than the solution containing micelles. Partitioning of fluorophores increases the fluorescence intensity, due to a higher local concentration.[13,14] In the micelle solution, the dye is encapsulated within the micelle and thus has a higher local concentration than the homogeneously dispersed dye in aqueous solution. As a result, this difference in fluorescence intensity between two solutions with equal Cy3 concentration proves that the dye is, at least for a large part, encapsulated within the micelles.
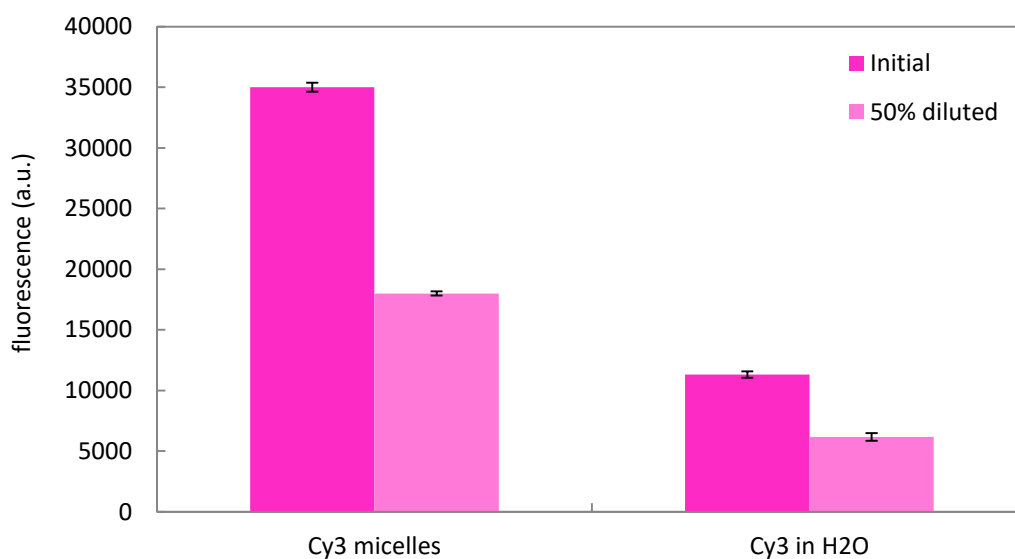
Figure 3.5:   Fluorescence intensity of aqueous solutions of Cy3 micelles and of cyanine3 alkyne, and fluorescence intensities of 50% diluted solutions. The error bars represent the 95% confidence interval based on measurements from three different samples.

3.3.6   Summary

UV-Vis spectroscopy experiments demonstrated solubilization, presumably by encapsulation, of dyes by micelles in a qualitative manner. Dyes are likely encapsulated within the micelles with a minimum efficiency of 40%, and possibly

much higher, as determined by ultracentrifugation experiments. The encapsulation of cyanine3 alkyne was verified by fluorescence intensity measurements of a micelle solution and a free dye solution. Octanol-water partition coefficients demonstrated that cyanine3 alkyne is only slightly hydrophobic. Dialysis experiments confirmed that Cy3 is not stably encapsulated within the micelles and equilibrates with the aqueous phase outside of the micelles. BHQ-2 amidite was determined to be highly hydrophobic based on its octanol-water partition coefficient. Dialysis experiments showed that BHQ-2 does not migrate out of the micelles and also seemed to indicate that little BHQ-2 was free in solution, considering the concentration of BHQ-2 did not decrease after dialysis.

3.4 Dye exchange between micelles

Solutions of Cy3 and BHQ-2 micelles were added together and were kept under quiescent conditions, magnetically stirred, or vortex mixed. The fluorescence was normalized to the fluorescence of a solution of Cy3 micelles. A solution of BHQ-2 micelles does not have any fluorescence intensity. The fluorescence of a 50% diluted solution of Cy3 micelles was measured as well, so the dilution effect on the fluorescence intensity due to mixing Cy3 micelles with BHQ-2 micelles could be isolated from the quenching effect. Quenching occurs when Cy3 and BHQ-2 molecules into close proximity (< 10 nm) of each other.
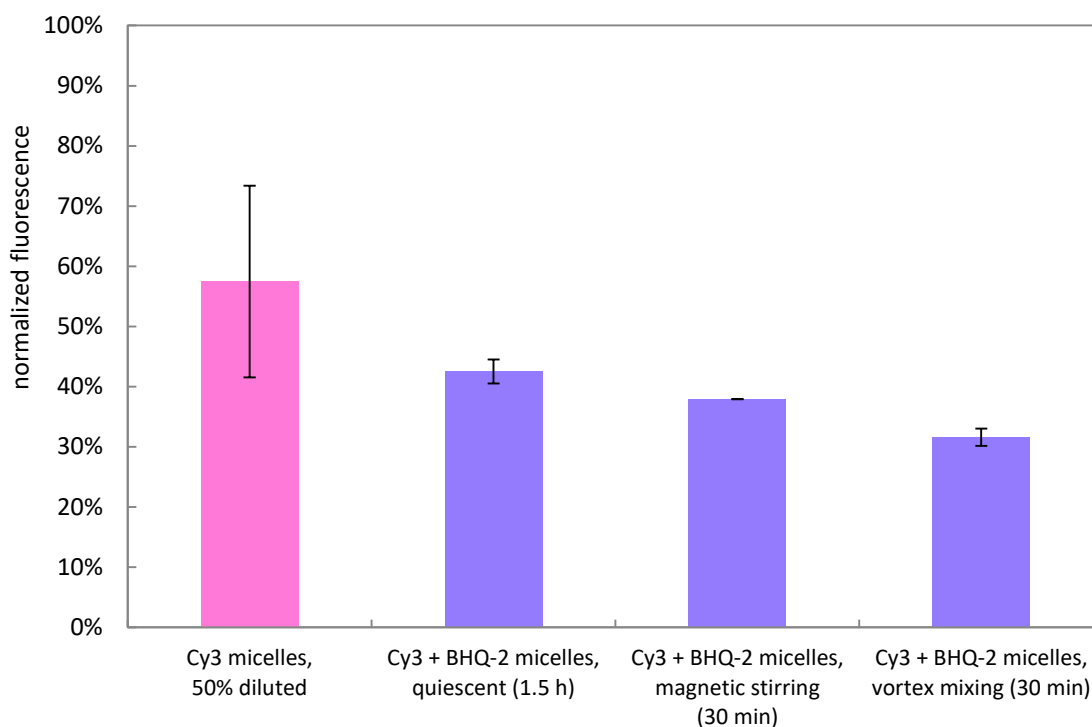
Figure 3.6:   Normalized fluorescence intensities of a diluted Cy3 micelle solution and solutions of Cy3 and BHQ-2 micelles under quiescent, magnetically stirred or vortex mixed conditions. Fluorescence intensities were normalized to the fluorescence intensity of the Cy3 micelle solution. The error bars represent the 95% confidence interval based on measurements from three different samples.

Figure 3.6 shows the difference in normalized fluorescence between the quiescent, magnetically stirred and vortex mixed Cy3 and BHQ-2 micelle solutions, compared to the diluted Cy3 micelle solution. The fluorescence of the quiescent sample is within error of the dilution sample, however, the large error on the fluorescence of the dilution sample is solely due to one outlier in the measurements. As will be further discussed and proven later (section 3.4.1), there seems to be a significant quenching effect for the quiescent sample. The sample that was

magnetically stirred has a slightly lower fluorescence intensity than the quiescent sample and will be compared to quiescent samples in a separate experiment (section 3.4.2). Vortex mixing seems to induce dye exchange between micelles, because the fluorescence is much lower than the diluted sample, as will be covered in section 3.4.3.

3.4.1 Exchange of dyes under quiescent conditions

Several hypotheses are presented to explain the apparent exchange of dyes between micelles in quiescent solutions. First, the hypothesis that the quenching effect is a product of free dye coming into close proximity or binding together in the aqueous phase is investigated. Second, actual exchange of dye between micelles due to a diffusion-based exchange mechanism, with Cy3 dye leaching out of the micelles into solution and consequently diffusing into BHQ-2 micelles, is examined as a possible explanation. Finally, a hypothesis is presented that attributes the apparent exchange of dyes to processing conditions, for example pipetting. Experiments or calculations were carried out to test these hypotheses.

3.4.1.1 Apparent exchange due to free dye in solution

The quenching effect observed during quiescent conditions is usually attributed to the dye molecules being exchanged between micelles. However, if dye molecules free in solution come into close proximity or bind, the total Cy3 fluorescence is also affected and could lead to an incorrect conclusion about apparent exchange of dyes between micelles, while this process is actually not occurring. Previous experiments demonstrated that Cy3 may not be completely encapsulated. A dialysis experiment indicated that BHQ-2 molecules are likely almost fully encapsulated into micelles.

Because both Cy3 and BHQ-2 dye molecules should be present in solution, likely the quiescent quenching effect is not due to free dye in solution. Also, due to the low concentration of Cy3 and BHQ-2 in solution, even if a significant amount is not encapsulated, it is highly unlikely that molecules would be in such close proximity to induce FRET because distances on the order of nanometers are necessary for FRET to occur. Binding of Cy3 and BHQ-2 molecules, which would induce contact quenching, is unlikely without any form of agitation.
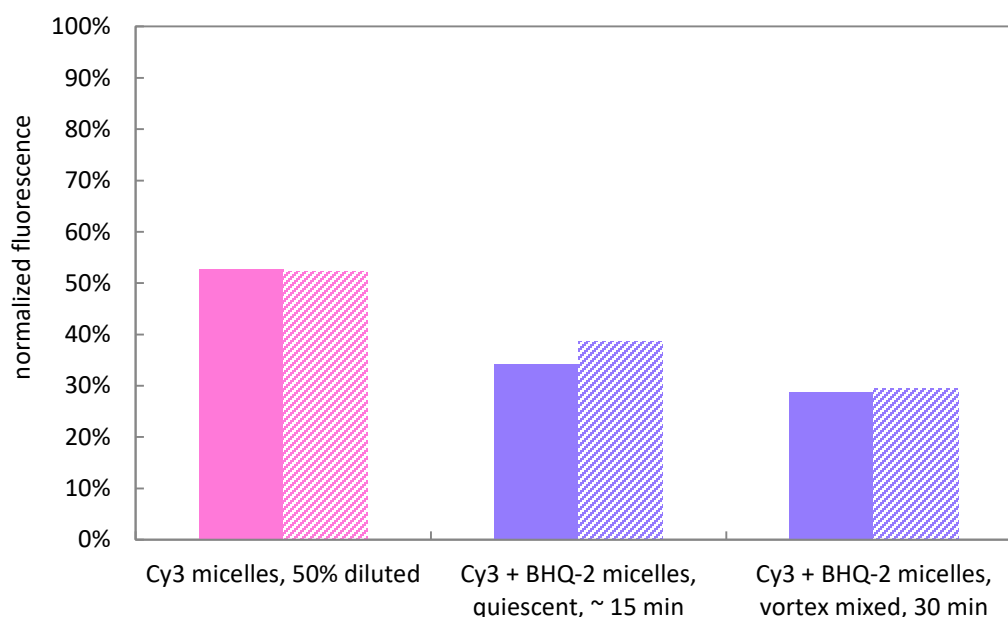

Figure 3.7:   Normalized fluorescence intensities of a diluted Cy3 micelle solution, and solutions of Cy3 and BHQ-2 micelles under quiescent and vortex mixed conditions, before (solid bars) and after (hatched bars) dialysis. Fluorescence intensities were normalized to the fluorescence intensity of the Cy3 micelle solutions before and after dialysis.

In Figure 3.7, the fluorescence of dialyzed Cy3 and BHQ-2 micelle solutions is compared to non-dialyzed solutions. The quenching effect is still visible for a quiescent mixture of Cy3 and BHQ-2 micelles: 26% decrease in fluorescence compared to 48% before dialysis. Considering Cy3 is not stably encapsulated into micelles, some free Cy3 might be present in the aqueous phase after dialysis. However, no BHQ-2 molecules should be present in the aqueous phase. Therefore, the quenching effect cannot be attributed to quenching of free dye molecules in solution.

3.4.1.2 Exchange through a diffusion-based mechanism

Based on the quenching of quiescent mixtures of dialyzed Cy3 and BHQ-2 micelle solutions (Figure 3.7), a diffusion-based process is proposed. In the diffusion-based mechanism, Cy3 molecules leach out of the micelles into the aqueous phase and then diffuse through the solution before entering the BHQ-2 micelles, causing quenching of the fluorescence intensity. The diffusion-based pathway is unlikely for micelles with a highly hydrophobic core like PB-PEO.[1] However, the diffusion-based pathway is also dependent upon the solubility of the compound being exchanged.[2] In this case, the partition coefficient indicates that Cy3 molecules could go into an aqueous solution. The hypothesis of Cy3 molecules leaching out of the micelles and into the aqueous phase is supported by a large decrease in Cy3 concentration after dialysis (section 3.3.2).

Figure 3.8 shows the normalized fluorescence over time for diluted Cy3 micelles and a quiescent solution of Cy3 and BHQ-2 micelles. The fluorescence of the diluted Cy3 micelles stays constant, as expected, as there is no change in fluorescence intensity when Cy3 is in core of micelle versus when leaching out into the solution when there is no self-quenching of Cy3 (section 3.4.4). If Cy3 were leaching out of the

micelles and into BHQ-2 micelles, a steady decrease in fluorescence intensity over time for the Cy3 and BHQ-2 micelle solution would be expected, which is not the case. The quenching effect also appears to be almost instantaneous because the drop in fluorescence compared to the dilution effect occurs within the lag time between set-up of the experiment and measurement, which is about 1 min.
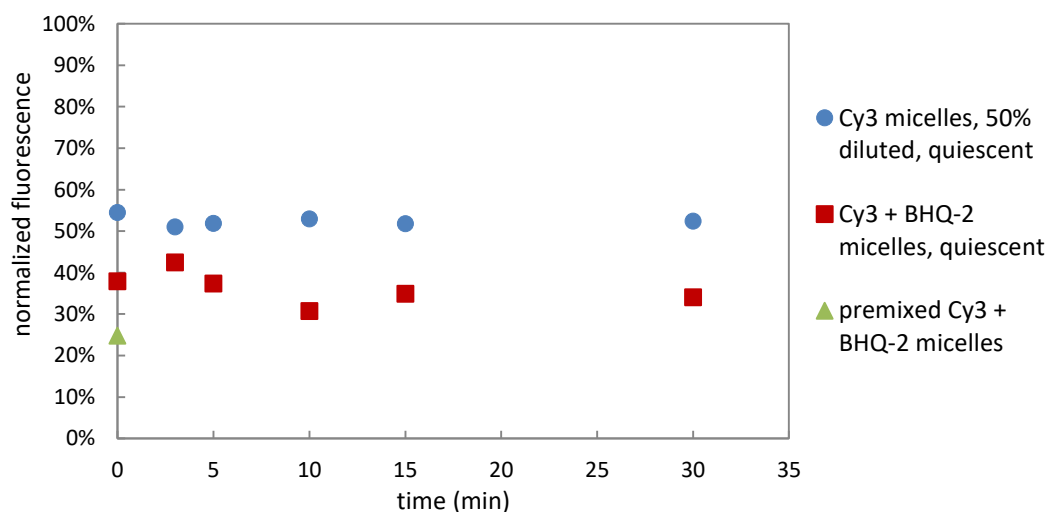
Figure 3.8:   Normalized fluorescence intensities of a diluted Cy3 micelle solution, and a solution of Cy3 and BHQ-2 micelles under quiescent conditions over various time spans. The normalized fluorescence intensity of a solution of premixed Cy3 and BHQ-2 micelles is included as a reference. Fluorescence intensities were normalized to the fluorescence intensity of the Cy3 micelle solution.

The diffusion-based mechanism consists of three steps: leaching out of Cy3 molecules into solution, diffusion through the solution and re-entry into BHQ-2 micelles. Considering the complete process could not be observed, the processes are isolated. The estimation of the partition coefficient and the dialysis experiment have

shown that it might be possible for cyanine3 to leach out of micelles. Now the last step in the diffusion-based pathway is investigated by observing if free cyanine 3 in solution would migrate into the BHQ-2 micelles. Without this process occurring alongside the other two, quenching due to the diffusion-based exchange is not possible.
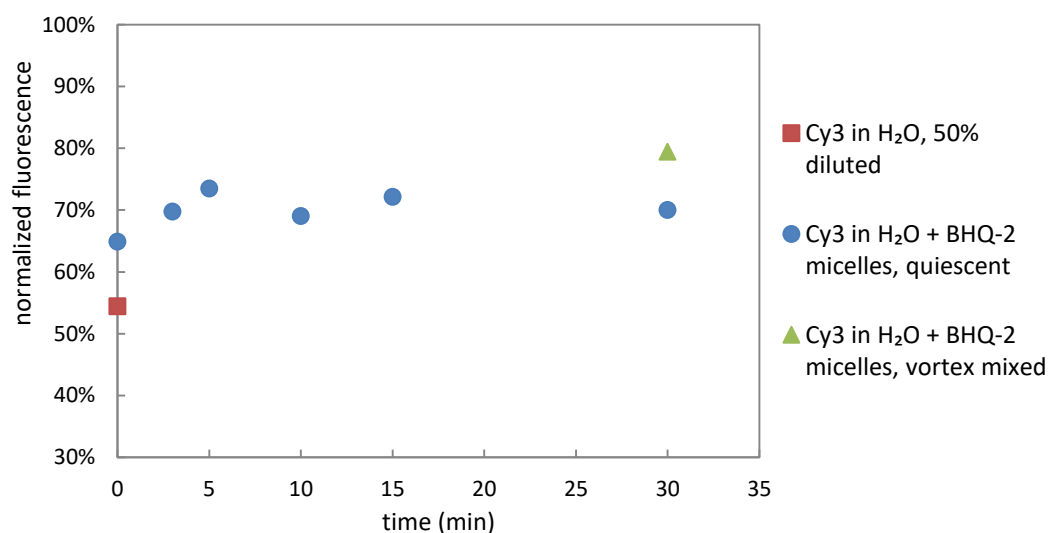
Figure 3.9:   Normalized fluorescence intensities of a mixture of a solution of Cy3 in water added to a BHQ-2 micelle solution, under quiescent conditions over various time spans. The normalized fluorescence intensities of a diluted Cy3 solution, and a vortex mixed solution of Cy3 in water and BHQ-2 micelles are also included as a reference. Fluorescence intensities were normalized to the fluorescence intensity of the Cy3 aqueous solution.

Figure 3.9 shows no decrease in fluorescence over time, which is what would be expected if Cy3 diffused from the solution into BHQ-2 micelles. Conversely, the fluorescence increases over time and is also higher for a vortex mixed Cy3 and BHQ-2

micelle solution. One possible explanation for this increase is that some Cy3 molecules would diffuse into corona of the BHQ-2 micelles, but do not move into the core. This relocation to the corona would cause a higher local concentration of Cy3, which results in a higher fluorescence (see section 3.3.5). Considering the partition coefficient of cyanine3 alkyne indicating that it is not very hydrophobic, the corona environment consisting of PEO chains may be a favorable location for Cy3 molecules. It is clear that free Cy3 molecules do not migrate into the core and cause quenching, thus making the diffusion-based process an unlikely cause of quenching under quiescent conditions.

3.4.1.3   Exchange due to processing conditions

The fluorescence of the quiescent Cy3 and BHQ-2 micelle solution does not decrease over time, but is lower than the fluorescence of the diluted Cy3 micelle solution. This "instantaneous" quenching suggests that the processing conditions during the experimental set-up may be the cause of the observed quenching under quiescent conditions. One possibility is that, during pipetting of the solutions, the air-water interface is disturbed enough to cause significant exchange of dyes between micelles. If the pipetting of the solution of BHQ-2 micelles into the solution of Cy3 micelles is represented as adding 3 μL drops, an estimate of the amount of micelles at the air-water interface which could undergo exchange of cargo can be made.

At a block copolymer concentration of 2.5 mg/mL and a molecular weight of 17 kg/mol, about 10^{17} chains of block copolymer per milliliter are present in the polymer solution. Kelley et al. determined that the aggregation number of PB-PEO micelles in aqueous is equal to 791.[15] This analysis was performed with a specific PB-PEO that included a 1,2-PB block and a PEO block that had a different molecular

100

weight. However, this aggregation number can be used as a rough estimate. Assuming all chains are incorporated into micelles, which is reasonable considering the very low CMC (on the order of 10^{-7} mol/L), the polymer solution contains about 10^{14} micelles per milliliter.[16] In a 3 μL droplet of this solution, approximately 10^{11} micelles are present. Zell et al. have shown that a PEO containing block polymer adsorbs strongly to the air-water interface so it is reasonable to assume that all of the available air-water interface area will be occupied by PB-PEO micelles.[7] By comparing the surface area of the droplet to the surface area one micelle takes up, which is about 100 nm x 100 nm (10^4 nm^2), the amount of micelles adsorbed to the air-water interface of the droplet can be calculated. About 10^9 micelles are located at the surface of the droplet, which is only 1% of the total amount of micelles present in the droplet. Even in the unrealistic case that every micelle at the air-water interface of the droplet exchanged cargo with another micelle during pipetting and complete exchange occurred, it would not cause an immediate quenching effect of the magnitude as seen here. It remains unclear why an immediate quenching effect is observed under quiescent conditions for Cy3 and BHQ-2 micelle solutions.

3.4.2 Exchange of dyes by magnetic stirring

Figure 3.10 indicates that Cy3 and BHQ-2 micelle solutions during quiescent conditions or after magnetic stirring have similar fluorescence intensities. No decrease in fluorescence is evident over several hours, which indicates that no dye exchange is occurring during this time span. A 30 min vortex mixed sample has a much lower fluorescence intensity than magnetically stirred samples. These results are consistent with the hypothesis that the dye exchange will occur through the air-water interface

and needs sufficient surface turnover, because magnetic stirring induces only a very small amount of surface turnover, about 200-fold less than vortex mixing.[17]
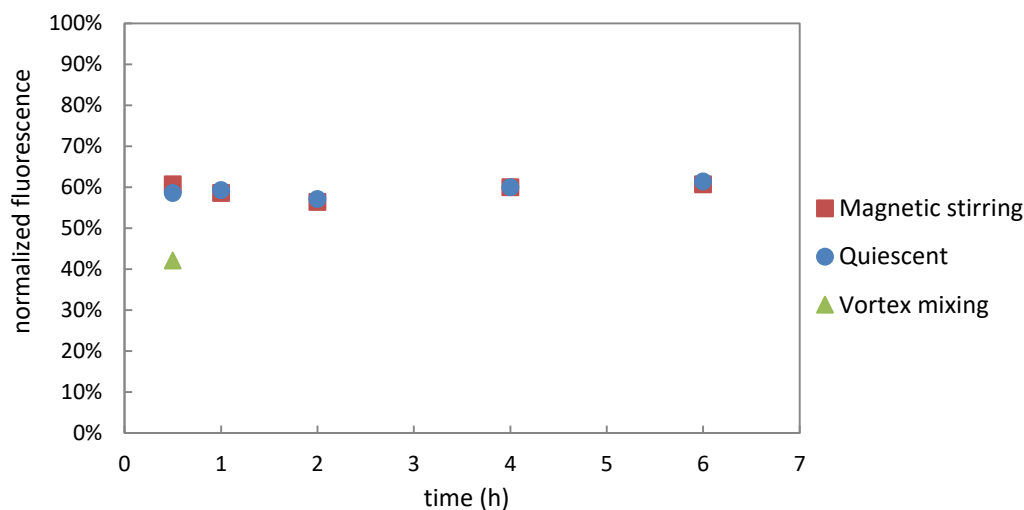

Figure 3.10: Normalized fluorescence intensities of mixtures of Cy3 and BHQ-2 micelle solutions, under quiescent and magnetically stirred conditions over various time spans. The normalized fluorescence intensities of a vortex mixed solution of Cy3 and BHQ-2 micelles is also included as a reference. Fluorescence intensities were normalized to the fluorescence intensity of the Cy3 micelle solution.

3.4.3 Exchange of dyes by vortex mixing

Figure 3.11 again shows how the fluorescence of a vortex mixed Cy3 and BHQ-2 micelle solution compares to a quiescent solution. The quenching during quiescent conditions seems to account for a large portion of the total quenching. However, the same fluorescence as the premixed Cy3 and BHQ-2 micelle sample is only obtained after vortex mixing.
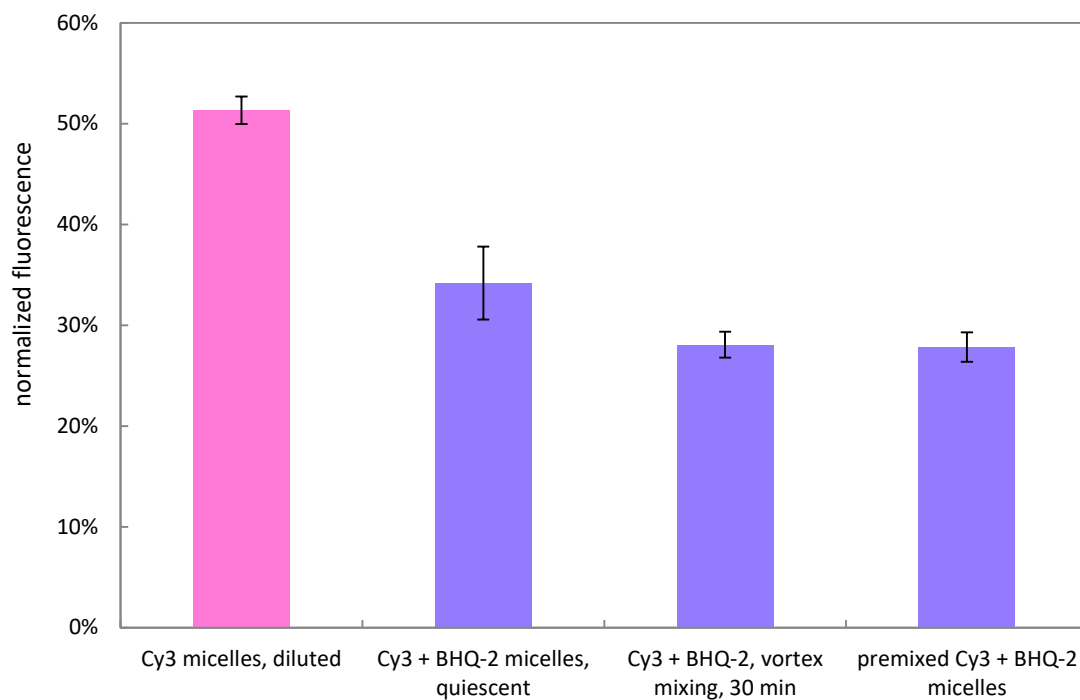
Figure 3.11: Normalized fluorescence intensities of a diluted Cy3 micelle solution and solutions of Cy3 and BHQ-2 micelles under quiescent and vortex mixed conditions. The normalized fluorescence intensity of a premixed Cy3 and BHQ-2 micelle solution is included as a measure for the fluorescence of a sample after complete dye exchange. Fluorescence intensities were normalized to the fluorescence intensity of the Cy3 micelle solution. The error bars represent the 95% confidence interval based on measurements from three different samples.

In Figure 3.12, the time frame of the dye exchange during vortex mixing is elucidated. The fluorescence of the Cy3 and BHQ-2 solution drops within the error of fluorescence of the premixed sample within 2 min of vortex mixing, indicating that complete exchange of dye occurs within this time span.
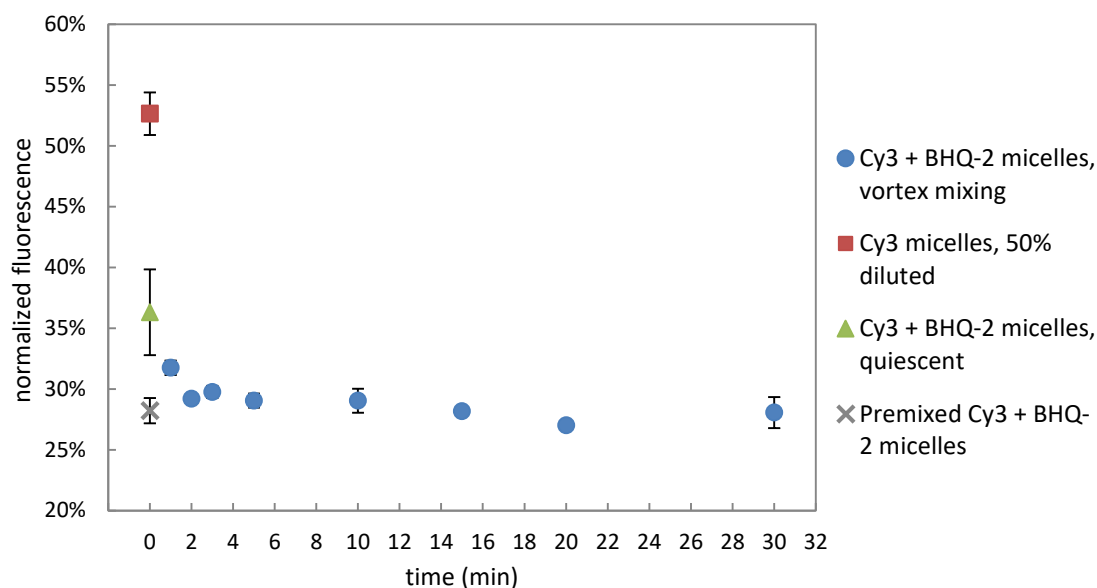
Figure 3.12: Normalized fluorescence intensity of a vortex mixed solution of Cy3 and BHQ-2 micelles over time. The normalized fluorescence intensities of the diluted Cy3 micelle solution, the quiescent mixture of Cy3 and BHQ-2 micelle solutions and the premixed Cy3 and BHQ-2 micelle solution are also included as references. Fluorescence intensities were normalized to the fluorescence intensity of the Cy3 micelle solution. The error bars represent the 95% confidence interval based on measurements from three different samples.

Theoretically, it is possible that the dyes exchange completely during this 2 min time frame. Bai et al. estimated a surface turnover rate of 200 cm^2/s for vortex mixing of a 1 mL solution in a 3 mL glass vial ($D_{inner} \approx 15$ mm) at 1000 rpm.[17] As calculated earlier, the number of micelles in 1 mL of 2.5 mg/mL PB-PEO solution is about 10^{14} and the area one micelle occupies at the air-water interface is estimated to be 10^4 nm^2. As a result, the timeframe for complete exchange of dyes between all micelles in the solution is estimated to be about 1 min. This result is in almost perfect alignment with what is observed from experiments. However, for a 2.4 mg/mL PB-PEO sample complete chain exchange was previously observed after only about 10

min of vortex mixing.[4] A possible explanation for this discrepancy between the theoretically estimated 1 min time frame and the experimental results, is that chain exchange was hypothesized to be a stepwise process with only a small fraction of chains exchanging with each interaction at the interface. Cargo exchange between micelles is a different process, even though it is closely related to chain exchange. For cargo exchange mediated through the air-water interface (Figure 3.1), multiple interactions are possibly not needed for the micellar cores to completely exchange the dyes considering diffusion of dye molecules through the core is likely fast. It must be noted that the parameters used to estimate the time scale of complete dye exchange might be very different in this particular system. The actual surface turnover rate will likely differ from the estimation of Bai et al. due to a larger surface to volume ratio because volumes of 130 µL in ½ dram glass vials ($D_{outer} \approx 11$ mm) are used in this case, instead of 1 mL in 3 mL vials ($D_{inner} \approx 15$ mm).[17] The surface turnover rate also depends on the speed of vortex mixing and experiments were done at about 1500 rpm instead of 1000 rpm.

3.4.4 Self-quenching of Cy3

Self-quenching occurs when fluorophores absorb the fluorescence emission of other fluorophores of the same kind. An increasing concentration of fluorophores then does not result in a proportional increase in fluorescence intensity and may even result in a reduction of the fluorescence. Cyanine dyes, including Cy3, are known to self-quench.[18-20]

3.4.4.1 Experimental evidence of self-quenching of encapsulated Cy3

Possible self-quenching of the Cy3 micelles was investigated by vortex mixing these solutions together with solutions of non-loaded ("empty") micelles. If the Cy3 molecules in the micelles are self-quenching, then an increase in fluorescence would be observed after these micelles are dispersed over a larger number of micelles. Figure 3.13 shows the fluorescence of the Cy3 micelle solution, the diluted solution and a vortex mixed solution of Cy3 and empty micelles for different batches with different concentrations of Cy3.
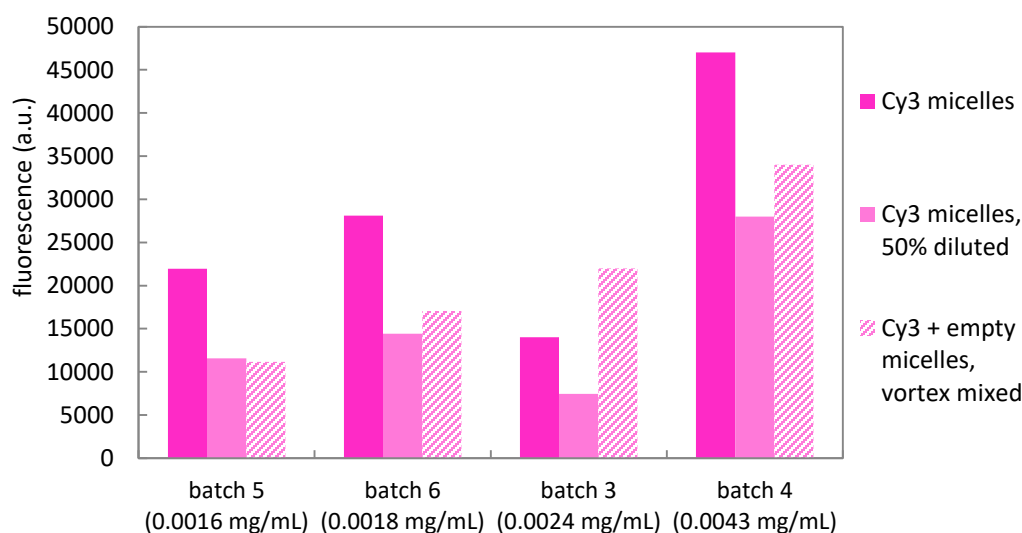

Figure 3.13: The fluorescence intensities of Cy3 micelle solutions, diluted Cy3 micelle solutions and vortex mixed solutions of Cy3 and empty micelles for different concentrations of cyanine3 alkyne.

The amount of self-quenching is defined here by the percentage increase of fluorescence between a diluted Cy3 micelle solution and the vortex mixed Cy3 and empty micelle solution. For batch 5, at a concentration of 0.0016 ± 0.0002 mg/mL

Cy3, does not have significant self-quenching. Batch 6, which has a slightly higher concentration of Cy3 at 0.0018 ± 0.0002 mg/mL, shows a small increase of 18% when comparing the diluted sample to the Cy3 and empty micelles vortex mixed sample. This small increase may be due to the removal of self-quenching, but could also be interpreted as an increase in fluorescence intensity because of a higher local concentration of Cy3 molecules due to free dye molecules diffusing into the corona of the empty micelles (see sections 3.3.5 and 3.4.1.2).

Increasing the concentration of Cy3 usually means increasing fluorescence, as seen for batch 6 compared to batch 5. But at a Cy3 concentration of 0.0024 ± 0.0002 mg/mL, the fluorescence of batch 3 is significantly lower than for batch 6. This decrease in fluorescence is due to substantial self-quenching: an increase in fluorescence intensity of 196% for the solution with vortex mixed Cy3 and empty micelles, compared to the diluted Cy3 micelle solution, is observed. For the vortex mixed solution of dye-loaded and empty micelles, it is expected that self-quenching effects have been removed, considering the concentration of Cy3 is decreased by half (to about 0.0012 mg/mL) and it is established that at these low concentrations (batch 5), no self-quenching occurs.

Surprisingly, the fluorescence increases again for batch 4, with a higher Cy3 concentration (0.0043 ± 0.0002 mg/mL). A possible explanation for this effect is that for these high concentrations of dye the encapsulation capacity of the micelles is superseded. Consequently, more dye would be free in solution or located in the coronas, where it is not self-quenched and contributes to the fluorescence intensity. When comparing the fluorescence of a diluted Cy3 micelle sample with the vortex mixed dye-loaded and empty micelles, there is apparently less self-quenching of the

107

dyes within the micelles occurring: 21% increase in fluorescence for batch 4 versus 196% for batch 3. This difference is thought to be only an artificial effect. First of all, the self-quenching efficiency calculation does not take into account the fluorescence by free Cy3 molecules in solution or in the corona, which might be significant if the encapsulation capacity is superseded. Because these molecules are not self-quenched, its fluorescence intensity is equal for the diluted sample as for the Cy3 and empty micelles vortex mixed sample. Secondly, due to the high concentration, the Cy3 molecules in the micelles of the vortexed mixed solution of dye-loaded and empty micelles could still be self-quenching. In this vortex mixed sample, the Cy3 concentration is decreased by half, to about 0.0022 mg/mL. At this concentration, significant self-quenching occurs, as the batch 3 sample indicates. Possibly, the self-quenching was only partially reduced and not completely removed when the dye molecules were dispersed over twice as many micelles.

In general, the fluorescence of Cy3 micelles can already indicate self-quenching occurring when it does not increase consistently for increasing concentration of dye, as evident in Figure 3.13. The fluorescence intensity does increase with increasing concentration for the vortexed mixing solution of Cy3 micelles and empty micelles, as expected because self-quenching effects should be severely diminished or removed in these samples (possibly excluding batch 4).

3.4.4.2   Theoretical determination of self-quenching of Cy3

Lee et al. reported lateral self-quenching as a phenomenon that does not usually happen until fluorophore densities reach ~1.5 molecules/nm^2.[20] This result was in part based on the work of Schmitt et al. on cyanine dyes, for which energy-transfer effects occurred between 0.6 and 0.7 nm^2/molecule (dye densities of 1.4

molecules/nm^2 to 1.7 molecules/nm^2).[21] The results from Schmitt et al. can be transformed into an estimate for the required distance between two dye molecules for self-quenching: 0.4 nm to 0.5 nm.

ThermoFisher reports that for goat anti-rabbit IgG antibody conjugates of Cy3 dye, self-quenching starts occurring at around 2 mol fluorophore per mol of protein. The size of the goat anti-rabbit IgG antibody is estimated to be around 9 nm, based on work determining the size of rabbit IgG antibody.[22] A rough estimate for the distance requirement for two Cy3 molecules to self-quench of 4.5 nm is obtained from these parameters.

Earlier, it was determined that about 10^{14} micelles are present in a 1 mL PB-PEO sample of concentration 2.5 mg/mL. The number of Cy3 molecules per micelle can be determined through the molecular weight of cyanine3 alkyne and Avogadro's number for different concentrations of Cy3 dye. The PB-PEO micelle core has a radius of 12 nm for aqueous solutions, which results in a core volume of 7.2 x 10^3 nm^3.[15] Then the density of Cy3 molecules in the core of the micelle and subsequently an estimate for the distance between two molecules can be determined. For different concentrations of Cy3, the results are shown in Table 3.5. The results indicate that self-quenching would start at a distance between fluorophores of about 4.6 nm to 4.4 nm, considering batch 5 did not show any self-quenching and possibly some self-quenching was observed for batch 6. Significant self-quenching is observed for distances of 4.0 nm. Compared to the estimate obtained from the work of Schmitt et al. (0.4 nm to 0.5 nm), this result is an order of magnitude larger, possibly because of the extrapolation of lateral quenching to quenching in three-dimensional space does not hold. A distance of 0.4 nm to 0.5 nm is also extremely low and not realistic. The

distance between fluorophores for which self-quenching is observed in experiments (4.6 nm to 4.4 nm) is very close to the estimated distance based on data supplied by ThermoFisher, which was 4.5 nm.[19]

Table 3.5:   The number of cyanine3 alkyne molecules per micelle, the density of molecules in the core of the micelle and the distance between the molecules within the core for different concentrations of cyanine3 alkyne.

	concentration Cy3 (mg/mL)	Molecules per micelle	Density in core (molecules / nm^3)	$d_{molecules}$ (nm)
batch 5	0.0016	18	2.5×10^{-3}	4.6
batch 6	0.0018	20	2.8×10^{-3}	4.4
batch 3	0.0024	27	3.8×10^{-3}	4.0
batch 4	0.0043	49	6.8×10^{-3}	3.3

3.4.4.3   Effect of self-quenching on BHQ-2 quenching

If Cy3 molecules encapsulated within the micelle core are self-quenching, the fluorescence intensity increases when these molecules are exchanged with other micelles. If the exchange happens with micelles loaded with BHQ-2 dye, two contradicting effects influence the fluorescence because the fluorescence intensity decreases once Cy3 molecules come into close proximity with BHQ-2 molecules. The fluorescence can thus stay constant due to cancellation of the BHQ-2 quenching effect by the increase in fluorescence due to the loss or decrease in self-quenching effect. To

avoid any possible confusion, all previous experiments were performed with Cy3

micelle solutions at concentrations for which no significant self-quenching occurred.
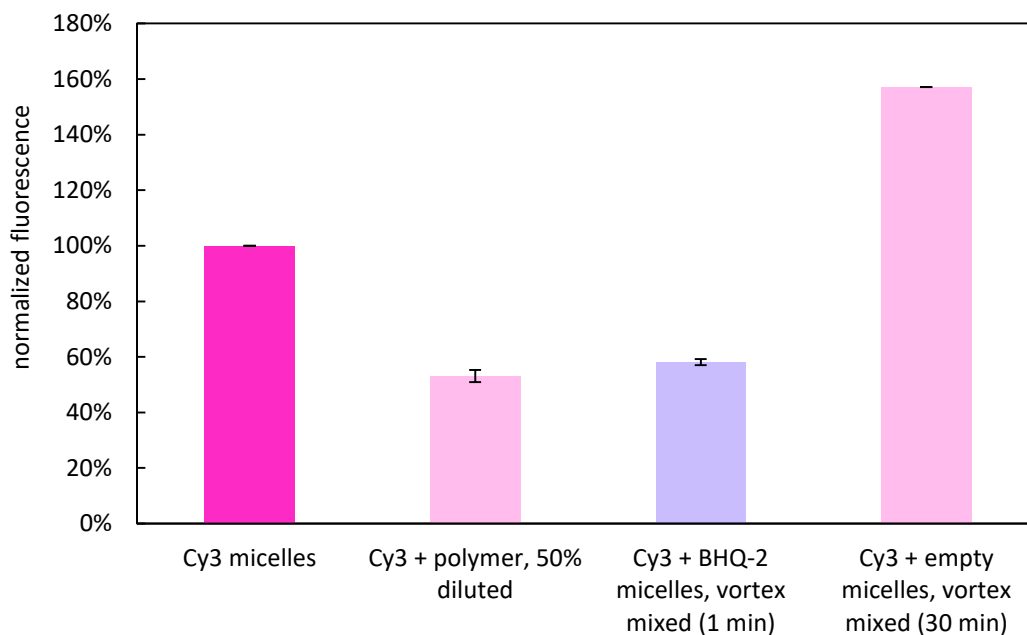

Figure 3.14: Normalized fluorescence intensities of a Cy3 micelle solution, a diluted
Cy3 micelle solution, a vortex mixed solution of Cy3 and BHQ-2
micelles and a vortex mixed solution of Cy3 and empty micelles.
Fluorescence intensities were normalized to the fluorescence intensity of
the Cy3 micelle solution. The error bars represent the 95% confidence
interval based on measurements from three different samples.

Figure 3.14 illustrates why Cy3 self-quenching micelle solutions should ideally

be avoided in combination with BHQ-2 micelle solutions. The fluorescence of a 1 min

vortex mixed Cy3 and BHQ-2 micelle solution is higher than the diluted Cy3 micelle

solution. The increase in fluorescence due to Cy3 molecules being released from the

micelle core is probably not fully compensated by the quenching by the BHQ-2

molecules, because a large amount of self-quenching occurs as proven by the large fluorescence intensity of the vortex mixed Cy3 and empty micelle solution.

The distance between Cy3 molecules in the core of the micelles was estimated previously to be around 4.6 to 4.4 nm (for non-self-quenching batches). It can be assumed that the dye density stays about the same after exchange, because the density of BHQ-2 in the micellar core is similar to the Cy3 density. The distance between the dye molecules after exchange is thus about the same as well, i.e. around 4.5 nm. The Förster radius of Cy3 and BHQ-2 is 5 nm, so the FRET efficiency is 50% this distance. As a result, with these dye densities, the maximum attainable FRET efficiency is only about 50%, which is consistent with measurements of the fluorescence of the premixed Cy3 and BHQ-2 solutions compared to the diluted Cy3 micelle solutions (about 47% to 57%). Ideally, the FRET efficiency would be very high so that the premixed sample would have a negligible fluorescence intensity and the decrease in intensity due to dye exchange would be much more clearly visible. However, higher loading densities to obtain this higher efficiency are not advisable due to exceeding the loading capacity of the micelles, resulting in significant amount of free dye in solution, and the self-quenching effects.

Even though self-quenching may cause confusion when comparing a diluted Cy3 micelle solution and a vortex mixed Cy3 and BHQ-2 micelle solution due to the two counteracting effects (Figure 3.14), the self-quenching does help when elucidating the time scale of vortex mixing. Due to the low FRET efficiencies because of the lower dye densities to avoid self-quenching, decreases in fluorescence are small. Due to the increase in fluorescence because of the self-quenching effect, the decrease in fluorescence is not as large during exchange and the dye exchange time frame is more

easily visible. From Figure 3.15, it can be concluded that dye exchange happens within the first 3 min to 5 min of vortex mixing because the fluorescence intensity plateaus, which is close to the 2 min time span determined earlier.
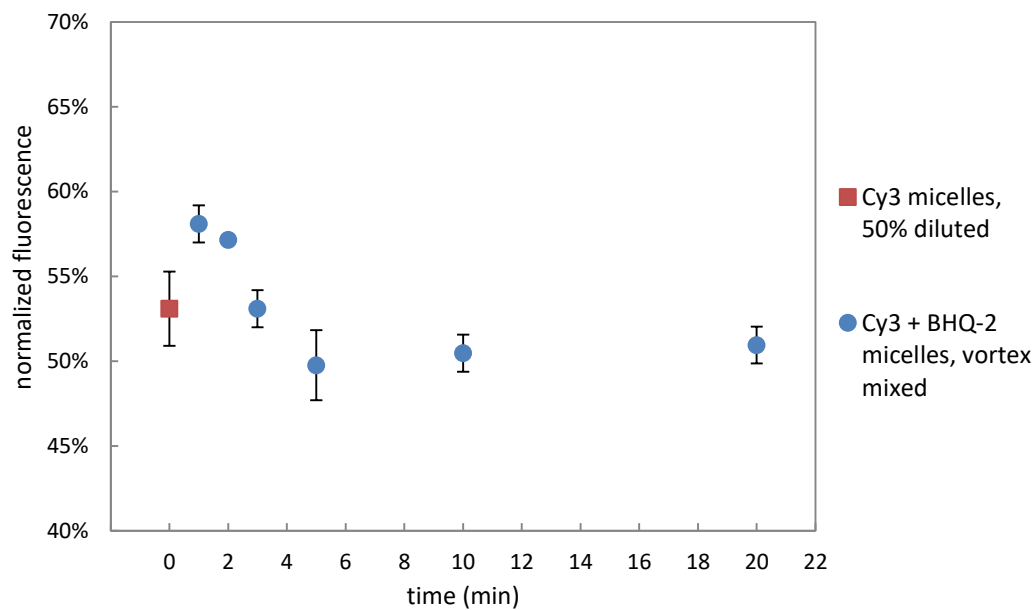

Figure 3.15: Normalized fluorescence intensities of a vortex mixed solution of Cy3 and BHQ-2 micelles over different time spans. The normalized fluorescence intensity of a diluted Cy3 micelle solution is included as a reference. Fluorescence intensities were normalized to the fluorescence intensity of the Cy3 micelle solution. The error bars represent the 95% confidence interval based on measurements from three different samples.

REFERENCES

1. Li, L.; Thayumanavan, S. Environment-Dependent Guest Exchange in Supramolecular Hosts. *Langmuir*, **2014**, *30*, 12384–12390.

2. Rharbi, Y.; Winnik, M. A. Solute exchange between surfactant micelles by micelle fragmentation and fusion. *Advances in Colloid and Interface Science*, **2001**, *89–90*, 25–46.

3. Won, Y. Y.; Davis, H. T.; Bates, F. S. Molecular exchange in PEO-PB micelles in water. *Macromolecules*, **2003**, *36*, 953–955.

4. Murphy, R. P.; Kelley, E. G.; Rogers, S. A.; Sullivan, M. O.; Epps, T. H. Unlocking Chain Exchange in Highly Amphiphilic Block Polymer Micellar Systems: Influence of Agitation. *ACS Macro Letters*, **2014**, *3*, 1106–1111.

5. Bijsterbosch, H. D.; de Haan, V. 0.; de Graaf, A. W.; Mellema, S. M.; Leermakers, F. A. M.; Stuart, M. A. C.; van Well, A. A. Tethered Adsorbing Chains: Neutron Reflectivity and Surface Pressure of Spread Diblock Copolymer Monolayers. Langmuir, 1996, 11, 4467–4473.

6. Gonçalves da Silva, A. M.; Filipe, E. J. M., d'Oliveira; J. M. R.; Martinho, J. M. G. Interfacial Behavior of Poly(styrene)-Poly(ethylene oxide) Diblock Copolymer Monolayers at the Air-Water Interface. Hydrophilic Block Chain Length and Temperature Influence. Langmuir, 1996, 12, 6547–6553.

7. Zell, Z. A.; Isa, L.; Ilg, P.; Leal, L. G.; Squires, T. M. Adsorption Energies of Poly(ethylene oxide)-Based Surfactants and Nanoparticles on an Air−Water Surface. Langmuir, 2014, 30, 110–119.

8. Bhattacharjee, S. DLS and zeta potential – What they are and what they are not? Journal of *Controlled Release*, **2016**, *235*, 337–351.

9. Geißler, D.; Gollwitzer, C.; Sikora, A.; Minelli, C.; Krumrey, M.; Resch-Genger, U. Effect of fluorescent staining on size measurements of polymeric nanoparticles using DLS and SAXS. *Analytical Methods*, **2015**, *7*, 9785–9790.

10. ThermoFisher Fluorescence SpectraViewer. https://www.thermofisher.com/us/en/home/life-science/cell-analysis/labeling-chemistry/fluorescence-spectraviewer.html (accessed January 26, 2017)

11. O'Hare, S. Product Specialist Biosearch Technologies, Novato, CA. Personal correspondence, 2017.

12. Leo, A.; Hansch, C.; Elkins, D. Partition Coefficients and Their Uses. *Chemical Reviews*, **1971**, *71*, 525–616.

13. Xie, M.; Wang, S.; Singh, A.; Cooksey, T. J.; Marquez, M. D.; Bhattarai, A.; Kourentzi, K.; and Robertson, M. L. Fluorophore exchange kinetics in block copolymer micelles with varying solvent– fluorophore and solvent– polymer interactions. *Soft Matter*, **2016**, *12*, 6196–6205.

14. Buboltz, J. T. Steady-state probe-partitioning fluorescence resonance energy transfer: A simple and robust tool for the study of membrane phase behavior. *Physical Review E*, **2007**, *76*, 21903.

15. Kelley, E. G.; Smart, T. P.; Jackson, A. J.; Sullivan, M. O.; Epps, T. H., III. Structural changes in block copolymer micelles induced by cosolvent mixtures. *Soft Matter*, **2011**, *7*, 7094–7102.

16. Topel, Ö.; Çakır, B. A.; Budama, L.; Hoda, N. Determination of critical micelle concentration of polybutadiene-block-poly(ethyleneoxide) diblock copolymer by fluorescence spectroscopy and dynamic light scattering. *Journal of Molecular Liquids,* **2013**, *177*, 40-43.

17. Bai, G.; Bee, J. S.; Biddlecombe, J. G.; Chen, Q.; Leach, W. T. Computational fluid dynamics (CFD) insights into agitation stress methods in biopharmaceutical development. *International Journal of Pharmaceutics*, **2012**, *423*, 264–280.

18. Berlier, J. E.; Rothe, A.; Buller, G.; Bradford, J.; Gray, D. R.; Filanoski, B. J.; Telford, W. G.; Yue, S.; Liu, J.; Cheung, C.-Y.; Chang, W.; Hirsch, J. D., Beechem, J. M.; Haugland, R. P.; Haugland, R. P. Quantitative Comparison of Long-wavelength Alexa Fluor Dyes to Cy Dyes: Fluorescence of the Dyes and Their Bioconjugates. *The Journal of Histochemistry & Cytochemistry*, **2003**, *51*, 1699–1712.

19. ThermoFisher. https://www.thermofisher.com/us/en/home/life-science/cell-analysis/fluorophores/cy3-dye.html (accessed January 13, 2017)

20. Lee, C.-Y.; Gong, P.; Harbers, G.M.; Grainger, D. W.; Castner, D. G.; Gamble, L. J. Surface Coverage and Structure of Mixed DNA/Alkylthiol Monolayers on Gold: Characterization by XPS, NEXAFS, and Fluorescence Intensity Measurements. *Analytical Chemistry*, **2006**, *78*, 3326–3334.

21. Schmitt, F.-J.; Meller, P.; Ringsdorf, H.; Knoll, W. Specific dye adsorption at oriented monolayers. In: *Interfaces in Condensed Systems*; Findenegg, G. H., Ed.; Progress in Colloid and Polymer Science, Vol. 83.; Steinkopff-Verlag: Heidelberg, 1990; pp 136-145.

22. Pease, L. F., III; Elliott, J. T.; Tsai, D.-H.; Zachariah, M. R. ; Tarlov, M. J. Determination of Protein Aggregation With Differential Mobility Analysis: Application to IgG Antibody. *Biotechnology and Bioengineering*, **2008**, *101*, 1214–1222.

Chapter 4

SUMMARY AND FUTURE RECOMMENDATIONS

4.1   Conclusions

Many applications of polymer nanocarriers, including drug delivery, catalysis and self-healing materials, require the encapsulation of cargoes.[1] The stability, performance and lifetime of the nanocarriers are dependent on the guest exchange dynamics and the chain exchange dynamics.[1,2] It is therefore important to understand these dynamic processes thoroughly. This thesis explored the encapsulation of dyes by polymer micelles and the exchange of these dyes between micelles, using DLS, UV-Vis spectroscopy, and FRET methods.

Chapter 1 offered an introduction into block copolymers and the self-assembly into micelles. The solubilization of compounds in these micelles, the release of solubilized drugs from micelles and the guest exchange between micelles was also discussed briefly.

Chapter 2 discussed polymer and dye selection and properties, as well as different micelle solution preparation methods. Solution characterization methods like DLS, FRET, and UV-Vis spectroscopy were introduced.

Chapter 3 revealed that Cy3 dye was not stably encapsulated and could migrate into the corona and aqueous solution, contrary to the encapsulation of the very hydrophobic BHQ-2 amidite. Solutions of Cy3 and BHQ-2 micelles under quiescent conditions, magnetically stirred and vortex mixed were investigated by FRET. The results suggested quiescent and magnetically stirred solutions exhibiting the same

trends. The fluorescence intensity was constant over several hours after an "immediate" (< 1 min) initial drop in fluorescence intensity compared to a diluted Cy3 micelle solution. Several hypotheses were examined, but no conclusive theory could be presented as to why an immediate quenching effect was observed. No change in fluorescence intensity occurred over time and complete exchange of cargo could not be achieved under quiescent conditions or during magnetic stirring, even after several hours. Vortex mixing did decrease the fluorescence intensity of a Cy3 and BHQ-2 micelle solution over the time span of minutes, due to exchange of dyes between micelles. Complete exchange occurred after about 2 min to 5 min, in concurrence with theoretical estimates of exchange of dye molecules between micelles through an air-water interface mediated exchange process.

Several effects occurred simultaneously when investigating the exchange of dyes between micelles. Self-quenching was observed for cyanine3 alkyne molecules at concentrations of 0.0024 mg/mL in micelle solutions. Solutions of cyanine3 alkyne had much less fluorescence intensity than solutions of the same concentration where block copolymer micelles were present, due to higher local concentrations of cyanine3 alkyne inside the micelles. Possibly, due to its limited hydrophobicity, cyanine3 alkyne molecules in solution may also move into the corona of newly added micelles and have an effect on the fluorescence intensity by increasing the local concentration.

Overall, new insights were developed into the exchange of encapsulated dyes between micelles. While magnetically stirred and quiescent solutions did not show any additional dye exchange over several hours after an apparent immediate quenching effect, vortex mixing could induce complete exchange within minutes. The dye exchange is thought to occur through the air-water interface and preliminary results of

a comparison with magnetic stirring experiments seemed to align with this hypothesis. These results are important for understanding the stability and lifetime of block copolymer micelles loaded with dyes or drugs under different processing conditions.

4.2 Future recommendations

The self-quenching behavior and limited hydrophobicity of cyanine3 alkyne resulted in some additional difficulties in determining the effect of agitation on the exchange of dye between micelles. Self-quenching should be avoided because self-quenched dye molecules in micelles result in opposite effects on the fluorescence intensity when the solution is mixed with a solution of micelles loaded with quencher molecules. Due to self-quenching, it was not possible to increase the dye density to obtain a higher FRET efficiency so the dye exchange process would induce a higher fluorescence intensity decrease and be clearer to detect. A more hydrophobic dye would be solubilized within the core and not leach out into the aqueous phase, so the diffusion-based process should not have to be considered. Therefore, ideally, a more hydrophobic dye should be used that does not exhibit significant self-quenching, which is not an easy feat considering the two other hydrophobic dyes identified earlier in this work, TRITC, a rhodamine derivative, and BODIPY® FL, also exhibit substantial self-quenching.[3-5] Possibly, a less hydrophobic and non-self-quenching dye molecule could be chemically modified. Kolmakov et al. have reported on the synthesis of hydrophobic and hydrophilic derivatives of rhodamine.[6] Rhodamine is not an advisable choice considering its self-quenching behavior, but possibly a similar strategy could be used to obtain a hydrophobic derivative of a fluorescent dye that does not self-quench.

Determination of encapsulation of dye within the micelle was challenged due to the low precision of the UV-Vis experiments. Molar extinction coefficients were used to determine the concentration of dyes, but these coefficients are dependent upon the solvent in which the dyes are present. Other methods should be explored to obtain more precise measurements of the dye concentration. One possibility would be using a calibration curve obtained specifically for the dyes in water. Here, the use of a calibration curve was not possible considering the limited available quantity of dyes, the limited resolution (0.0001 g) balance, and the low solubility of BHQ-2 amidite in water without polymer.

Ideally, determination of the location of dye molecules within a micelle solution would be done with a microscopy technique. Cryo-TEM can visualize the micelles, but would likely not have enough resolution to locate the dye molecules. For the fluorescent cyanine3 amidite molecules, a fluorescent microscopy technique could be used. However, the resolution of fluorescence microscopy is about 200 nm to 300 nm, which is too large to visualize polymer micelles of about 85 nm and cannot determine whether dye molecules are in the core or the corona of the micelle.[7] Some new high-resolution fluorescence microscopy techniques have been developed with a resolution as high as $\sim$ 20 nm in the lateral direction.[7] In theory, this resolution would be sufficient to distinguish between the core and the corona of the PB-PEO micelles, considering the core is about 24 nm in diameter.[8]

To determine the influence of the air-water interface turnover rate, a more controlled process than vortex mixing is necessary for changing the interface. Agitation of mixtures of dye-loaded micelles with a rotator could control the surface turnover rate and look at the influence of different turnover rates of the exchange of

120

dyes between micelles. With experiments using a rotator, a kinetic model for the interface mediated dye exchange could be elucidated by relating the surface turnover rate to the fluorescence intensity. Using different filling levels of vials, the influence of the surface-to-bulk level could also be determined, in conjunction with additional vortex mixed experiments. A completely filled vial, as negative control, would confirm undoubtedly whether the guest exchange is surface limited.

REFERENCES

1. Li, L.; Thayumanavan, S. Environment-Dependent Guest Exchange in Supramolecular Hosts. *Langmuir*, **2014**, *30*, 12384–12390.

2. Murphy, R. P.; Kelley, E. G.; Rogers, S. A.; Sullivan, M. O.; Epps, T. H. Unlocking Chain Exchange in Highly Amphiphilic Block Polymer Micellar Systems: Influence of Agitation. *ACS Macro Letters*, **2014**, *3*, 1106–1111.

3. Swiecicki, J.-M.; Thiebaut, F.; Di Pisa, M.; Gourdin -Bertin, S.; Tailhades, J.; Mansuy, C.; Burline, F.; Chwetzoff, S.; Trugnan, G.; Chassaing, G.; Lavielle, S. How to unveil self-quenched fluorophores and subsequently map the subcellular distribution of exogenous peptides. *Scientific Reports*, **2016**, *6*, 20237.

4. Lakowicz, J. R. *Principles of Fluorescence Spectroscopy*; Springer US: Boston, MA; 2006.

5. ThermoFisher. https://www.thermofisher.com/us/en/home/references/molecular-probes-the-handbook/fluorophores-and-their-amine-reactive-derivatives/long-wavelength-rhodamines-texas-red-dyes-and-qsy-quenchers.html (accessed April 23, 2017)

6. Kolmakov, K.; Belov, V. N.; Bierwagen, J.; Ringemann, C.; Müller, V.; Eggeling, C.; Hell, S. W. Red-Emitting Rhodamine Dyes for Fluorescence Microscopy and Nanoscopy. *Chemistry: A European Journal*, **2010**, *16*, 158–166.

7. Huang, B.; Bates, M.; Zhuang, X. Super-resolution fluorescence microscopy. *Annual Review of Biochemistry*, **2009**, *78*, 993–1016.

8. Kelley, E. G.; Smart, T. P.; Jackson, A. J.; Sullivan, M. O.; Epps, T. H., III. Structural changes in block copolymer micelles induced by cosolvent mixtures. *Soft Matter*, **2011**, *7*, 7094–7102.

Appendix

COPYRIGHT PERMISSION STATEMENT

Figure A.1.: Permission statement for *Science,* **2003**, *300*, 460–464.